Improving Polymer-Mediated DNA Vaccine Delivery

A DISSERTATION SUBMITTED TO THE FACULTY OF THE GRADUATE SCHOOL OF THE UNIVERSITY OF MINNESOTA

BY

Rebecca Noelle Palumbo

IN PARTIAL FULFILLMENT OF THE REQUIREMENTS FOR THE DEGREE OF DOCTOR OF PHILOSOPHY

Advisor: **Chun Wang, Ph.D.**

June, 2011

Acknowledgements

This work was partially funded by the National Institutes of Health (grant number R01CA129189), the Wallace H. Coulter Foundation (Early Career Translational Research Award), and a subcontract award from DOD.

Special thanks to Dr. Matt Mescher for providing the OT-1/PL mice, Kathy Pape and Sandy Johnson for helpful suggestions regarding tissue sectioning and immunostaining, and Prof. Bob Tranquillo for making a cryotome available for us to use.

We are also grateful to the Biomedical Image Processing Lab (BIPL) at the University of Minnesota, in particular, John Oja for assistance with Maestro live animal imaging analysis

Dedication

This thesis is dedicated to all those who helped me write it. To my advisor, Dr. Chun Wang, for providing me with support and flexibility, particularly in the last two years, and the rest of my Wang Lab comrades for all their help. And, of course, this is dedicated to my family. To my husband, Matt, for putting up with my sneaking off to work every time he entered the door, leaving him to make dinner and clean the house alone. To my daughter, Ayla, for maintaining her sunny attitude even when I spent most of the time hidden from her trying to write. And to my son, Adden, who had to endure the stress of the situation right along with me. I also include my babysitter, Liz, without whose willingness to work different hours every week to fit my schedule I would probably still be writing today.

Abstract

Vaccination using antigen-encoding plasmid DNA has great potential to generate strong immune response against delivered antigen. In order to effectively generate immune response, antigen must be delivered to antigen presenting cells, primarily dendritic cells (DCs). Using cationic polymers as a delivery vehicle can provide many advantages, including protection of DNA from degradation, ability to add targeting moieties, and easy modification of structure to optimize various properties. We have investigated the use of polyplexes as a DNA delivery vehicle in a variety of settings. We demonstrated the feasibility of using the CD40L as a DC targeting moiety, a protein capable of both binding and stimulating DC maturation, using coated nanoparticles. We have also studied the possibility of delivering antigen through transfection of bystander cells rather than direct expression by DCs using an in vitro model. We confirmed the ability of these DCs to present antigen, become mature, and stimulate T cells. Finally, we studied the interaction of cationic polymer complexes in vivo, both in respect to local tissue dispersion and interaction with specific cell types, using fluorescently labeled DNA. Through these experiments we have illuminated potential pathways for optimizing DNA vaccine efficiency using polymer complexes with slightly different structures.

Table of Contents

List of Figures

Chapter 1: Introduction

1.1. DNA Vaccines

The goal of vaccination is to manipulate the immune system into responding against a delivered antigen. To accomplish this antigen must be delivered to antigen presenting cells (APCs), along with an effective adjuvant, for processing, presentation, and subsequent immune response stimulation. The delivered antigen can take many forms, including peptides, protein, RNA, DNA, cell lysate, or even whole tumor cells.[1-5] However, vaccination with plasmid DNA encoding specific antigens has the potential for effective and efficient immune response generation. Transfection of cells with plasmid DNA will result in expression of the protein by those cells. This is an ideal method of vaccination because in situ antigen expression carries the potential for long term antigen generation capable of stimulating responses from both arms of the immune system to multiple epitopes.[4,6-8] In addition, plasmid DNA is easy to modify, replicate, and is very stable compared to materials such as peptides or proteins.[8]

1.2. Dendritic Cells and the Immune Response

Though there are several types of antigen presenting cells, including B cells and macrophages, dendritic cells (DCs) are considered by far the most efficient[9-11] and play a large role in controlling immune response. They are the only APC capable of stimulating a primary immune response and immunologic memory.[9,10] In an immature state DCs are located primarily in peripheral tissues and are able to acquire antigen from different sources through several different processes, including phagocytosis, pinocytosis, and

receptor-mediated endocytosis.[10,12] Antigen is digested and presented on major histocompatibility complex (MHC) class I or II molecules for presentation to effecter cells (T and B cells) in the lymph nodes[10,12,13] (Fig. 1.1). In the absence of any 'danger signals', such as inflammatory cytokines or pathogenic material, DCs will remain immature and stimulate the induction of tolerance, a process important for maintaining control of the immune system's response to self antigens.[14] However, in the presence of immunostimulatory signals, DCs undergo a process known as maturation,[10,12] which is characterized by increased antigen processing and presentation and migration to the lymph nodes where they interact with naïve T cells and B cells.[13] Maturing DCs also upregulate their expression of co-stimulatory molecules such as CD40, CD80, and CD86 among others, order to enhance stimulation of effecter cells for generation of a specific immune response to displayed antigen.[10,12,13] Traditionally, antigen obtained exogenously is processed for presentation on MHC class II, which primarily stimulates B cells and a humoral immune response, characterized by enhanced antibody production. Endogenously produced antigen, that expressed by DCs themselves after, for example, viral transfection, are processed on MHC class I molecules, leading to stimulation of T cells and a cellular immune response. It is known, however, that exogenous antigen can be processed for MHC class I presentation through a process known as cross-presentation.

Stimulation of T and B cells to a specific antigen is known as the adaptive immune response, but DCs are also known to be important in the generation of the innate immune response.[4,9] This branch of the immune system is characterized by activation of non-specific effecter cells such as natural killer (NK) cells and granulocytes. These cells

destroy foreign material in part by the identification of molecular targets shared by most pathogens. The innate immune response takes place primarily at the entry points for foreign material and is stimulated by an inflammatory response.[12] DCs are capable of stimulating this inflammation through the release of various cytokines such as type I IFNs and IL-12 and have been shown to interact directly with NK cells.[9,12] These characteristics all make DCs an ideal target cell for vaccination.

Initial attempts to utilize the great potential of dendritic cells' immostimulatory functions include many studies, some early clinical trials, done by loading cells with antigen ex vivo. In this method, precursor cells are first isolated from patients[1] and then expanded and differentiated into DCs by culturing with cytokine mixtures, usually GM-CSF and IL-4, for 3-5 days.[1] These cells must then be loaded with antigen and further cultured with various stimuli to induce maturation[1] before being re-injected into the patient. This process can result in enhanced immune response and has been the focus of several clinical trials.[15-17] However, culturing and antigen loading is time consuming, expensive, and can be suboptimal.[18,19] It was, for example, shown that DCs are just as, if not more, effective at immune stimulation when matured in situ, likely because the cell culture methods are not optimized and the process in vivo is more natural.[18] This suggests that targeting DCs for antigen loading and maturation entirely in vivo may be the optimal situation, which would eliminate the need for expensive and time consuming cell isolation and culture.

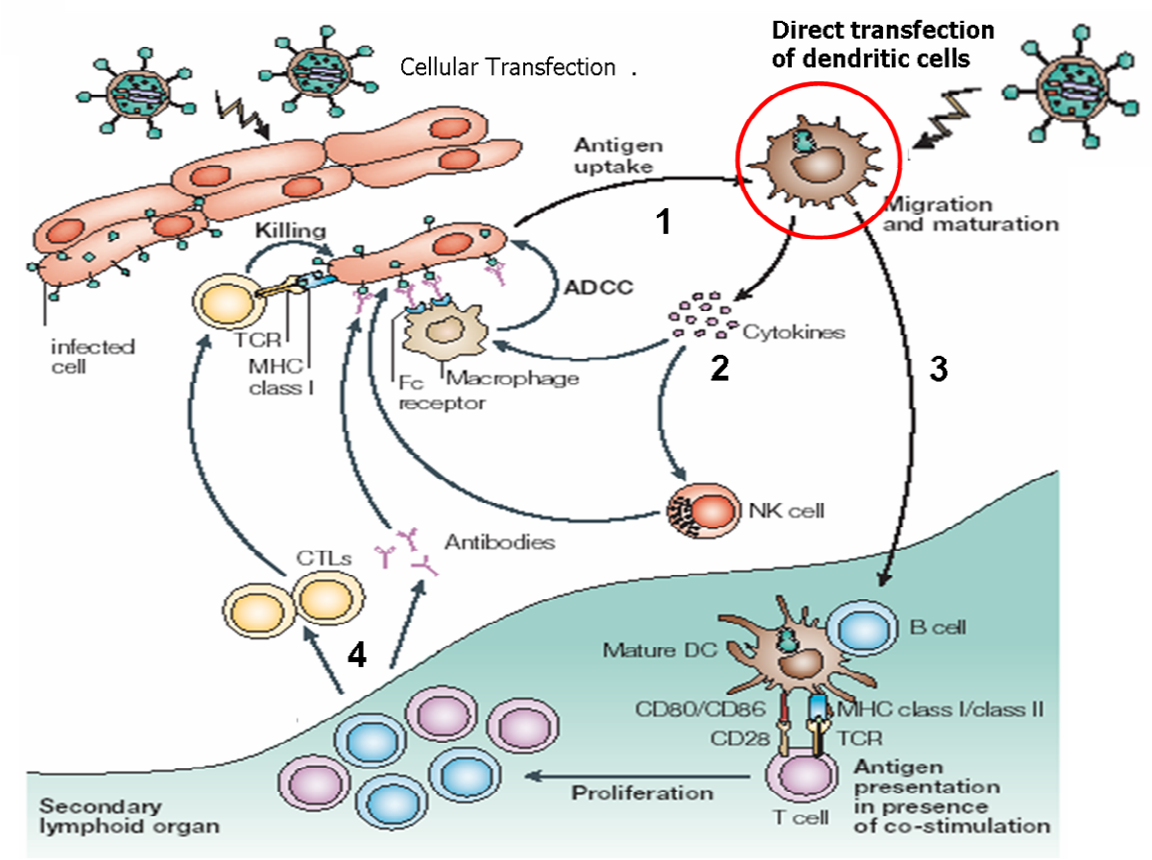

Figure 1.1: Dendritic cell control of immune response. (1) DCs ingest pathogenic material in the peripheral tissues, leading to antigen processing and maturation. (2) Cytokines are released at infection site for innate immune response stimulation. (3) DCs migrate to lymph nodes where antigens are presented along with costimulatory molecules to T and B cells. (4) Depending on how antigen is presented and DC stimulation, antibodies or cytotoxic T lymphocytes (CTLs) are produced to remove foreign material. Figure altered from Banchereau et. al.[13] Figure reprinted with permission from Macmillan Publishers Ltd: [Nat. Rev. Immunol.] (v. **5**, p. 296), copyright (2005)

1.3. Polymer-Mediated Delivery

The initial method of DNA vaccination in vivo involved the injection of naked plasmid DNA. However, though this can result in immune response, the efficiency of this method of delivery is generally low, presumably because the DNA itself is not able to efficiently enter cells and is easily degraded by nucleases extracellularly.[7,8,20] Various methods have been used to enhance transfection, therefore, including the use of gene guns and electroporation, which increase the ability of naked DNA to enter cells, as well as the use of delivery vehicles for packaging the plasmid. DNA delivery vehicles include viral vectors, liposomal formulations, and many different polymeric materials. All of these have the capability of protecting DNA from degradation and enhancing transfection efficiency. Viral vectors are by far the most efficient, but must overcome difficulties arising from clearance due to immune response against the carriers themselves as well as various safety concerns.[6,21]

The use of polymers for DNA delivery, though, has shown a lot of potential. They are able to provide protection to the DNA from degradation as well as potentially aid in targeting APCs, including dendritic cells.[22] Polymer systems are potentially ideal for delivering material to APCs because not only are they often moderate adjuvants on their own, but are also able to bind additional material to enhance DC stimulation or potentially improve targeting.[22]

One of the most explored polymers for APC targeting is poly-lactic co-glycolic acid (PLGA) because it is biodegradable and has already been determined biocompatible.[22] Initial attempts at using this polymer include simple encapsulation of plasmid DNA, which creates particles that have been shown to be taken up by phagocytic APCs,[23] and

specifically by dendritic cells both in vitro[24] and in vivo after intradermal injection.[25] However, the encapsulation techniques have several limitations. For example, the degradation rate of PLGA is too long,[23] perhaps longer than the lifespan of the dendritic cells themselves.[22] Also, DNA can be damaged both by the encapsulation procedure and the environment within the PLGA particles.[22,23] Therefore, alternatives or improvements to this basic carrier have been devised.

1.4. Cationic Polymers

In the search for improvement upon PLGA many have turned to positively charged materials, which are able to bind to the negatively charged phosphate groups of DNA directly, eliminating the need for encapsulation. For example, DNA has been absorbed onto the surface of PLGA microparticles treated with a cationic surfactant.[26] This increased the amount of DNA that could be delivered on each microparticle and was shown to induce a CTL immune response greater than naked DNA alone against a p55 gag antigen.[23,26] The cationic PLGA compound was also shown to transfect bone marrow derived dendritic cells in vitro.[27] Others have experimented with naturally cationic polymers such as polyethelyneimine (PEI), or polylysine (PLL). The positive charges, usually from amine groups, are often in excess to allow the polymer to bind not only to DNA but also to negatively charged glycoproteins and proteoglycans on the cell surface, which facilitates cellular entry.[7,28-30] However, the high charge ratio of these polymer complexes also leads to high toxicity.[31] Therefore, cationic polymers are often used in conjunction with other more biocompatible materials. For example, PEI has been blended[32] and covalently attached[33] to PLGA. These particles were able to enhance in

vitro transfection compared to PLGA alone without toxicity,[32] demonstrate endosomal release,[33] and transfect phagocytic cells.[33]

The excess positive charges of these vehicles, however, often lead to low complex stability in the presence of serum proteins. Aggregation in these conditions can lead to rapid clearance and toxicity. Interactions with serum proteins, blood, or solutes in the interstitial fluid can also lead to complex destabilization and DNA release.[7] Therefore, cationic polyplexes are also often shielded with small biocompatible polymers such as poly(ethylene glycol) (PEG),[31] pluronic, polyacrylic acid, or POE[7,28] to reduce their negative side effects. The polyplexes are coated or blended with these materials, shielding the extra positive charges, which has been shown to reduce both the toxicity and non-specific interactions, with elements such as negatively charged blood serum proteins, associated with polymer delivery vehicles. This helps to increase the stability, and therefore circulation time, of the polymeric material.[31] PEGylation has also been shown to significantly enhance the amount of polyplex that can be concentrated without precipitation, important when considering the amounts required for therapeutic effects, though it also significantly reduces the transfection efficiency.[34] In fact, shielding generally reduces the transfection efficiency of cationic polymers by reducing the high charge ratio, and therefore their interactions with cells. To overcome this, many groups have experimented with direct targeting.[35,36] In vitro, EGF-targeted shielded polyplexes actually had higher transfection efficiencies to EGFR expressing cells than PEI polyplexes alone, and similar levels to polyplexes conjugated to EGF without PEG shielding.[35] When complexes conjugated to either EGF or transferrin were injected into

mice, expression of a reporter gene was significantly higher in a distant tumor when compared to non-shielded transferrin-targeted polyplexes.[36]

1.5. Subcellular Trafficking

Non-viral DNA must overcome several hurdles to achieve transfection, the first being entry into the cell. Uptake of extracellular material, including polymeric delivery systems, typically occurs through either phagocytosis or one of various endocytic processes. Phagocytosis is mainly restricted to specialized cell types, such as macrophage and DC, so most other cells ingest polymeric particles through either clathrin-mediated endocytosis, caveolae-mediated endocytosis, macropinocytosis, or clathrin/caveolae-independent endocytosis[29] (Fig. 1.2). These pathways all differ in terms of the mechanism of uptake and the cargo fate upon entry. Several pathways, including phagocytosis, clathrin-mediated endocytosis, and, to a lesser extent, macropinocytosis, result in acidification of the resulting intracellular compartment. Only caveolae-mediated endocytosis does not lead to a decrease in pH, suggesting that this may be an ideal target for gene delivery, though release from the intracellular compartment will still need to be facilitated. Clathrin-mediated endocytosis is generally stimulated by ligand attachment, and can be induced by targeting with molecules such as transferrin.[29] This is an efficient method of material ingestion and may be an ideal way to enhance delivery of polymeric particles. It is unclear which of these pathways is primarily responsible for cationic polyplex uptake, though there is evidence to suggest primary contributions from clathrin-mediated endocytosis and macropinocytosis.[29]

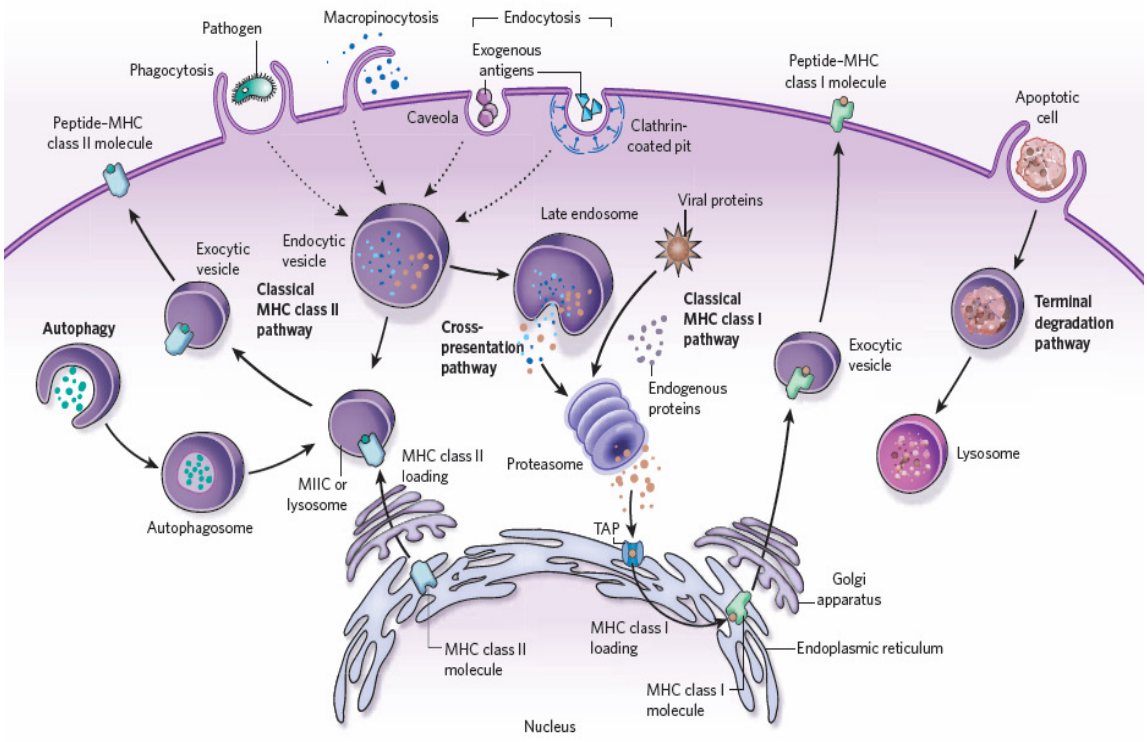

Figure 1.2: Routes of cellular entry. Material can be ingested either by phagocytosis, by specialized cells, or one of various routes of endocytosis. Most routes of endocytosis lead to either acidification or recycling of cargo back to the plasma membrane. Classical routes of antigen processing and presentation, as well as cross-presentation, are also displayed. Figure copied from Hubbell, et. al.[11] Figure reprinted with permission from Macmillan Publishers Ltd: [Nature] (v. **462**, p. 449), copyright (2009)

It is agreed upon, however, that regardless of method of entry, all polyplexes must facilitate endosomal escape to be effective. All endocytic pathways lead to either degradation or recycling back to the membrane, so DNA must be released from intracellular compartment into the cytoplasm before it can enter the nucleus for expression.[7,29,30] Some cationic polymers, such as PEI, are able to facilitate this escape, likely by creating endosomal disruption due to osmotic pressure caused by the 'proton sponge' buffering effect.[7,28-30,37,38] In the 'proton sponge' hypothesis, the hydrogen atoms pumped into the endosome during acidification are absorbed by the polymer, causing continued influx of the chlorine ions used by the cell to maintain electroneutrality. Eventually the resulting increase in osmotic pressure causes disruption of the endosomal membrane facilitating complex release into the cytoplasm (Fig. 1.3). For this reason, polymers such as PEI have been widely used as at least a partial component of many polymer-based delivery systems.[32,33,39] Other methods of facilitating endosomal escape include the use of fusogenic and pore-forming peptides.[29,30] These peptides facilitate endosomal escape by forming pores in the endosomal membrane, either in acidic environments, such as the diphtheria toxin translocation domain or GALA peptides, or neutral pH conditions as in the case of melittin, a component of bee venom.[29,30] There are also several lysomotropic agents available, such as chloroquine, which diminish acidification of, and potentially destabilize, endosomes. However, their use is often associated with toxicity and therefore these agents are not useful for in vivo applications.[7,29]

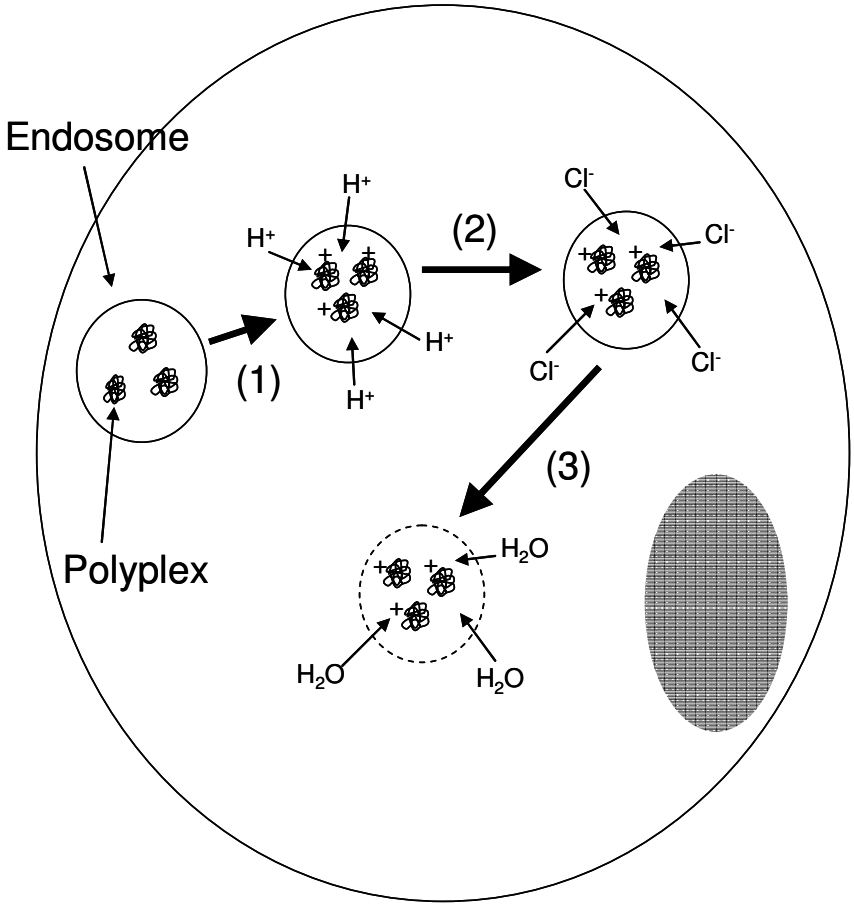

Figure 1.3: Endosomal disruption by 'proton sponge' mechanism. Polymeric material absorbs hydrogen atoms pumped into endosome during acidification (1), leading to a continued influx of chlorine atoms (2). Eventually the endosomal membrane is ruptured due to osmotic pressure (3).

Another significant barrier to transfection is passage into the nucleus. The pores of the nuclear envelope only allow entry to particles about 70 kDa in size, smaller than plasmid DNA.[29] Probably entry is gained only during replication, when the nuclear membrane loses integrity.[29] Some success has been seen using nuclear transport proteins, known as karyopherins or importins, coupled with the DNA. These proteins induce active transport into the nucleus, during which time the pores are expanded, facilitating DNA entry into non-dividing cells.[29,30] Once in the nucleus, it is thought that competition with genomic DNA causes release of plasmid from cationic polymers for expression.[29,30]

1.6. Size

Greater understanding has been obtained recently about the effect of particle size on transfection efficiency. Complexes can be divided into two basic categories, microparticles and nanoparticles, based on the order of magnitude of their size. Nanoparticles are less than 1 μm in diameter. It has been shown that DCs will ingest larger microparticles,[25] mainly through phagocytosis.[22,40] In fact, it may be possible to indirectly target APCs using microparticles between 1 and 10 μm because they are the only cells capable of effective phagocytosis[22] and they have been shown to work with some success.[41,42] However, it has been demonstrated that nanoparticles under 100 nm are taken up more efficiently than larger particles by DCs in vivo,[40,43,44] and particles as small as 20 nm may indirectly target DCs by entering the lymphatic system where a there is a high concentration of these cells.[69,44] Nanoparticles are also advantageous because they are generally distributed better in vivo than their larger counterparts.[40]

1.7. Current Hurdles for DNA Vaccines

DNA vaccination strategies must take into account not only delivery to cells and efficient transfection, but also must ensure antigens are presented properly and appropriate maturation stimuli are received. DCs have various receptors, known as pattern-recognition receptors (PRRs), to detect endogenous signals and foreign materials in order to stimulate an appropriate response.[11] Endogenous signals that lead to the development of adaptive immunity are generally associated with tissue damage and cell stress.[11] Foreign material, generally that associated with various pathogens, is identified primarily through toll-like receptors (TLRs) and can be detected either upon interaction with the plasma membrane or in the endosome after endocytosis. Interaction with DC TLRs, as well as other receptors, plays a role in determining the type of immune response generated. For example, lipopolysaccharide (LPS), a bacterial protein, interacts with TLR4 and has been shown to enhance $CD8^+$ T cell stimulation and the cellular immune response.[11] Therefore it is important to take stimulation, and the location of its corresponding receptor, into account when designing a DNA delivery system. In addition, both the delivered DNA and polymeric material have been shown to be potentially immunostimulatory themselves,[7] which could aid in immune response generation especially if delivered in the appropriate manner.

The delivery route also plays an important role in determining the type of antigen presentation and therefore type of immune response generated. For example, for presentation on MHC class II molecules and humoral immune response generation, antigen would ideally be present in the endosomal compartments of DCs. However, for presentation on MHC class I molecules and cellular immune response generation, antigen

must reach the DC cytoplasm.[11] The target cell for transfection can therefore significantly affect the type of antigen presentation on DCs and therefore type of immune response. Direct transfection of DCs will lead primarily to antigen presentation on MHC class I molecules, while transfection of bystander cells will be followed either by presentation on MHC class II or be dependent on cross-presentation pathways for presentation on MHC class I. Therefore, when designing delivery systems not only must general hurdles for transfection be overcome, but the specific effects on DCs and immune response stimulation must also be considered.

1.8. Thesis Overview

Much work has been done with various polymer formulations and delivery routes to optimize the immune response generated by delivery with these vehicles. However, overall efficiency is generally still low. We have investigated several different methods to improve delivery effectiveness. Chapter 2 focuses on our investigations into the feasibility of using the CD40 ligand (CD40L) as a targeting moiety to deliver DNA directly to DCs. The CD40L is a protein present on T cells that binds to the CD40 receptor on DCs, and is capable of stimulating potent maturation responses. We therefore hypothesized that targeting nanoparticles to DCs using the CD40L would be able to simultaneously enhance uptake and stimulate maturation. We tested this using polystyrene nanoparticles coated with a monomeric CD40L peptide. In Chapter 3 we studied the feasibility of generating a cellular immune response by transfecting bystander cells instead of directly delivering DNA to DCs. To do this we developed an in vitro model system using a NIH 3T3 fibroblast cell line and the DC 2.4 dendritic cell line to

measure antigen cross-presentation after bystander cell transfection. We quantified transfection, MHC class I antigen presentation and maturation on DCs, and T cell response using PEI as the model polymeric delivery system. Finally, we investigated the in vivo interactions of polyplexes made with various cationic polymers in Chapter 4. The local dispersion and cell-specific interactions were quantified for all polymers after intradermal injection and compared to naked DNA. These studies illuminated potential methods of enhancing the effectiveness of DNA delivery using polymer-based delivery systems.

Chapter 2: Recombinant Monomeric CD40 Ligand for Delivering Polymer Particles to Dendritic Cells

SUMMARY: Dendritic cells (DCs) are considered the most efficient antigen-presenting cells and are therefore ideal targets for *in vivo* delivery of antigen for vaccines. We are investigating the strategy of using CD40 ligand (CD40L) as a targeting moiety because this protein has the potential to not only target DCs but also stimulate cell maturation, leading to more potent immune responses. We have shown that a recombinant, monomeric CD40 ligand fusion protein conjugated to polystyrene micro- and nanoparticles led to significantly enhanced uptake by DCs *in vitro*. This enhancement was observed for particles of both sizes and in both a murine DC cell line and primary DCs. The uptake appeared to be specifically mediated by CD40L binding to CD40 expressed on DCs. Enhanced uptake of nanoparticles in draining lymph nodes of mice was not observed, however, 48 hours after subcutaneous injection. These findings suggest that CD40 ligand may be a potentially useful targeting moiety for delivery of particulate vaccines to DCs, and that further optimization of both CD40L and the polymer carriers is necessary to achieve efficacy *in vivo*.

2.1. Introduction

Dendritic cells (DCs) are the most efficient antigen-presenting cells (APCs)[9,10] and play important roles in modulating immune responses. These cells are involved in orchestrating either immune tolerance[14] or various types of antigen-specific immunity that involve both humoral and cellular responses.[4] DCs are also the only APCs capable of generating immunological memory[9] and are instrumental in activities such as directing effector cells to the site of infection and stimulating non-specific (innate) immune responses.[4,9] These capabilities make the DCs an ideal target for immunotherapy. Because of the biological versatility of DCs and their dichotomy in inducing either immune suppression or activation, it is not only important to deliver antigens efficiently to DCs but also crucial to provide appropriate co-stimulatory signals that will ensure the generation of the desired immune response. Under homeostatic conditions DCs are immature. They are highly phagocytic and their primary function is to sample the antigen content in their tissue environment.[10] Once exposed to 'danger signals' such as inflammatory cytokines or pathogenic material such as bacteria and viruses, DCs become mature.[10] The maturation process is characterized by reduced phagocytic activity, increased antigen processing and presentation, and higher expression level of co-stimulatory molecules.[9] Matured DCs also begin to secrete cytokines such as IL-12 and TNF-α, and they migrate from the peripheral tissue to the draining lymph nodes and the spleen, where they engage naïve T cells and B cells to produce antigen-specific immune responses.[9,10] In the absence of phenotypic maturation, however, DCs will instead stimulate the induction of tolerance to the antigen.[14] Therefore, the ideal approach to immunotherapy or vaccination must address two equally important problems: the

delivery of antigens to DCs and the delivery of appropriate stimulatory signals to induce DC maturation.

Synthetic polymer particles are attractive delivery systems for transporting both antigen and maturation signals efficiently to DCs, because the properties of polymer particles can be tuned to maximize the delivery efficiency of a variety of chemical and biological molecules and to achieve DC-specific delivery.[7] Particle size is known to have significant impact on DC uptake and attempts have been made to use size alone as a means for achieving preferential uptake by DCs.[45] Although passive targeting to DCs through controlling particle size is an appealing approach due to its simplicity, it can be technologically challenging to produce particles with precisely defined sub-100-nm size using a wide range of polymer materials and to maintain their size *in vivo*. It is also infeasible to rely only on nonspecific passive targeting by size when sometimes it is more desirable that antigen be delivered to a subset of DCs rather than all DCs.

To promote and enhance specific interactions between polymer particles and DCs, the surface of particles can be decorated with different electric charges or with targeting moieties that are recognized specifically by DCs via cell surface receptors.[10,11] The properties of particle surfaces, particularly surface charge and surface chemistry, are known to affect both DC uptake and maturation. For example, positively charged cationic particles in general have greater initial affinity toward cell surface than negatively charged or neutral particles.[40] Chemical characteristics of particle surface alone have also been demonstrated to affect DC maturation, and some polymers seem able to act as adjuvants on their own more potently than other polymers,[41,46,47] although the stimulation can often be increased with the inclusion of additional adjuvants, either incorporated into

the delivery system itself or injected simultaneously with the vaccine. DC maturation by simple chemical polymers is an intriguing phenomena that involves perhaps pattern recognition by toll-like receptors, but the exact mechanism is yet unknown.[48, 49] A number of DC targeting ligands have been used to modify polymer particles for vaccine delivery. These include mannose,[50] DC-sign,[51] DEC205 antibody,[52] and so on. These previous studies have reported significant enhancement of antigen uptake by DCs through active targeting, but DC maturation could only be achieved by incorporating additional "danger signals", or adjuvants, into the delivery system.

Polymer particles modified by a DC-targeting ligand that can simultaneously provide a strong DC maturation stimulus would be the ideal approach to vaccine delivery, and one molecule with the potential to accomplish this is the CD40 ligand (CD40L). CD40L is transiently expressed on activated $CD4^+$ T-helper cells and its engagement with the CD40 receptor on DCs is important for their complete maturation and transformation into competent antigen-presenting cells.[53] CD40 stimulation by CD40L has been shown to be particularly important in generating CD8 T cell response[54] and is required even in addition to the stimulation by other well-known immunostimulatory adjuvants.[55] CD40L in the form of cDNAs encoding CD40L multimers has been used to enhance the efficacy of DNA vaccines.[56] More often, recombinant CD40L protein has been used to target soluble protein antigens and adenoviral vectors to DCs.[57,58] In the case of CD40L-retargeted viral vector, enhanced transfection and stimulation of DCs *in vitro* and increased immune response *in vivo* have been achieved.[57] CD40L is also the focus of two separate ongoing clinical trials designed to evaluate primarily its potential as an immune adjuvant.

Given that CD40L not only binds DCs specifically via CD40 but also provides an excellent maturation signal, we aim to explore the possibility of using CD40L to enhance the uptake of polymer particles in DCs and to cause DC maturation without the need for additional adjuvant. Here we report the development of a recombinant monomeric murine CD40L fusion protein that can be produced in *E. coli* with high yield. The protein can be easily purified and has high water solubility and stability. We prepared polymer micro- and nanoparticles conjugated with the CD40L, characterized their average size and surface charge, and examined the uptake of these particles in a murine DC cell line (DC2.4) and in primary DCs and their maturation *in vitro*. Finally, we determined the *in vivo* uptake of conjugated nanoparticles by DCs in the draining lymph nodes of mice after subcutaneous injection.

2.2. Experimental Methods

2.2.1. Gene cloning, protein expression and purification.

Two different recombinant plasmids were constructed to allow different methods of protein purification to be used. First, the DNA encoding the extracellular portion of the mouse CD40L was obtained by polymerase chain reaction (PCR) using the full-length CD40L cDNA (American Type Cell Culture, ATCC) as template and the following primers: forward primer, 5'- GCC CTC GAG TCA GAG TTT GAG TAA GCC A - 3' and reverse primer, 5'- GGC AAG CTT GAG GAT CCT CAA ATT GCA G -3'. The PCR product was end-digested, ligated into a pRSF-1b bacterial vector (Novagen), placing a six-histidine repeat at the N-terminus of the CD40L sequence, and transformed into *E. coli* DH5α competent cells (Invitrogen) for amplification. The recombinant

plasmid was isolated using a QIAprep Spin Miniprep Kit (Qiagen) and transformed into BL21(DE3)pLysS competent cells (Invitrogen) for protein expression. These cells were grown in 500 mL Luria-Bertani (LB) media for 4 hours at 37^{o}C and aerated at 210 rpm, at which point protein expression was induced by the addition of isopropyl-β-D-thiogalactopyranoside (IPTG) to a final concentration of 0.5 mM, followed by another four hours of culture. Cell suspension was centrifuged at 4000 rpm for 30 minutes to pellet cells. The pellets were resuspended in 25 mL of buffer A (20 mM Tris, 500 mM NaCl, pH 7.0) containing 1 mM phenylmethylsulfonyl fluoride (PMSF) and 0.1% Tween 20. Cells were then lysed by sonication and centrifuged at 14,000 rpm for 30 minutes to remove cellular debris. The supernatant was loaded onto a Ni-NTA affinity column (Qiagen) with 1-mL bed-volume, washed with buffer A, and the His-tagged CD40L was eluted by three fractions of 1-mL Buffer A containing 300 mM imidazole. The purified protein was characterized by SDS-PAGE and Western blot using an anti-His-tag antibody raised in mouse (Sigma) following standard procedures.

Alternatively, to increase protein yield, the CD40L extracellular domain was expressed as a fusion with an N-terminal maltose-binding protein (MBP). The cDNA of CD40L extracellular domain was amplified by PCR using the following primers: forward primer, 5'- GCC AAG CTT TCA GAG TTT GAG TAA GCC A - 3' and reverse primer, 5'-GGC GAA TTC GAG GAT CCT CAA ATT GCA G - 3'. The PCR product was then inserted into the pMALTM vector (New England Biolabs), transformed into BL21(DE3)pLys cells, and protein expression was induced by IPTG. The harvested cells were resuspended in Phosphate Column Buffer (PCB, containing 77 mM Na_2HPO_4, 23 mM NaH_2PO_4, 250 mM NaCl, 50 mM PMSF), and lysed by sonication. The supernatant

of the lysate was loaded onto a column packed with amylose resin (New England Biolabs). The column was washed with PCB and purified protein was eluted from the column with PCB containing 10 mM maltose. Elution fractions containing the protein were identified using the Bradford assay (BioRad), pooled, and transferred into PCB using Amicon Ultra-4 centrifugal filters (Millipore) to remove maltose. The final protein solution had a concentration of between 1 and 5 mg/mL and was analyzed by SDS-PAGE. MBP alone without the CD40L domain was also expressed and purified using the same method.

2.2.2. Mammalian cell culture.

DC2.4 murine dendritic cell line (ATCC) was maintained in DMEM media (1 mg/mL D-glucose, 2 mM L-glutamine, and 1 mM sodium pyruvate) supplemented with 10% fetal bovine serum (FBS), 100 units/mL penicillin/streptomycin (Pen/Strep), and 10 mM HEPES. Cells were cultured at 37°C and in 5% CO_2. Immature mouse bone-marrow derived dendritic cells (BMDCs) were generated using a method similar to what was reported by Inaba *et al*.[59] Briefly, the femur and tibia were removed from BALB/c mice, cleaned, and soaked in 70% ethanol for one minute. The bones were then washed twice with phosphate buffered saline (PBS) and transferred into RPMI medium (Gibco) supplemented with 10% FCS, 100 U/mL Pen/Step, 2 mM L-glutamine, and 1 mM sodium pyruvate. The bones were cut at both ends and the marrow was flushed out with RPMI media. The cells were filtered through a cell strainer, spun down at 1000 rpm for ten minutes, and resuspended in RPMI media containing 50% ACK lysis buffer (Lonza) for five minutes at 37°C to lyse red blood cells. The cells were then pelleted again by

centrifugation, resuspended in BM media (RPMI media supplemented with 50 mM 2-mercaptoethanol and 1 ng/mL granulocyte macrophage-colony stimulating factor, GM-CSF), and seeded at 5×10^6 cells in 3 mL per well into 6-well plates. On days 2 and 4 of culture most of the cell media was removed and replaced with fresh media. On day 6 the clusters of developing DCs were harvested by vigorous pipetting and centrifugation at 1300 rpm for five minutes. These cells were resuspended in BM media and plated at 1×10^6 cells per well in 6-well plates. Most of the cells attached and spread on the plate surface after approximately two and a half hours, at which point the polymer particle uptake and DC maturation experiments were conducted.

2.2.3. Competitive cell binding assay

The specific binding capacity of recombinant MBP-CD40L to $CD40^+$ DCs was verified by competitive inhibition of anti-CD40 antibody binding to the cells. DC2.4 cells were plated in 6-well plates and treated overnight with 10 µg/mL of lipopolysaccharide (LPS) from *E. coli* strain 0111:B4 (Santa Cruz Biotechnology) to enhance the expression of CD40 to approximately 70% $CD40^+$. The cells were harvested and suspended in 100 µL of FACS buffer (PBS containing 1% BSA and 1 mM sodium azide). The CD40L fusion protein MBP-CD40L was added to the cells at increasing concentrations and incubated for 15 minutes. Then 0.5 µL of a mouse PE-labeled anti-CD40 antibody (BioLegend) was added and incubated for another 20 minutes. Finally, the cells were washed, suspended in 500 µL of FACS buffer for analysis by flow cytometry using a FACSCalibur flow cytometer (Becton Dickson) and the data was processed using Flowjo

software. In parallel the competitive inhibition was tested using the MBP only and buffer (PBS) only.

2.2.4. Protein conjugation to particles

The recombinant protein MBP-CD40L, MBP, and bovine serum albumin (BSA) were covalently conjugated to the surface of polystyrene particles of micrometer and nanometer size. The typical conjugation protocol is as follows. One milligram of protein was transferred into 200 µL of 50 mM MES buffer (pH 6.5) using Centricon centrifugal filters. To the protein solution 50 µL of yellow-green fluorescent carboxylated polystyrene micro or nanoparticles (FluoSpheres, Molecular Probes, 1 µm and 100 nm in diameter) were added and mixed in a low protein-absorbing glass reaction tube. *N*-ethyl-*N'*-(3-dimethylaminopropyl)carbodiimide (EDC, 0.01 M) was then added and the reaction mixture was incubated at room temperature for two hours with constant mixing. To purify polymer particles from any unreacted protein and reaction byproducts, the microparticles were centrifuged at 7000 rpm for 5 minutes to pellet and resuspended in PBS. This step was repeated two more times, and the last resuspension was in 500 µL of PBS containing 1% BSA, in order to block any unreacted sites on the microparticles. To purify protein-conjugated nanoparticles, the reaction mixture was diluted with 200 µL of PBS and dialyzed against PBS using membrane with molecular-weight-cut-off of 300 Da (Spectrum Laboratories). The dialysis lasted two hours at room temperature with one buffer change and continued against PBS containing 1% BSA overnight at 4°C. Both purified micro and nanoparticles were stored at 4°C.

2.2.5. Particle characterization

The average size of particles was measured by dynamic light scattering using a 90Plus Particle Size Analyzer (Brookhaven Instruments) at 1 μg/mL particle concentration in PBS. Zeta-potential of the particles was determined using a Zeta-sizer (Brookhaven Instruments). The efficiency of protein conjugation to the polymer particles was estimated by determining, using gel electrophoresis, the reduction in protein concentration in solution before and after conjugation.

2.2.6. In vitro particle uptake

DC2.4 cells or BMDCs were seeded in 6-well plates at 1×10^6 cells per well. Micro or nanoparticles (30 μg) conjugated with MBP-CD40L, MBP, or BSA, were added separately to the cells and incubated for one hour at 37°C. The cells were washed three times with cold PBS to remove excess unbound particles. For flow cytometry analysis cells were removed from plates using trypsin-EDTA and the particle fluorescence was analyzed using a FACSCalibur flow cytometer (Becton Dickson) and the data was processed using Flowjo software. For confocal fluorescence microscopy analysis cells were stained for one hour with 50 μg/mL of Alexa Fluor 594-labeled concanavalin A (Molecular Probes) to visualize cell membrane, washed with PBS, and analyzed using a Bio-Rad MRC 1000 laser on an upright microscope equipped with a Nikon Optiphot camera. Image analysis was conducted using Bio-Rad Laser Sharp 3.0 and Image J software.

2.2.7. In vitro DC maturation

Immature BMDCs were prepared from murine bone marrow as described above and plated on day 6 in 6-well plates 1×10^6 cells per well. These cells were incubated with either 10 μg protein per well, 10^6 nanoparticles per well, or 2 ng/mL LPS as a positive control, for 24 hours. Cells were then removed from the plates using trypsin, resuspended in 100 μL FACS buffer (PBS containing 1% BSA and 0.01% sodium azide), and analyzed by flow cytometry. Cells were stained with either PE-labeled anti-CD40, PE-Cy5 labeled anti-CD80, PE-Cy5 labeled CD86. All cell samples were stained with APC-labeled CD11c antibody as a DC identification marker.

2.2.8. In vivo nanoparticle uptake

The housing and use of mice were conducted in accordance with guidelines from the University of Minnesota Institutional Animal Care and Use Committee. Protein conjugated nanoparticles were suspended in sterile PBS containing 1% BSA, and aliquots of 50 μL of this particle suspension were injected subcutaneously into three sites on BALB/c mice (Jackson Labs): the back of the neck and near both shoulders. After 48 hours the mice were sacrificed and the auxiliary and cervical lymph nodes were harvested. Single cell suspension was prepared by collagenase digestion. DCs were purified from the total cell population by Magnetically Activated Cell Sorting (MACS) using anti-CD11c magnetic microbeads and a MACS magnetic column (Miltenyi Biotec). Purified cells were stained with APC-labeled anti-CD11c antibody and analyzed by flow cytometry.

2.3. Results and Discussion

2.3.1. Protein expression

The gene sequence for the receptor binding region of the extracellular domain of CD40L was obtained from cDNA and amplified by PCR. The protein was expressed first with an N-terminal His-tag in *E. coli* BL21 (DE3)pLysS and purified from total cell lysate by metal affinity chromatography. The purified His-tagged protein migrated as a single band on a Coomasie-stained SDS-PAGE gel with an apparent molecular weight of approximately 18 kDa and was recognized by a His-tag antibody (data not shown). However, the yield of the protein was low, which is possibly due to poor solubility of the protein in water, and not sufficient for conjugation to polymer particles. Therefore, the CD40L domain was expressed as a fusion protein with MBP, a widely used strategy for enhancing solubility and promoting stable folding of recombinant proteins.[59] The MBP tag was positioned at the N-terminus of CD40L, leaving the C-terminal domain free to bind CD40 on DCs. After inducing expression with IPTG, a large amount of the fusion protein, MBP-CD40L, was produced by *E. coli*, as shown by the thick band present among the total soluble proteins of the bacteria (Fig. 2.1). The expression of MBP-CD40L was tightly controlled because its level was undetectable without IPTG induction. A single step of purification by affinity chromatography with an amylose column yielded the protein with good purity. Bacteria transformed with the empty vector, pMALTM, were induced to over-express MBP only, which was also purified with the amylose column. The apparent molecular weight of the two proteins run on a SDS-PAGE gel agreed well with the theoretical molecular weight of the proteins, that is, ~68 kDa (MBP-CD40L), ~50 kDa (MBP), ~18 kDa (CD40L extracellular receptor-binding domain).

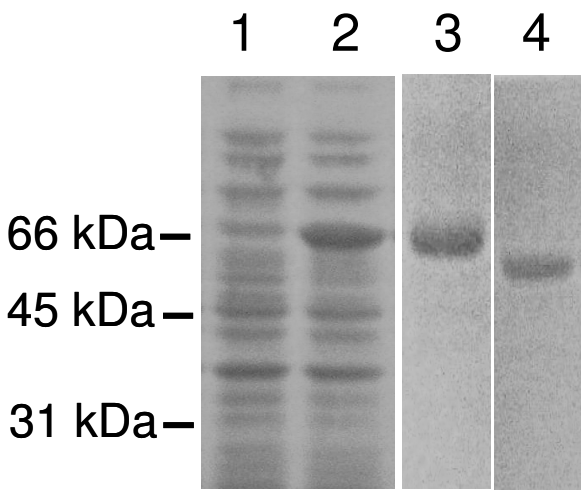

Figure 2.1. Expression and purification of recombinant monomeric CD40 ligand from E. coli. CD40L was expressed as a MBP fusion and purified by amylose resin with high yield. Lane 1: total cell lysate without induction; lane 2: total cell lysate induced by IPTG; lane 3, purified MBP-CD40L; lane 4: purified MBP control protein.

2.3.2. Evaluation of protein binding to CD40 receptor

In order to determine whether MBP-CD40L was able to bind to the CD40 receptor, we did a competition experiment using a fluorescently labeled murine anti-CD40 antibody, which binds very well to $CD40^+$ DCs. If the MBP-CD40L was also specifically binding to CD40 on DCs, then the antibody binding should be inhibited depending on the concentration of the competing MBP-CD40L. To this end, DC2.4 murine dendritic cells, which have intermediate CD40 expression levels (Fig. 2.2A), were pre-incubated with either MBP-CD40L or MBP proteins before being stained with a fluorescent anti-CD40 antibody. Flow cytometry analysis revealed a decrease in the level of anti-CD40 antibody bound to cells in the presence of MBP-CD40L protein, which was also concentration dependent, whereas MBP only had so such inhibitory effect (Fig. 2.2B). This suggests that the MBP-CD40L protein binds to CD40 receptor specifically, rendering them unavailable for anti-CD40 antibodies. Based on these results, the apparent binding constant (K_d) of the MBP-CD40L was estimated to be 0.11 mM, which is lower than the values reported for full-length CD40L or multimeric CD40L.[60] This can be explained by the fact that the CD40L reported here is monomeric and that the large hydrophilic MBP tag might affect receptor binding due to steric effect. Nonetheless, our results clearly confirm that the recombinant MBP-CD40L is capable of binding to $CD40^+$ DCs specifically.

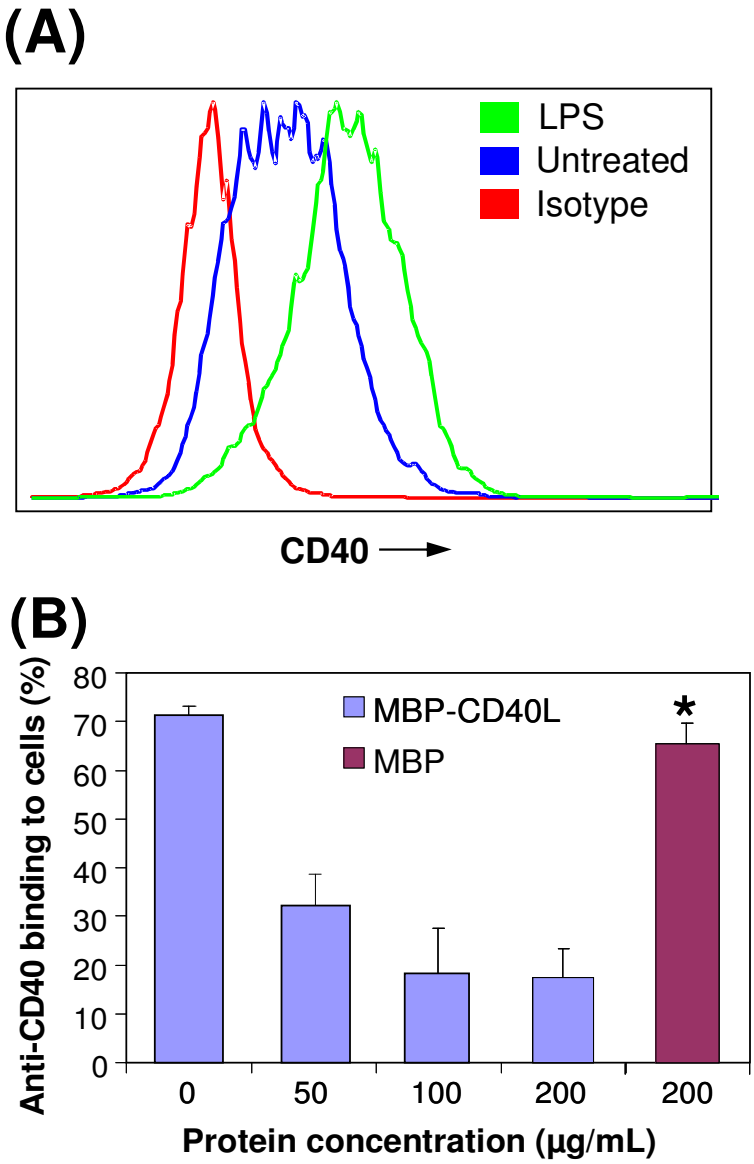

Figure 2.2. MBP-CD40L binds to CD40$^+$ dendritic cells specifically. (A) DC2.4 cells are CD40$^+$ and the CD40 level can be further elevated by LPS treatment. (B) Competitive binding of CD40$^+$ DC2.4 cells showing dose dependence and specificity of MBP-CD40L. DC2.4 cells were incubated with MBP-CD40L at increasing concentrations (50, 100, or 200 µg/mL), or MBP (200 µg/mL) alone, for 15 minutes before incubation with anti-CD40 antibodies. Anti-CD40 antibody binding was analyzed by flow cytometry.

2.3.3. Size and surface charge characterization of polymer particles

The recombinant MBP-CD40L could serve as an ideal ligand for vaccine targeting, due to its ability of binding to $CD40^+$ DCs. Therefore, we evaluated the protein's ability to facilitate DC uptake of polymeric particles by conjugating chemically the MBP-CD40L protein to fluorescent, carboxylated, polystyrene micro- and nanoparticles using carbodiimide chemistry. Additionally, MBP alone was conjugated the same way to demonstrate receptor specificity of cellular uptake. Furthermore, bovine serum albumin (BSA) conjugated particles were also prepared as an additional control to minimize potential nonspecific interactions between cells and polystyrene particles after serum protein adsorption onto the particle surface. It is known that both particle size and surface charge may influence uptake by cells.[11,40,46] For example, microparticles of 1 to 10 μm in size may be able to target DCs passively simply because the uptake by other non-phagocytic cells is much more limited.[11,45] It has been shown that DCs do ingest readily particles of this size range, and microparticles made from degradable and non-degradable polymers have been used to deliver antigens with some success in producing immune responses *in vivo*.[11,47,51] However, it has been demonstrated that nanoparticles under 100 nm are taken up by DCs more efficiently than microparticles *in vivo*,[11,44,48] due to better transport of small particles through tissues and that nanoparticles as small as 20 nm may be particularly capable of reaching resident DCs in the lymph nodes by entering the lymphatic system, rather than being retained at the peripheral tissues. As for the effect of surface charge, cationic particles appear to greatly enhance DC uptake over negatively charged or neutral particles during the initial few hours, although a study on smaller 100 nm particles demonstrated that charge may be not as important at later time points.[10]

Positive surface charge also increases the risk of non-specific tissue interactions *in vivo* due to uncontrollable adsorption of proteins.

To this end, micro and nanoparticles conjugated with the proteins (MBP-CD40L, MBP, BSA) were characterized in terms of their average size by dynamic light scattering and their zeta-potential or surface charge was also determined. Both the average particle size and surface charge varied only slightly depending on the protein that was conjugated. The average size of the microparticles was 1~3 μm with zeta-potential of -24~-44 mV. The average size of the nanoparticles ranges from 126 to 220 nm with zeta-potential of -22~-28 mV. Therefore, regardless of what protein was conjugated, all the microparticles and nanoparticles had similar average size and negative surface charge, which are not expected to influence cellular uptake substantially.

2.3.4. Targeted delivery of polymer particles to dendritic cells in vitro

DC 2.4 cells were incubated with conjugated microparticles (Fig. 2.3) and nanoparticles (Fig. 2.4) for one hour and then analyzed with flow cytometry and confocal fluorescence microscopy. Both particle sizes are taken up more efficiently by DCs when conjugated to the MBP-CD40L than when conjugated to control proteins of MBP alone and BSA. Since we have demonstrated that the MBP-CD40L protein binds to CD40 receptor specifically (Fig. 2.2), it is likely that the enhanced uptake of particles is also mediated through this interaction. Confocal microscopy analysis suggests that both the micro and nanoparticles are internalized by the DCs and are not simply attached to the outer cell membrane (Fig. 2.3B and 2.4B). All nanoparticles were taken up more efficiently than microparticles, which is in agreement with previous studies.[51]

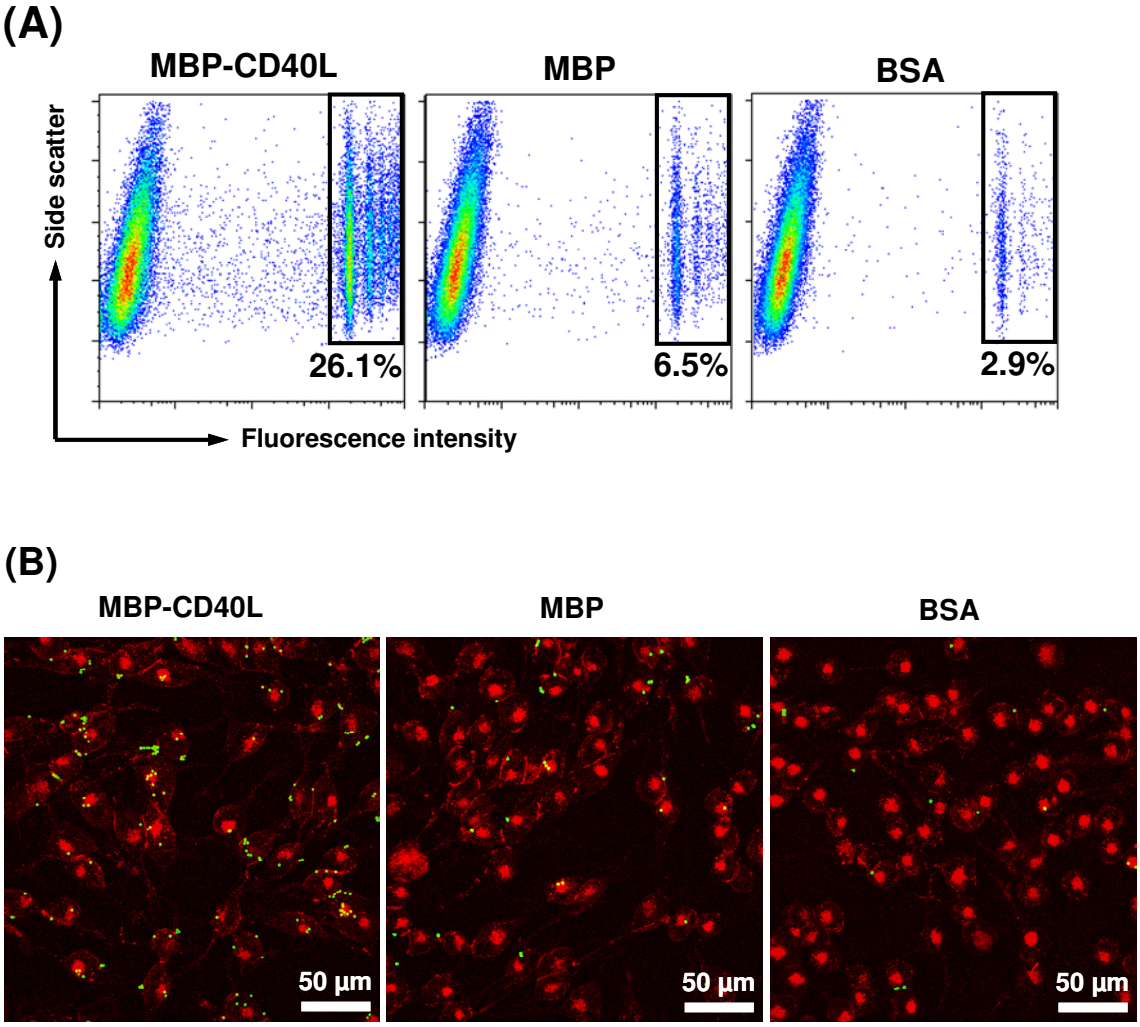

Figure 2.3. MBP-CD40L mediates enhanced uptake of microparticles in DC2.4 cells. Cells were incubated with polystyrene microparticles conjugated to either MBP-CD40L, MBP, or BSA. Microparticles conjugated to MBP-CD40L were taken up more effectively by the cells as determined by (A) flow cytometry and (B) confocal fluorescence microscopy. Confocal images show the middle plane of cells along the z-direction, indicating that many of the particles seen have been internalized. Scale bar: 50 µm.

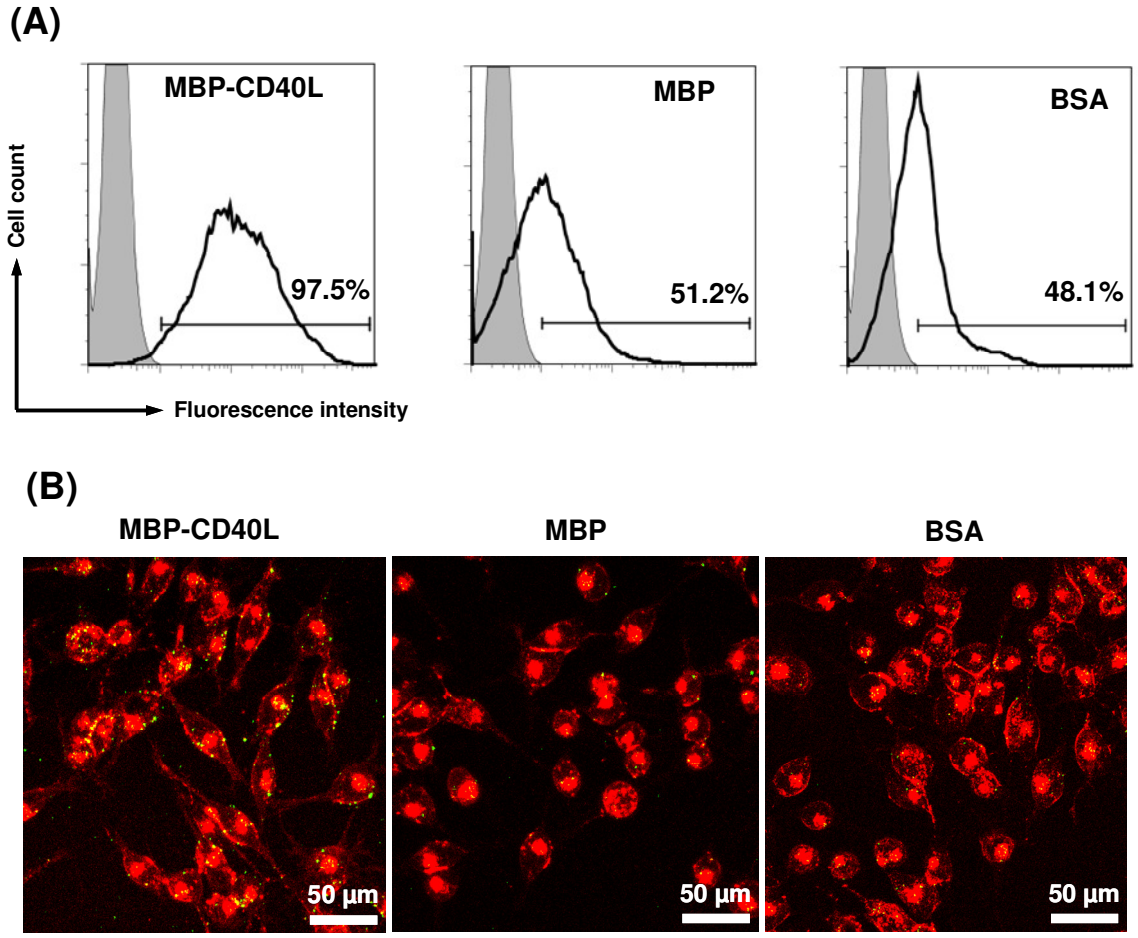

Figure 2.4. MBP-CD40L mediates enhanced uptake of nanoparticles in DC2.4 cells. Cells were incubated with polystyrene nanoparticles conjugated to either MBP-CD40L, MBP, or BSA. Nanoparticles conjugated to MBP-CD40L were taken up more effectively by the cells as determined by (A) flow cytometry and (B) confocal fluorescence microscopy. Confocal images show the middle plane of cells along the z-direction, indicating that many of the particles seen have been internalized. Scale bar: 50 µm.

Next, we focused on the protein-conjugated nanoparticles because of their potential in *in vivo* application (due to their much smaller size than the microparticles). We investigated the uptake of protein-conjugated nanoparticles by primary mouse dendritic cells derived from the bone marrow, BMDCs, and the effect on their maturation state. After one hour of incubation with immature BMDCs in culture, the uptake of particles were analyzed using flow cytometry and the maturation state of the cells was examined in terms of its level of CD40 expression. Similar to what was observed in the DC2.4 cells, BMDCs demonstrated preferential uptake of particles conjugated to MBP-CD40L compared to MBP and BSA conjugated particles (Fig. 2.5A). On the other hand, BMDCs incubated with MBP-CD40L proteins, either free or conjugated to polystyrene nanoparticles, did not show any up-regulation in CD40 level (Fig. 2.5B). The lack of DC stimulatory ability of the MBP-CD40L might be related to its apparent monomeric nature due to the bulky MBP fusion tag impeding sterically the multimerization of CD40-bound CD40L. The CD40L is naturally trimeric and DC stimulation is dependent its ability to cross-link the DC receptor.[53] It has been demonstrated that trimeric and multimeric formulations of the CD40L protein both bind more strongly to the CD40 receptor and provide stronger immune activating stimulus in B cells.[61,62] There are two major implications of the current finding that the MBP-CD40L is capable of promoting cellular uptake without causing the cells to become mature. First, the MBP-CD40L would be perfect for use in *ex vivo* DC therapy where the key issue is to load DCs cultured *in vitro* with particulate vaccines of the highest possible quantities.[63] After antigen loading, maturation of the DCs can then be initiated by adding additional adjuvants such as TLR-ligands. Second, because the recombinant CD40L lacks the DC stimulation function of

the wild-type protein, it could serve as an ideal DC targeting ligand for inducing tolerance toward particulate antigens in the treatment of allergic reactions and autoimmune diseases.

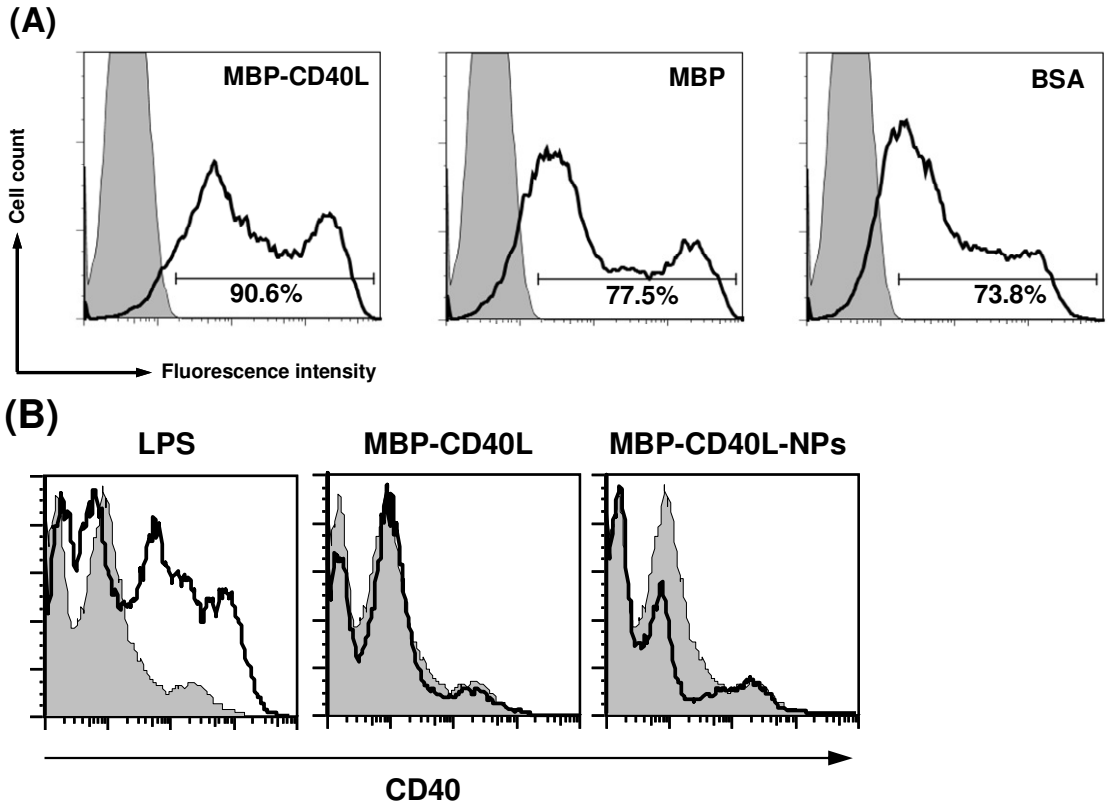

Figure 2.5. MBP-CD40L mediates enhanced uptake of nanoparticles in BMDCs (A) and do not alter the level of CD40 expression by the BMDCs before and after nanoparticle uptake (B). Polystyrene nanoparticles conjugated to either MBP-CD40L, MBP, or BSA were incubated with BMDCs on day 6 of culture and fluorescence of nanoparticles and CD40 was analyzed by flow cytometry.

2.3.5. Uptake of conjugated nanoparticles by dendritic cells in vivo

Since polymer particles, particularly nanoparticles, conjugated to MBP-CD40L, are taken up efficiently by both a DC cell line and primary DCs *in vitro*, we performed experiments to determine if the same effect could be achieved *in vivo*. Nanoparticles conjugated with MBP-CD40L and control proteins were injected subcutaneously into mice and DCs in the draining lymph nodes were analyzed 48 hours later. The experiment was conducted with nanoparticles rather than microparticles because we had previously found that the smaller particles were taken up at a higher rate by DCs in mouse lymph nodes at 24 and 48 hour time points (data not shown). To our surprise, nanoparticles conjugated to the MBP-CD40L were not taken up more efficiently *in vivo* than particles conjugated to control proteins (Fig. 2.6). In fact, MBP-CD40L conjugated nanoparticles are consistently the least capable of reaching DCs in the draining lymph nodes, with BSA coating particles being consistently the best. There could be several factors contributing to this finding. The stability of the conjugated nanoparticles in the biological milieu is not clear. Interaction with blood components might have altered the surface properties of the particles and caused different degrees of agglomeration to affect DC uptake. Polystyrene is known to be highly attractive to serum protein adsorption, in particular, fibrinogen adsorption.[64] BSA modification might have passivated the surface and reduced nonspecific adsorption of proteins. Another possibility is that some epithelial cells may express CD40 receptor[53] that could bind to CD40L coated nanoparticles, trapping them before they could have the opportunity of reaching the lymph nodes and binding to DCs. The elucidation of these *in vivo* mechanisms will require further study in the future. In summary, the *in vivo* uptake study reported here underscores the challenge of achieving

cell-specific targeting in the complex physiological environment, and it emphasizes the importance of careful optimization of physico-chemical and biological properties of the polymer particle surface.

CD40L has shown considerable promise as an immune modulator, primarily as an adjuvant to augment immunotherapy against cancer. In one early phase clinical study, injection of a recombinant human trimeric CD40L protein has shown some success in cancer patients, presumably due to enhanced immune response.[65] A separate trial demonstrated that injection of bystander cells genetically modified to express CD40L and produce GM-CSF, a molecule linked to DC recruitment and differentiation, along with radiated autologous tumor cells, was able to induce T-cell responses to tumor antigens and recruitment of activated DCs to tumor site in some cancer patients.[66] The trimeric protein appeared to induce some dose-dependent liver toxicity, while the CD40L-expressing bystander cells did not appear to have any significant negative effect. Both therapies are currently undergoing phase II clinical trials. The recombinant monomeric MBP-CD40L described here may also be further developed for stimulating immune responses, particular for use in *ex vivo* DC therapy. In this case, it is highly advantageous to achieve enhanced uptake of antigen in DCs, as shown in this study. The ability of induce DC maturation, however, will need to be improved, perhaps by incorporating a trimeric CD40L domain instead. On the other hand, the lack of DC maturation bodes well for the MBP-CD40L to be used to induce immune tolerance, and may find applications in combating autoimmune diseases, preventing allergies, and ameliorating immune rejection of transplants.

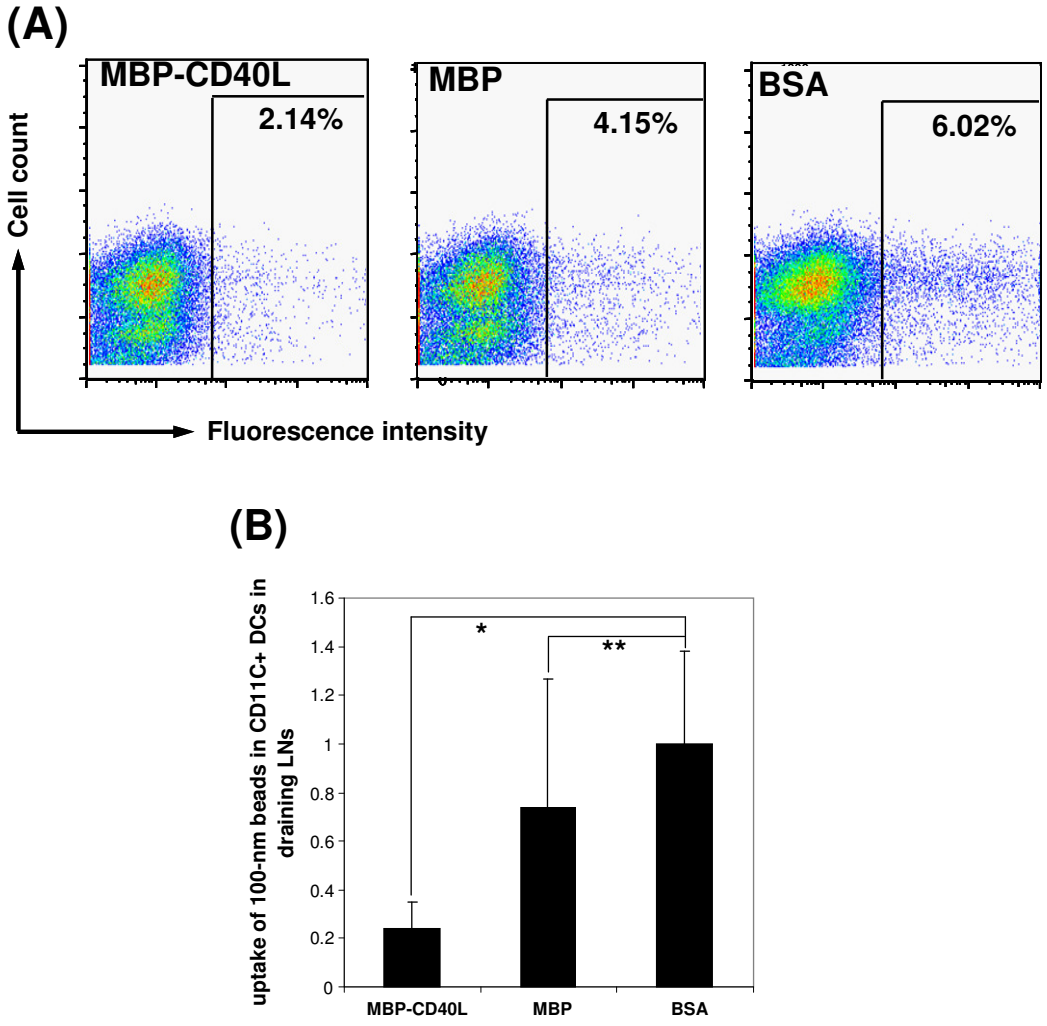

Figure 2.6. MBP-CD40L does not enhance DC uptake of nanoparticles in vivo. BALB/c mice were injected subcutaneously with polystyrene nanoparticles conjugated to either MBP-CD40L, MBP, or BSA. CD11c+ DCs were isolated from draining lymph nodes and analyzed for nanoparticle fluorescence by flow cytometry. Nanoparticles conjugated to MBP-CD40L did not show increased uptake when compared to particles conjugated to control proteins. (A) Histogram of flow cytometry analysis of uptake in a typical mouse group. (B) Collective representation of uptake in CD11c+ DCs in the draining lymph nodes of 3 mice per experimental group. * $p<0.05$, **$p>0.05$, student t test.

2.4. Conclusions

We have developed a recombinant fusion protein containing the CD40-binding domain of mouse CD40L. The protein is able to bind to DCs and mediate enhanced uptake of polymeric micro and nanoparticles *in vitro* without affecting the maturation state of the cells. This effect is seen both in a dendritic cell line (DC2.4) as well as in primary DCs derived from the bone marrow. However, enhanced uptake of nanoparticles conjugated with MBP-CD40L was not observed in mice after subcutaneous injection. This study suggests that the monomeric MBP-CD40L protein could be useful in targeting DCs for *ex vivo* immunotherapy and in inducing tolerance of antigens. It also underscores the challenge and importance in optimizing nanoparticle properties and protein-based ligands to achieve DC targeting *in vivo*.

Chapter 3. Polymer-Mediated DNA Vaccine Delivery via Bystander Cells Requires a Proper Balance between Transfection Efficiency and Cytotoxicity

SUMMARY: Direct targeting of dendritic cells is an ideal goal for DNA vaccine delivery in order to stimulate both arms of the immune system. However, dendritic cells are often difficult to transfect using nonviral polyplexes. Here we show that transfecting bystander cells such as fibroblasts with PEI/DNA complexes leads to efficient cross-presentation of a model antigen by dendritic cells and subsequent activation of antigen-specific $CD8^+$ T cells. Maturation of dendritic cells is also stimulated after co-culture with transfected fibroblasts. Such outcomes depend on a proper balance between transfection efficiency and polyplex-induced cytotoxicity in the fibroblasts. In fact, substantial cytotoxicity is desirable and even necessary for cross-presentation and cross-priming of T cells. This study illustrates a new pathway of polymer-based DNA vaccine delivery via bystander cells without direct targeting of antigen-presenting cells.

3.1. Introduction

Dendritic cells (DCs) are considered the most important antigen-presenting cells and play a central role in modulating immune responses. They are a very attractive target for DNA vaccine delivery because they are able to present antigen on both MHC class I and II molecules for generation of cellular and humoral immune responses. The classical antigen processing pathways lead to MHC class II presentation and a humoral immune response from exogenously obtained antigen, characterized by $CD4^+$ T cell stimulation and antibody production. In the case of directly transfected DCs, endogenously expressed proteins are processed through the MHC class I pathway, leading to cellular immune response, characterized by $CD8^+$ T cell activation and cytotoxic T lymphocyte (CTL) generation.[10] The CTL response is essential to the defense against viral infections and cancer.[67] Therefore, targeting DNA vaccine to DCs using properly designed carriers and achieving direct transfection of DCs has been widely accepted to be crucial for the generation of cellular immunity.

Many methods have been explored to efficiently deliver antigen to dendritic cells, including manipulation of carrier size,[43] targeting of the carrier,[52,68,69] or targeting of the antigen itself.[70] Many of these methods have resulted in some increased immune response, confirming that delivery of antigen to DCs is important. Many studies suggested that for DNA vaccine, direct transfection of DCs that leads to antigen expression in these cells is indeed a very effective vaccination pathway. Hattori et al. were able to directly demonstrate enhanced in vivo DC transfection using mannose-targeted liposomes,[68,71,72] leading to some enhancement in T cell stimulation. Intradermal transfection with a DC-restricted expression plasmid also showed enhanced $CD8^+$ T cell

stimulation when compared to a keratinocyte-restricted plasmid.[73] Unfortunately, DCs remain difficult to target directly because of their relative rarity in vivo.[10] In addition, DCs as well as other APCs, are notoriously difficult to transfect, especially by nonviral vectors. It is possible that they have enhanced protection against nuclear entry by foreign nucleic acids due to their functional role of pathogen uptake and processing.[7] Even when DC tranfection in vivo is observed, the level is usually very low. Hattori et al, for example, was only able to detect transfection through transcriptional amplification by RT-PCR.[68,71,72] Using cationic polymer carriers, Jilek et. al. reported a very low frequency of DC transfection of one per 10,000 cells.[74]

An alternative pathway does exist for generating $CD8^+$ T cell responses through DNA vaccination without directly transfecting DCs. It has been well documented that DCs can present exogenous antigen on MHC class I molecules in a process known as cross-presentation. The subsequent stimulation of $CD8^+$ T cells is known as cross-priming.[67, 75] Cross-presentation is a pathway distinctly different from endogenous MHC class I peptide loading[76] and is regulated, at least in part, by the transporter associated with antigen processing (TAP) protein.[67,76] Antigen from various sources has been efficiently cross-presented, including soluble protein at high concentrations, protein or peptide associated with particles, as well as protein and peptide from autologous cells.[67] Also, a particularly effective way of delivering antigen to DCs for cross-presentation is to have it ingested through damaged and dying cells.[67,77,78] Therefore, if DNA vaccination results in some antigen expression by cells other than DCs, it can still contribute to the overall immune response through cross-presentation and cross-priming.

While most DNA vaccination studies do not differentiate between direct and cross-primed responses, there is evidence that the cross-presentation pathway alone may have been sufficient. For example, it was reported that when antigen expression is limited only to muscle cells, cross-presentation can generate CTL responses.[79,80] Cho et al. determined that CTL responses were generated more effectively when expression of plasmid DNA delivered by gene gun was under the control of a nonspecific CMV or K14 promoter. When expression was controlled by a APC-specific CD11b or MHC II promoter, both Ab and CTL responses were weakened, suggesting that cross-presentation, rather than direct transfection of DCs, could be the primary mechanism for immune response generated by DNA vaccination.[81,82] In the case of polymer-based DNA vaccine delivery, it has been speculated that cross-presentation may be important.[83-85] However, cross-presentation and its importance in generating cellular immune response by polymer-delivered DNA vaccine have not been evaluated. Furthermore, how polymer carrier design might affect cross-presentation and cross-priming is not known.

Here we developed a co-culture system to test the hypothesis that polymer-mediated transfection of non-DCs, or bystander cells, can be sufficient in generating MHC class I restricted antigen presentation on DCs and subsequent $CD8^+$ T cell stimulation. To mimic the in vivo situation typical of vaccination and immune activation, our co-culture system consists of bystander cells (fibroblasts), DCs, and naïve $CD8^+$ T cells mixed sequentially and cultured for certain periods of time (Fig. 3.1). The bystander cells were transfected by complexes of polyethylenimine (PEI) and plasmid DNA encoding a model antigen, ovalbumin (OVA), and OVA-specific $CD8^+$ T cell activation was quantified. Since cell death is known to have significant impact on cross-presentation, we further investigated

the relationship between polymer-mediated transfection efficiency and cytotoxicity in bystander cells, in order to determine how antigen-presentation and DC maturation can be optimized.

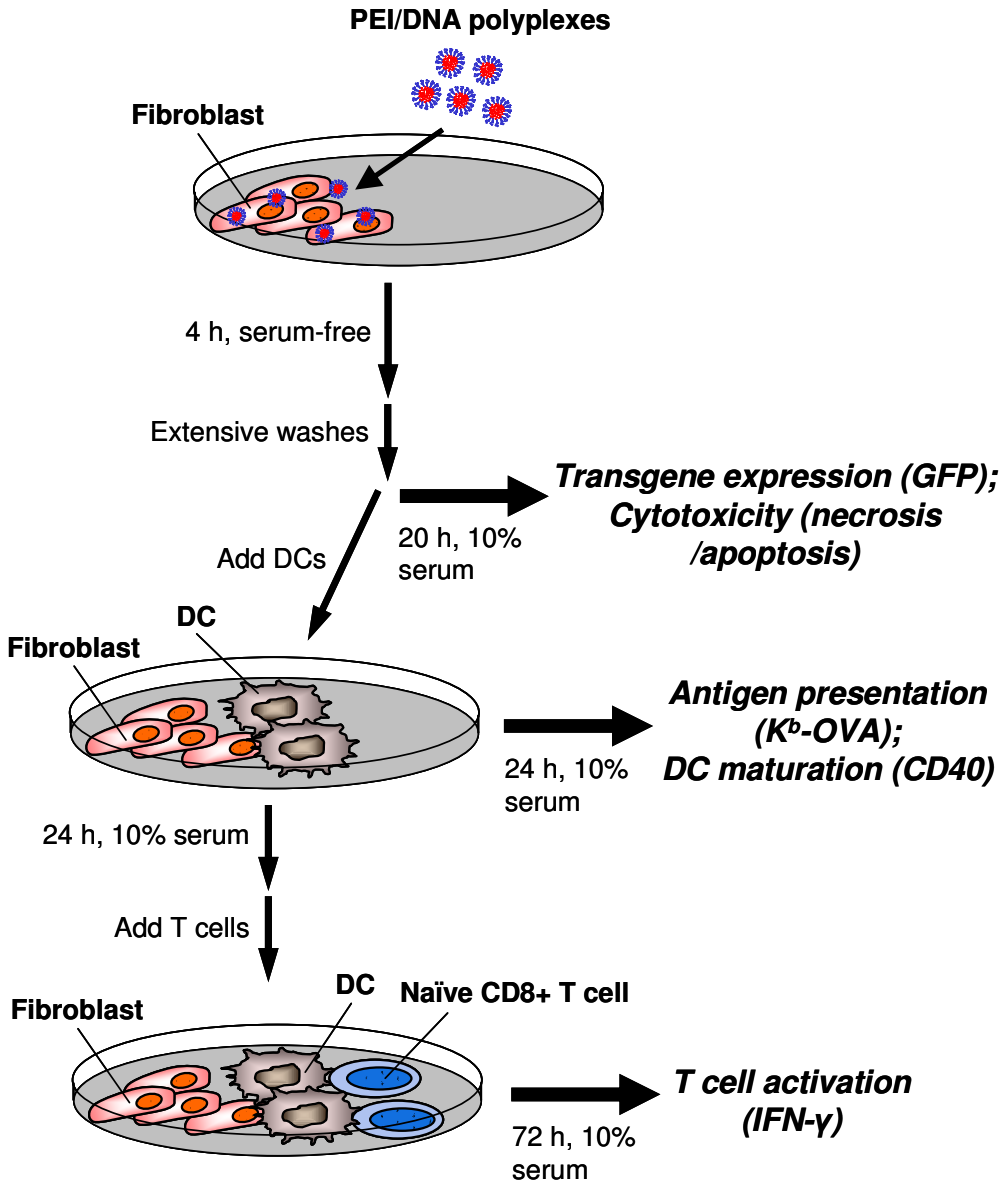

Figure 3.1. Experimental Design. NIH 3T3 fibroblast cells are transfected with polyplexes and then either analyzed or co-cultured with DC 2.4 cells. Cells are then analyzed for antigen presentation or cultured for an additional 3 days with antigen-specific $CD8^+$ T cells.

3.2. Experimental Methods

3.2.1 Cell Culture

NIH 3T3 murine fibroblast cell line was cultured in DMEM (1 g/L D-glucose, L-glutamine, 110 mg/L sodium pyruvate, Gibco) media supplemented with 10% fetal bovine serum (FBS, heat inactivated, Gibco) and 100 units/mL penicillin/streptomycin (Gibco). The DC 2.4 murine dendritic cell line (ATCC, provided by Dr. John Ohlfest) was maintained in the same media without additional glucose but also supplemented with 10 mM 4-(2-hydroxyethyl)-1-piperazineethanesulfonic acid (HEPES) buffer. Mouse $CD8^+$ T cells were cultured in RPMI medium (Gibco) supplemented with 10% FBS, 100 U/mL penicillin/streptomycin, 2 mM L-glutamine, and 1 mM sodium pyruvate). All cells were incubated at 37°C in 5% CO_2.

3.2.2 Preparation of PEI/DNA Polyplexes

Polyplexes were prepared using PEI (branched, 25 kDa, Sigma) and plasmid DNA in 20 mM HEPES buffer. PEI and DNA solutions were both diluted to 0.1 mg/mL in 20 mM HEPES, mixed in equal volumes to a total of 100 µL, vortexed briefly, and allowed to incubate at room temperature for 30 minutes prior to use. For transfection experiments polyplexes were prepared with a plasmid encoding enhanced green fluorescent protein (GFP) (pEGFP-N1, Elim Biopharmaceuticals). A plasmid encoding the luciferase gene (pCMV-Luc, Elim Biopharmaceuticals) was used for toxicity studies and as a no-antigen control. For antigen presentation and maturation studies, a plasmid encoding the full-length chicken OVA and a CMV promoter was used (Clontech). The plasmids were either purchased from Elim Biopharmaceuticals with high purity and free of endotoxin,

or were amplified in *E .coli* DH5α cells and purified using an Endo-free MAXI plasmid purification kit (Qiagen). Purity and quantity of DNA was verified by UV absorbance at 260 and 280 nm, and endotoxin level was verified to be below 3 EU/mg using a Pyrogent Gel Clot LAL assay (Lonza).

3.2.3 Transfection of Bystander Cells

NIH 3T3 cells were plated at 5 x 10^4 cells/well in 6-well plates and allowed to adhere overnight. The cell media was replaced by serum-free media and polyplexes of GFP plasmid were added and allowed to incubate for 4 hours. Four µg of DNA was added per well in 6-well plates. The amount of polymer was varied based on the N/P ratio used (4, 8, 12, 16, 20). For some experiments to reduce cell death, the caspase inhibitor Z-VAD FMK (vendor?) was added to cells at 50 µM 30 minutes prior to adding polymer complexes. After transfection, cells were washed three times with phosphate buffered saline (PBS, pH 7.4) and replaced with media containing 10% serum. Twenty-four hours after initial addition of polyplexes cells were harvested by trypsinization and suspended in FACS buffer (PBS, 1% BSA, 1 mM sodium azide) and analyzed directly by flow cytometry. Samples were run on either a FACSCalibur or LSR II flow cytometer (Becton Dickson) and analysis was done using FlowJo software. GFP-positive cells were gated against a sample transfected with luciferase-encoding DNA using the same transfection procedure to control for any increased autofluorescence of cells caused by polyplexes nonspecifically.

3.2.4 Toxicity in Bystander Cells

NIH 3T3 cells were prepared and treated with polyplex as stated above for transfection experiments. Polyplexes were made with luciferase-encoding plasmid instead of GFP plasmid to avoid GFP signal overlap with cytotoxicity detection. N/P ratios of 4, 8, 12, 16, 20 were tested. In some cell samples labeled "N/P=8x2", fibroblasts were transfected with one dose of polyplex containing Luc plasmid plus an equal dose of polyplexes containing OVA plasmid. The polyplex dose was therefore doubled while the amount of antigen-encoding DNA delivered remained constant. The purpose of this was to increase polyplex-induced toxicity without affecting antigen expression. After the 24 hr incubation, cells were harvested, tryspinized, and washed once with 1 mL of Annexin V staining buffer (BioLegend). Cells were then resuspended in 100 µL of Annexin V staining buffer and stained with Alexa Fluor 647-labeled Annexin V (BioLegend) and propidium iodide (PI) (BioLegend), followed by analysis by flow cytometry.

3.2.5 Antigen Presentation and Maturation

NIH 3T3 cells were cultured at 2.5 x 10^4 per well in 12-well plates and allowed to adhere overnight. Cells were incubated with polyplexes of OVA DNA for 4 hours in serum free media as described in the transfection experiments. Two µg of DNA was per well. Afterwards, the fibroblasts were washed three times with 1 mL of PBS, and DC 2.4 cells were added to each well at 1 x 10^5/well. All the cells were cultured in media containing 10% serum for another 24 hrs and then harvested by trypsinization, resuspended in FACS buffer, and stained with PE-labeled anti-mouse OVA-K^b antibody (e-Biosciences) and APC-labeled anti-murine CD40 antibody (BioLegend). Cells were

washed once with 1 mL of FACS buffer and analyzed using flow cytometry. The OVA-K^b antibody recognizes MHC class I-restricted SIINFEKL, an OVA-derived peptide. Fibroblasts were gated out using forward and side scatter profiles. This gating method was compared to that based on cells staining positive for CD40 - NIH 3T3 cells were shown to stain negative for this marker - and no significant difference was observed between the two gating methods in terms of antigen presentation.

3.2.6 $CD8^+$ T Cell Activation

To isolate antigen-specific $CD8^+$ T cells, lymph nodes from an OT-1/PL TCR transgenic mouse were harvested, combined, homogenized against a wire mesh, and strained through a 70-µm cell strainer. The cells were then washed once with PBS containing 2% FBS and resuspended in T Cell media. An aliquot of cells was stained with PE-labeled anti-murine CD8 (BioLegend) and PerCP Cy 5.5-labeled anti-murine CD90 (CD90.1) (BioLegend). The fraction of naïve $CD8^+$ T cells present in the whole lymph node cell population was approximately 40% as determined by sizing the population staining positive with both antibodies. To determine T cell activation, NIH 3T3 cells were transfected followed by co-culture with DC 2.4 cells for 24 hours as described above. Lymph node cells from OT-1/PL TCR transgenic mouse were added to the co-culture so that approximately 6 x 10^5 $CD8^+$ T cells were present in each well. After culturing for 3 days, the cell media was analyzed for IFN-γ by ELISA using a Ready-Set-Go IFN-γ "Femto-HS" kit (e-Bioscience) following standard protocol provided by the manufacturer. In separate experiments, DCs alone were incubated with SIINFEKL

peptide (New England Peptide, LLC) at 1 μM for 1 hour or with lipopolysaccharide (LPS, Sigma) at 2 ng/mL overnight before T cells were added.

3.3. Results

3.3.1 Correlation between transfection efficiency and cytotoxicity in bystander cells

NIH 3T3 cells were transfected with PEI/DNA complexes of various N/P ratios for 4 hours in serum-free condition and analyzed by flow cytometry after 24 hours (Fig. 3.2A). The gate of GFP-positive cells was set based on cells treated with polyplexes of Luc plasmid as the GFP-negative population, which controls for any increase of cell autofluorescence frequently observed after exposure to cationic polyplexes. As expected, the polyplexes were able to transfect fibroblasts effectively, especially at lower N/P ratios (4 and 8), but the fraction of GFP^+ cells decreased at higher N/P ratios (12, 16, 20). Toxicity in polyplex-treated cells was also determined by staining with annexin-V and PI, a common method for quantifying apoptosis and necrosis. At relatively low N/P ratios (4 and 8), there was very minor toxicity with over 90% of cells having low levels of annexin-V and PI staining (Fig. 3.2B). With increasing N/P ratio (to 12, 16, 20), the fractions of apoptotic and necrotic cells increased as shown with high level of either annexin-V or PI staining. Comparing transfection efficiency (quantified by the percentage of GFP^+ cells) with cytotoxicity (quantified by the percentage of annexin-V-high and PI-high populations), it is noted that at low N/P ratios (4, 8) when the cell death due to apoptosis/necrosis was minimal (<10%), transfection efficiency was high (Fig. 3.2C). As higher N/P ratios (12, 16, 20) caused more cytotoxicity, transfection efficiency declined accordingly. To further elucidate the effect of transfection efficiency and

cytotoxicity on antigen presentation, we focused on N/P ratios of 8 (high transfection/low toxicity) and 16 (low transfection/high toxicity) in the following studies.

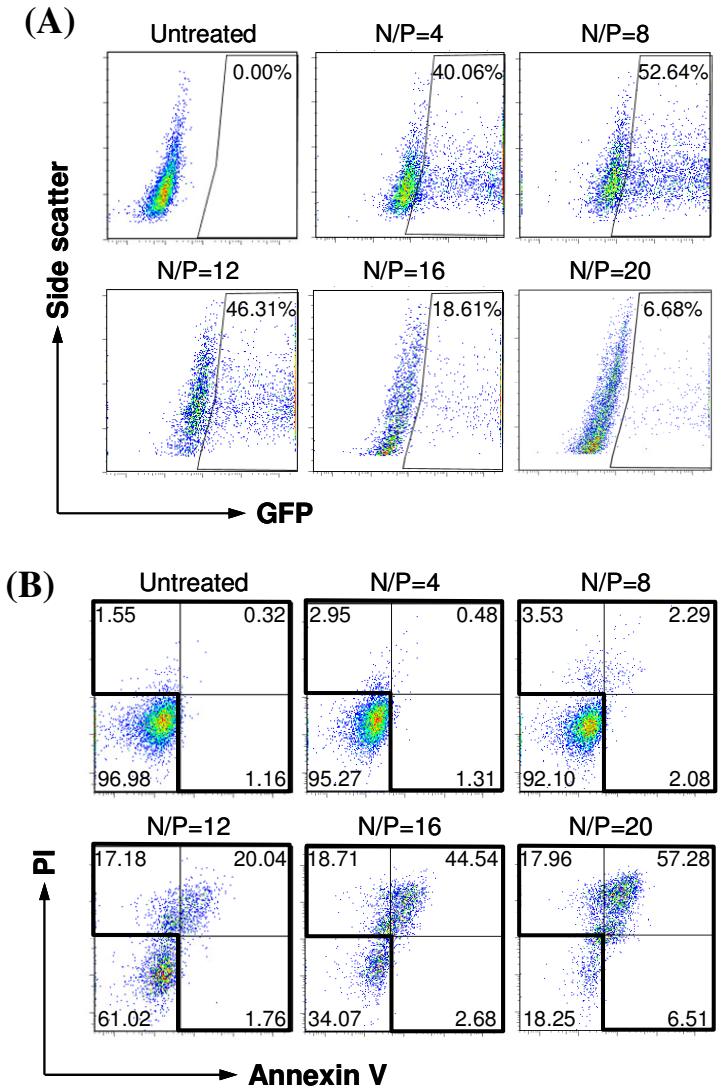

Figure 3.2. PEI-mediated transfection efficiency in bystander cells is inversely correlated to toxicity. NIH 3T3 cells were tranfected and analyzed by flow cytometry after 24 h for either transfection efficiency (A) and apoptosis/necrosis (B). Fraction of cells either expressed GFP or stained positive for annexin V or PI were quantified (C). Experiments were performed in triplicate and statistical significance between samples (*) was determined as $p < 0.0001$.

3.3.2 Transfecting bystander cells leads to cross-presentation by DCs

To determine if transfected fibroblasts were able to transfer antigen to DCs to be cross-presented, polyplexes were prepared with DNA encoding the model antigen OVA and transfected 3T3 cells at N/P ratios of 8 and 16. To ensure that only the bystander cells were transfected and not DCs, fibroblasts were washed repeatedly with buffer to remove any free polyplexes before adding DCs. The subsequent fibroblast/DC co-culture was conducted in serum-containing media because PEI/DNA polyplexes do not transfect well in the presence of serum. After the co-culture, DCs were stained for the OVA-derived peptide SIINFEKL presented specifically on MHC I complexes (Fig. 3.3). Despite not being directly transfected, DCs did stain positive for antigen presentation (~7%) at N/P 16, which strongly suggests that they were able to obtain the OVA antigen from transfected fibroblasts and process it for MHC I presentation. Fibroblasts transfected with polyplexes of GFP plasmid at N/P 16 did not result in any cross-presentation, confirming that cross-presentation seen with the OVA plasmid was antigen-specific. When transfected fibroblasts alone were stained for antigen presentation, the signal was similar to untreated cells, indicating that DCs are responsible for presenting the OVA antigen. Surprisingly, despite much higher transfection efficiency than N/P 16 (Fig. 3.2), there was no detectable cross-presentation for polyplexes of N/P 8 (Fig. 3.3), suggesting that cytotoxicity in bystander cells, rather than transfection efficiency, might be more important in causing cross-presentation.

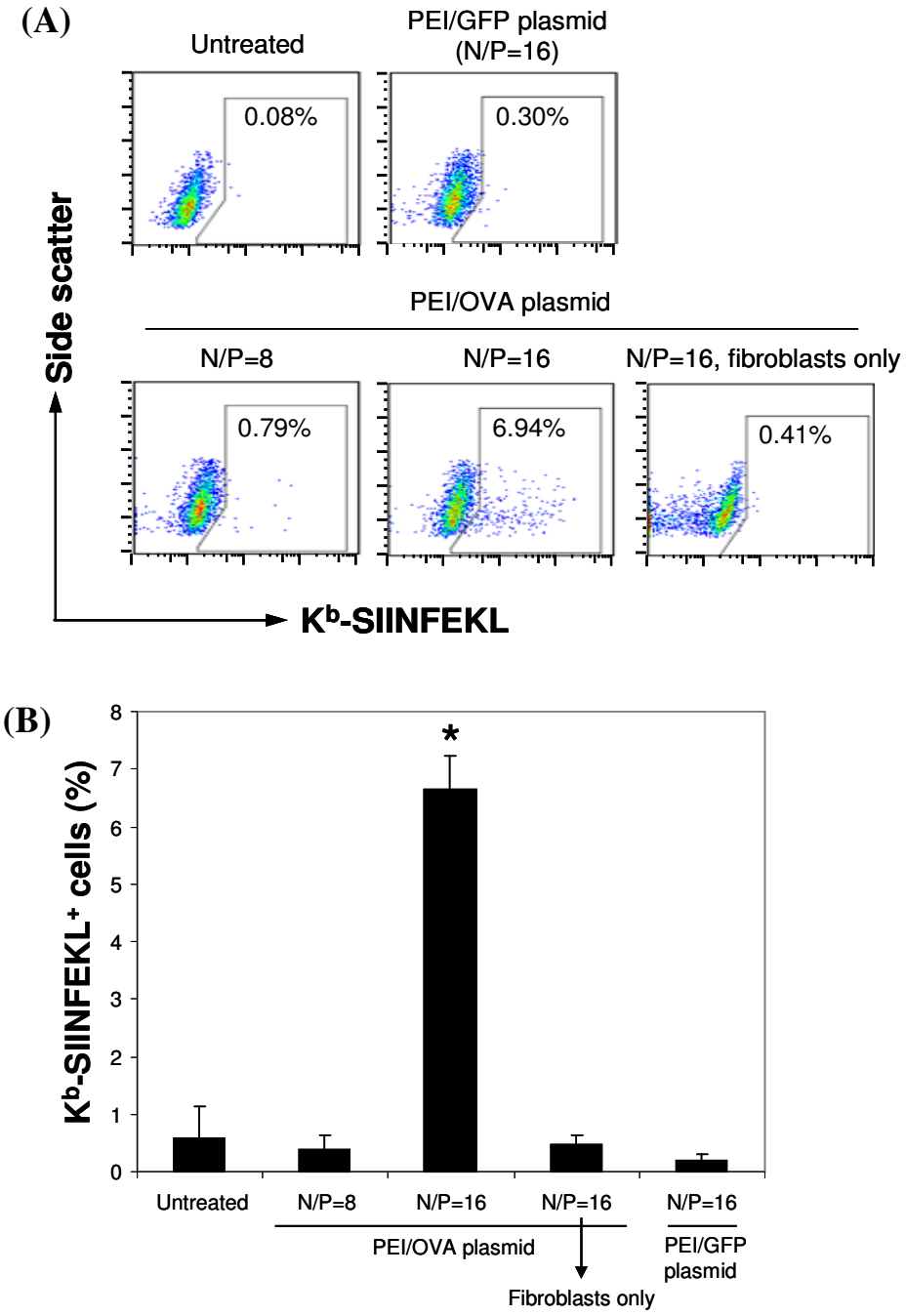

Figure 3.3. Cross-presentation of OVA antigen by DCs co-cultured with transfected bystander cells. MHC-I-restricted SIINFEKL peptide was detected by immuno-fluorescence staining and analyzed by flow cytometry. Shown are a representative set of dot plots (A) and quantification of three experiments (B). *Statistical significance of the "N/P 16" sample compared to all other samples was determined as $p < 0.0002$.

3.3 Toxicity in bystander cells directly affects cross-presentation by DCs

To further elucidate the correlation between bystander cell toxicity and cross-presentation, we characterized the influence on presentation of OVA antigen in co-culture by either aggravating toxicity in fibroblasts (without altering transfection) or reducing toxicity in fibroblasts through inhibiting apoptosis (Fig. 3.4). First, we transfected the fibroblasts with polyplexes containing 2 μg OVA plasmid at N/P 8, which showed very mild toxicity (~10%) (Fig. 3.4A) and no antigen presentation (Fig. 3.4B). We then doubled the dose by adding extra polyplexes containing 2 μg non-antigen-encoding Luc plasmid at N/P 8, so that cytotoxicity increased to ~45% without altering OVA expression. As a result, OVA antigen presentation went up to ~4%. Moreover, compared to N/P 8, polyplexes of N/P 16 induced much higher cytotoxicity (~60%) as well as much higher OVA presentation (~6.5%). On the other hand, treating the fibroblasts with 50 μM ZVAD 30 min prior to transfection effectively reduced cytotoxicity compared to those without ZVAD – from ~45% to ~25% (N/P 8 double-dose) and >60% to <40% (N/P 16). The amount of OVA presentation after ZVAD treatment went down accordingly, from an average of 4 to <3% (N/P 8 double-dose, not statistically significant) and 6.5% to 4% (N/P 16, $p<0.05$) (Fig. 3.4B). These observations establish a direct correlation between toxicity in fibroblasts and cross-presentation by DCs.

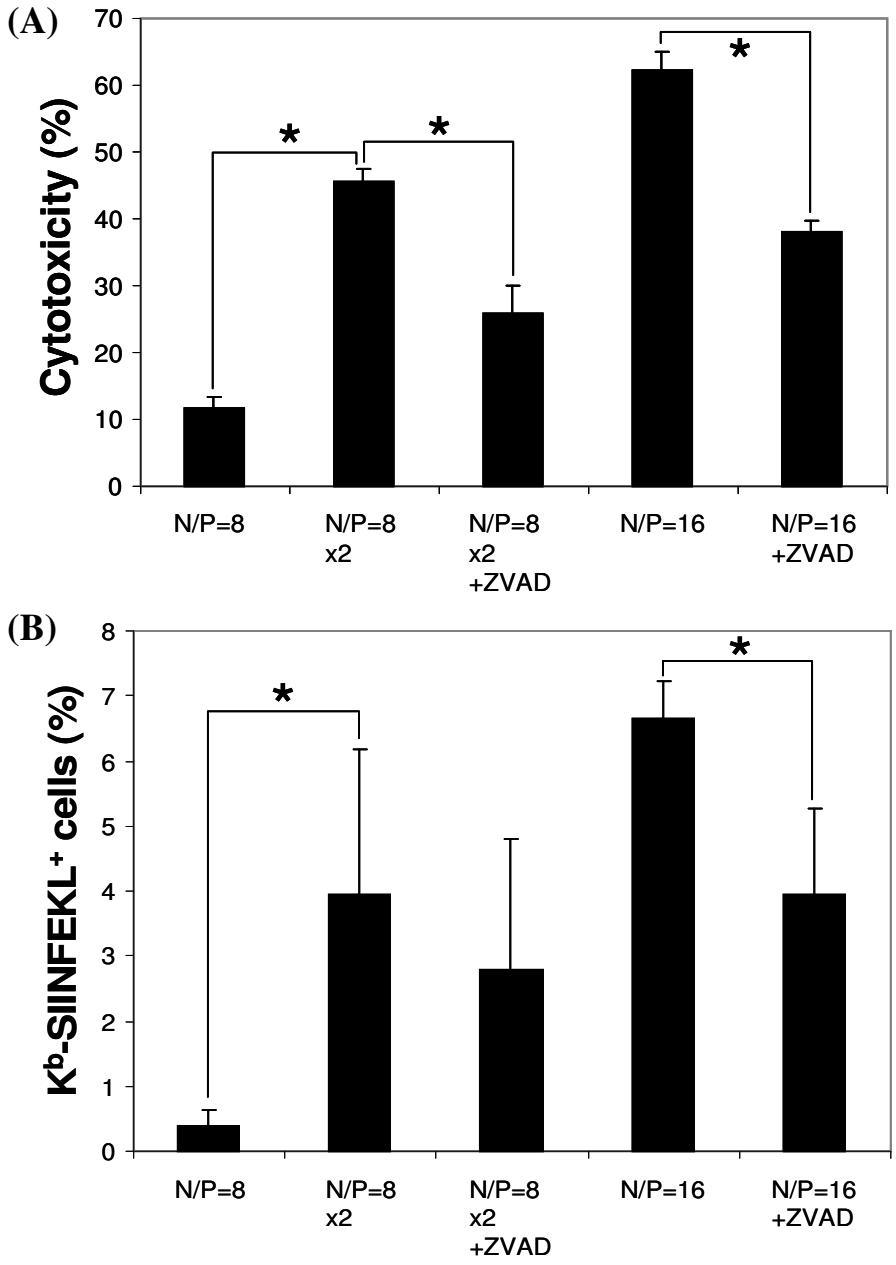

Figure 3.4. Cross-presentation of SIINFEKL peptide by DCs is dependent on bystander cell toxicity. Fibroblasts were incubated with either an extra dose of polyplex at N/P=8 (Luc DNA) or treated with ZVAD during transfection. Fibroblasts were analyzed for cytotoxicity (A) and quantified for cross-presentation after co-culture with DCs (B). Experiments were performed in triplicate and statistical significance (*) was determined by (A) $p<0.01$, (B) $p<0.05$.

3.3.4 Toxicity in bystander cells directly affects DC maturation

For DCs to effectively activate an immune response against presented antigen, they must be stimulated to mature. To determine if transfecting bystander cells alone with polyplexes could lead to DC maturation, we measured the level of CD40, a receptor that is up-regulated on mature DCs (Fig. 3.5). We observed higher CD40 expression after co-culture with transfected fibroblasts than untreated DCs and LPS treated DCs (Fig. 3.5A). CD40 level increased in response to either a higher N/P ratio (16 versus 8) or polyplex dose (single or double-dose at N/P 8), and decreased with the addition of the apoptosis inhibitor ZVAD (Fig. 3.5B). Polyplexes at N/P 16 containing Luc DNA caused the same degree of DC maturation as OVA DNA. Overall, DC maturation appears to be directly related to fibroblast cytotoxicity but independent of transfection efficiency and antigen expression.

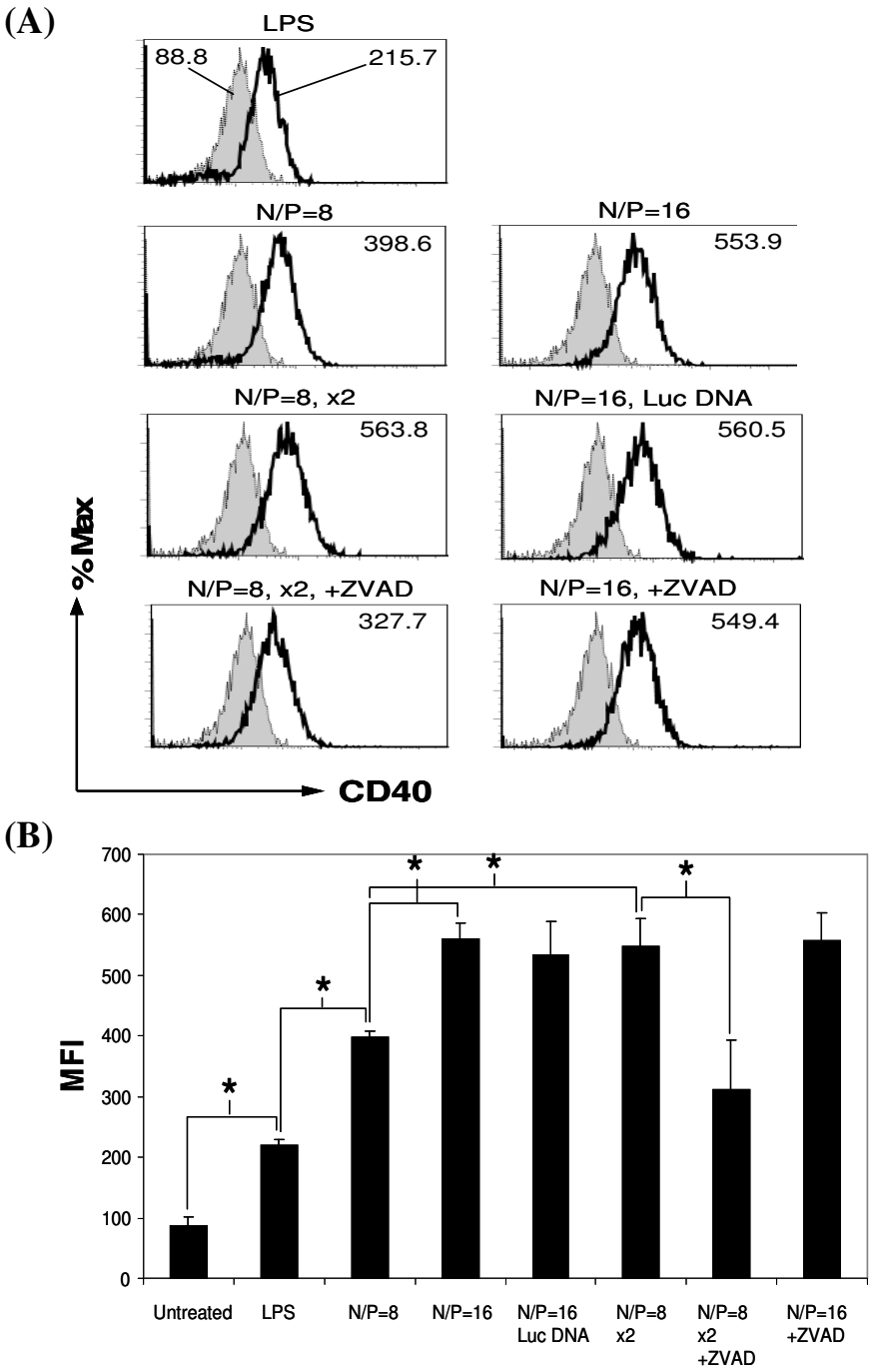

Figure 3.5. Effect on DC maturation state by bystander cell transfection. DCs were incubated with fibroblasts after transfection, stained for CD40 expression, and analyzed by flow cytometry. Shown are a representative set of histograms of CD40 level (A) and quantification of the MFI of treated cells (B). Experiments were performed in triplicate and statistical significance (*) was determined by $p<0.05$.

3.3.5 $CD8^+$ T Cell Activation

To induce an immune response, activated DCs must stimulate antigen specific naïve T cells in the lymph nodes. To determine if DCs could accomplish this after exposure to transfected bystander cells, fibroblasts were first transfected with polyplexes, co-cultured with DCs, followed by co-culture with naïve OVA specific $CD8^+$ T cells harvested from an OT-1 transgenic mouse. These T cells express the transgenic T-cell receptor that can recognize the MHC I-restricted SIINFEKL peptide presented on the surface of DCs, thereby becoming activated to secrete IFN-γ. We found that co-cultured DCs were able to induce IFN-γ secretion in the antigen-specific T cells as determined by ELISA (Fig. 3.6). Compared with untreated cells, T cells stimulated with DCs pulsed with the SIINFEKL peptide and matured by LPS secreted high level of IFN-γ, which serves as the positive control. At N/P 8, the T cells did not produce IFN-γ beyond the level of untreated cells, but cytokine production was significantly increased when fibroblasts were transfected with OVA plasmid at N/P 16 (Fig. 3.6). This is consistent with our data demonstrating higher DC antigen presentation and maturation at the more cytotoxic N/P 16 (Fig. 3.4B and Fig. 3.5B). No IFN-γ was produced after transfection at N/P 16 using the non-antigen-encoding GFP plasmid, suggesting that observed T cell activation with OVA plasmid was antigen-specific and that both antigen expression and DC maturation are necessary. Finally, additional treatment of DCs with LPS during co-culture with fibroblasts transfected by OVA DNA polyplexes at N/P 16 resulted in a further increase in T cell stimulation to the same level of the positive peptide control, suggesting that exogenous adjuvants such as LPS may augment the effect by polyplex-induced cytotoxicity.

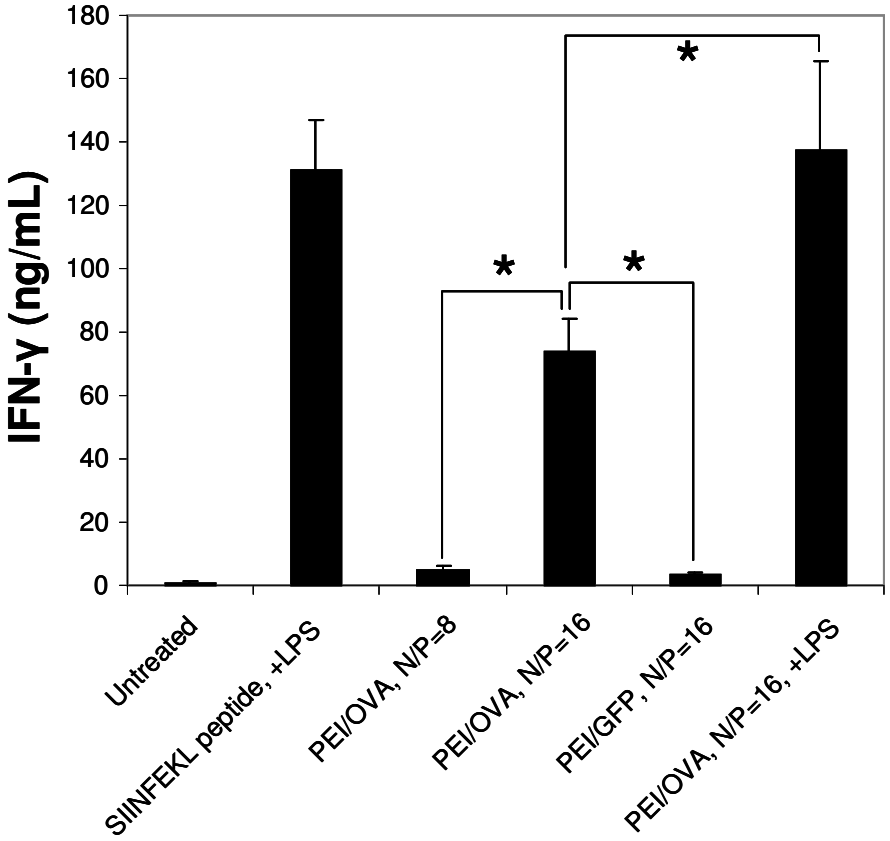

Figure 3.6. Transfecting bystander cells leads to activation of antigen-specific naïve $CD8^+$ T cells. SIINFEKL-specific OT-1 T cells were co-cultured with DCs and transfected fibroblasts and the amount of IFN-γ secretion was determined by ELISA. Experiments were performed in triplicate and statistical significance (*) was determined by $p<0.001$.

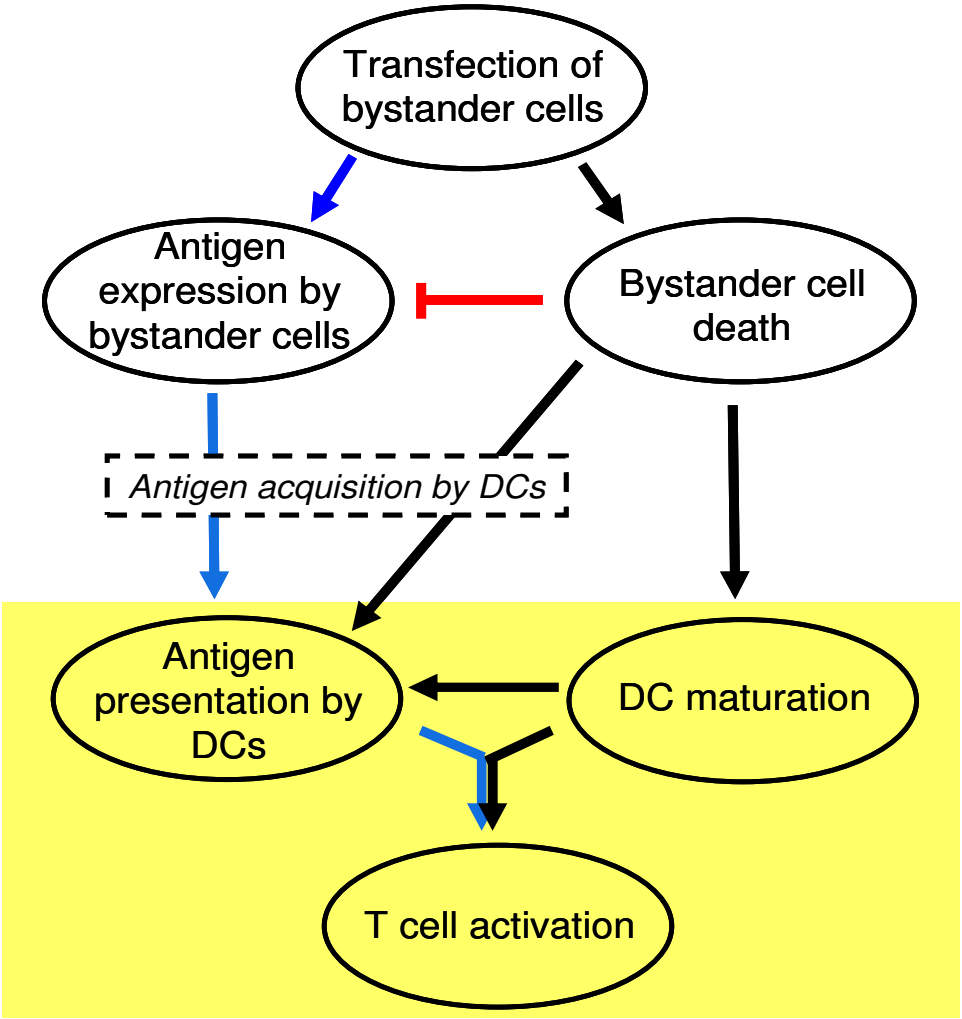

Figure 3.7. A proposed mechanism of polymer-mediated DNA vaccine delivery through targeting bystander cells to achieve T cell activation. Solid circles depict cellular events that are quantified in this study. Effective T cell activation requires antigen-presentation by mature DCs. Polymeric carriers can achieve high transfection efficiency and antigen expression in bystander cells. Expressed antigen is then acquired by immature DCs and cross-presented (blue arrows). On the other hand, intrinsic polymer-induced toxicity in bystander cells may enhance antigen acquisition and maturation by DCs (black arrows). Finally, maintaining a proper balance between transfection efficiency and cytotoxicity in bystander cells is crucial, because too much cell death reduces antigen expression (red blunt arrow).

3.4. Discussion

What are the ideal target cells for polymer-based DNA vaccine delivery? Directly transfecting dendritic cells is an attractive means of promoting antigen display on MHC class I molecules for $CD8^+$ T cell stimulation and a cellular immune response. However, this strategy requires overcoming intrinsic hurdles associated with DCs, a relatively rare cell type inherently challenging to transfect with foreign genes. Here we have demonstrated an alternative pathway for polymer/DNA vaccine delivery. We have shown that bystander cells such as fibroblasts transfected with PEI/DNA complexes are able to provide antigen to DCs for presentation on MHC class I molecules and trigger subsequent T cell stimulation in vitro. It is envisioned that for in vivo delivery, transfecting bystander cells, such as fibroblasts, at the site of injection may circumvent the difficulties in DC targeting/transfection and potentially generate robust T cell responses.

Another difficulty associated with directly targeting DCs is the inherent toxicity associated with many cationic polymer gene carriers. DCs need to remain functional after acquiring antigen to be able to prime naïve T cells, and toxicity in DCs resulted from direct transfection will compromise the immunostimulatory capacity and limit the life-time of these cells. When bystander cells are the intended target, however, the limitations of cytotoxicity can be lifted. Furthermore, we have shown here that some bystander cell death is even necessary for efficient antigen presentation. Dying cells are known to be a particularly effective source of antigen for cross-presentation.[67] Kurt et. al. demonstrated that DCs obtaining antigen from apoptotic cells were as efficient at stimulating $CD8^+$ T cells as directly transfected cells.[86] Perhaps the reason is that peptides may form

complexes with heat shock proteins (HSPs) produced by cells under stress, which have been shown to increase cross-presentation when used to deliver antigen to DCs.[87, 88] It has been shown that HSPs seem better able to simulate $CD8^+$ T cell effector function rather than that of $CD4^+$ T cells when complexed to peptide antigen.[89] In fact, the addition of hsp70 has been observed to enhance immune response when delivered along with cytotoxicity-inducing DNA.[90-93] Dying cells could also be a potent source of antigen for cross-presentation simply because the protein antigen is rendered into particulate form by association with cellular debris.[67] Apoptotic bodies themselves have also been shown to enhance cross-presentation.[77] We also observed that transfection of bystander cells at N/P ratios high enough to cause significant cytotoxicity enhanced DC maturation. This suggests that bystander cell cytotoxicity could be used not only to enhance cross-presentation but also as an adjuvant. Apoptotic and necrotic cells are known to release many factors capable of both recruiting and maturing DCs, including HMGB-1, HSPs and uric acid, among others,[94] which can activate immature DCs. While cytotoxicity of the polymer gene carrier is undesirable in many gene therapy applications, it could in fact be an advantage within the context of DNA vaccine delivery and immune activation. Thus, as depicted in Fig. 3.7, we propose a two-fold mechanism for how polyplex-induced bystander cell death can lead to $CD8^+$ T cell response – by enhancing DC cross-presentation of acquired antigen and by stimulating phenotypic maturation of DCs.

The idea of causing toxicity in healthy cells deliberately in exchange for enhanced immune response and therapeutic benefit is not unheard of.[95] It has been shown that delivering naked DNA encoding a cytotoxic gene to healthy cells can cause regression of tumors in cancers of the same cell type.[90-93] It was also determined that unlike a bacterial

adjuvant such as Complete Freund's Adjuvant, cytoplasm from damaged cells enhances both $CD4^+$ and $CD8^+$ responses specifically against particulate antigen.[96,97] By analogy, polymer carriers of DNA vaccine could be designed and used in such a way to transfect bystander cells and to promote the death of these same cells to achieve immune activation against antigens. Future designs of DNA vaccine carriers for cancer therapy may incorporate the following considerations: 1) targeting not only healthy somatic cells, but also stromal cells within the tumor microenvironment or even cancer cells themselves; 2) maintaining a proper balance between cellular stress and transfection efficiency; 3) modulating the pathway of cell death to optimize antigen acquisition and DC maturation; and 4) delivering additional synergistic signals (such as TLR ligands) to boost the cross-priming of CD8 T cells.

3.5. Conclusions

Fibroblasts transfected with PEI/DNA complexes are effectively able to transfer antigen to DCs for presentation on MHC I molecules and to achieve subsequent T cell stimulation in vitro. Antigen presentation and T cell stimulation are both more effective when fibroblasts are transfected at high polyplex N/P ratios, despite lower protein expression in these conditions. This suggests the balance between transfection and polyplex-induced toxicity in the fibroblasts is important for stimulating immune responses. Fibroblasts transfected at higher polyplex N/P ratios also induce higher DC maturation. These experiments highlight an alternative pathway to directly targeting DCs for polymer-mediated DNA vaccine therapy.

Chapter 4: Tissue and Cellular Distribution of Naked and Polymer-Condensed Plasmid DNA After Intradermal Administration in Mice

SUMMARY: DNA vaccination using cationic polymers as carriers has the potential to be a very powerful method of immunotherapy, but typical immune responses generated have been less than robust. To better understand the details of DNA vaccine delivery in vivo, we prepared polymer/DNA complexes using three structurally different cationic polymers and fluorescently labeled plasmid DNA and injected them intradermally into mice. We analyzed the local tissue and cellular distribution of the labeled DNA at the injection site at various time points (from hours to days). Live animal imaging revealed that naked DNA dispersed quickly in the skin of mice after injection and had a wider distribution than any of the three types of polyplexes. However, naked DNA level dropped to below detection limit after 24 h, whereas polyplexes persisted for up to 2 weeks. The PEGylated polyplexes had a significantly wider distribution in the tissue than the non-PEGylated polyplexes. PEGylated polyplexes also distributed more broadly among dermal fibroblasts and allowed greater interaction with antigen-presenting cells (APCs) (dendritic cells and macrophages) starting at around 24 h post-injection. By 4 days, substantial interaction of polyplexes with APCs was observed at the injection site regardless of polymer structure, whereas small amounts of polyplexes were found in the

draining lymph nodes. These in vivo findings demonstrate the superior stability of PEGylated polyplexes in physiological milieu and provide important insight on how cationic polymers could be optimized for DNA vaccine delivery.

4.1. Introduction

The goal of vaccination is to manipulate the immune system into responding against specific antigens. Theoretically, this strategy can work both to treat ongoing infections and malignancies as well as prevent disease by generating immunological memory. For successful immunization, antigen must be delivered to antigen-presenting cells (APCs), mainly dendritic cells (DCs) and macrophages, often along with an immunostimulatory adjuvant. These cells can then process and present the antigen and stimulate T and B cells in the lymph nodes and spleen.[4,9,10]

Transfection of cells with antigen-encoding plasmid DNA will result in the expression of the protein antigen by those cells. This is an attractive method of vaccination due to high stability of plasmid DNA formulations, the potential for long-term antigen production, and the capacity of generating both humoral and cellular immune responses to multiple epitopes.[4,6-8] The initial attempt of DNA vaccination involved the injection of naked plasmid DNA. However, though this can result in immune responses, the efficiency of this method of delivery is generally low.[7,8,20] Various delivery vehicles, including viral particles, liposomes, and polymeric materials, have since been used to help protect the DNA and increase transfection.[7,98] Polymeric carriers have the potential to be a very effective means of delivering antigen-encoding DNA for immunization because polymers can be easily modified and potentially display a wide

range of characteristics. Delivery of DNA vaccine with various polymer-based systems has shown improvement in both humoral and cellular immune responses, but overall immune responses have not been sufficiently robust.[7,11]

Over the years a large number of polymer DNA carriers with a large variety of chemical structures have been developed, many of which have been investigated for DNA vaccine delivery. It is not clear, however, how to best improve upon current designs because not much is known about the specific mechanisms of delivery in vivo, especially tissue and cellular processes that precede immune response generation. There have been studies conducted to investigate the uptake and transfection of specific cell types using various naked DNA delivery systems in the muscle and skin.[99-102] For example, it was shown that fibroblasts, endothelial cells, and adipocytes appeared to be the primary cell types transfected after naked DNA delivery via electroporation into the skin,[100] and that myocytes were the primary recipient of DNA after intramuscular injection.[99] More recently, van den Berg and others described the transfection of primarily keratinocytes after tattooing with PEGylated polyplexes.[8] These studies also reported some, if limited, DNA uptake by or transfection of, APCs. However, exactly which cell types are primarily involved in the interactions with polyplex-delivered DNA, as well as how those interactions may affect antigen presentation and the timeline and magnitude of immune responses, is not well understood. Furthermore, there is a lack of systematic understanding of the structure-function relationship of polymer carriers in the context of in vivo administration. To this end, we prepared polyplexes of plasmid DNA and three different cationic polymers: branched polyethylenimine (PEI), linear poly(2-aminoethyl methacrylate) (PAEM), and diblock copolymer PEG-*b*-PAEM (Fig. 4.1). We injected

these polyplexes into mice intradermally, and analyzed the local biodistribution of DNA both macroscopically on the tissue level and microscopically on the cellular level, in comparison to injections of naked DNA. We uncovered important differences in tissue and cellular distribution between polyplexes and naked DNA, and between PEGylated and non-PEGylated polyplexes. This information could be highly useful for improving the design of cationic polymer carriers for DNA vaccines.

4.2. Experimental Methods

4.2.1. Chemicals and Solvents for Polymer Synthesis

PEI (branched, 25 kDa) was obtained from Sigma. Monomethoxy-PEG (average M_n of 5000) was from Aldrich and was used after vacuum drying at 80 ºC for 2 h. Toluene (Aldrich) was dried by refluxing over sodium and distilled. The monomer *N*-(*tert*-butoxycarbonyl)aminoethyl methacrylate (*t*BAM) and the PEG macro-initiator for atom transfer radical polymerization (ATRP) was synthesized as described before.[103,104] Ethyl α-bromoisobutyrate, copper (I) chloride (CuCl) and 2,2'-dipyridyl (bPy) were purchased from Sigma. Other chemicals and solvents were purchased from Sigma and used without further purification.

4.2.2. Polymer Synthesis

The ATRP of P*t*BAM followed a procedure modified from Tang et. al.[105] A glass two-neck flask was charged with *t*BAM, CuCl, bPy, and the system was degassed three times. Dried degassed toluene and ethyl α-bromoisobutyrate were added, and the mixture was heated at 80 °C for 8 h. The reaction was terminated by exposing the system to air.

The reaction solution was then diluted by dichloromethane (DCM) and passed through a basic aluminum oxide column to remove the copper complex. The resulting product was precipitated in hexane twice and dried in vacuum at room temperature for 2 days. To remove the Boc groups, 0.8 g of P*t*BAM was dissolved in 5 mL of trifluoroacetic acid (TFA) and stirred for 2 h at room temperature. TFA was then removed by evaporation, and the oil residue was rinsed three times with diethyl ether. The resultant precipitate was collected by filtration, washed twice by diethyl ether, and dried overnight in vacuum. Afterwards, the polymers were washed with NaOH solution at pH 9.0, and immediately put into dialysis tubing (MW cut-off 3500) and dialyzed against distilled water for 3 days. The final PAEM polymer was obtained by lyophilization.

PEG-*b*-PAEM diblock copolymer was synthesized as described in Tang et al.[105] using a 5000 Da PEG block. The final polymer was washed by NaOH solution, dialyzed and lyophilized. The average values of M_n for P*t*BAM and PEG-*b*-P*t*BAM were 3.37×10^4 and 3.96×10^4 with narrow distribution (PDI 1.16 and 1.20). Therefore, the average chain-length of the PAEM homopolymer (degree of polymerization, DP: 150) was the same as the PAEM segment in the PEG-*b*-PAEM diblock copolymer.

4.2.3. Polyplex Preparation

Plasmid DNA encoding ovalbumin (OVA, kindly provided by Dr. Chris Pennell) was purified from *E. coli* DH5α cells using an EndoFree Plasmid Maxi plasmid prep kit (Qiagen). A luciferase plasmid (pCMV-LUC, Elim Biopharmaceuticals) was also used. Both plasmids were covalently labeled with Cy3 fluorophore using a Label IT nucleic acid labeling kit (Mirus) and purified according to manufacturer's instruction. Purified

plasmids were verified to contain less than 0.6 EU/mg of endotoxin using the Pyrogent Gel Clot LAL assay kit (Lonza) and stored at -20°C in sterile water. Polymer stocks were first diluted in 5% glucose, filter-sterilized, and stored in aliquots at -20°C. To form polyplexes, polymer stocks were further diluted in sterile 5% glucose before DNA was added and samples were vortexed to mix. A typical batch of polyplexes was made with 12 µg of DNA and enough polymer for an N/P ratio of 8 in 36 µL total volume. Naked DNA was diluted to the same volume with 5% glucose.

4.2.4 Polyplex Stability in Serum-Containing Medium

Fifteen µL of polyplex solution containing 5 µg of Cy3-labeled plasmid DNA was added to another 15 µL of either 5% glucose or cell culture medium comprised of DMEM medium (1 g/L D-glucose, L-glutamine, 110 mg/L sodium pyruvate) supplemented with 10% heat-inactivated fetal bovine serum (FBS), 100 units/mL penicillin/streptomycin, and 10 mM 4-(2-hydroxyethyl)-1-piperazineethanesulfonic acid (HEPES) (all cell medium components were from Gibco). Five µL of the polyplexes solution was removed immediately after dilution and after a 1-h incubation at room temperature, placed onto a glass microscope slide, covered with a glass coverslip, and was observed under an Olympus IX70 inverted microscope equipped with a standard FITC/TRITC/DAPI filter set, a 20× objective lens, an Olympus DP72 camera, and CellSens software. To see if there was any free DNA present after polyplexes were formed and after incubation in 5% glucose and serum-containing medium, polyplex solutions were analyzed on a 0.7% agarose gel stained with ethidium bromide.

4.2.5. Injections

Hair was plucked from a small section of skin on the hind leg of 10~16-week old male C57BL/6 mice (Jackson Labs) to mark injection site, and polyplex solutions were injected intradermally through a 29-gauge needle. Ten μg of DNA complexed with polymers at N/P ratio of 8 was prepared as described above and was injected into each mouse in a total volume of 30 μL. The same volume of naked DNA and buffer only injections were also administered. Polyplexes containing all three cationic polymers (PEI, PAEM, and PEG-*b*-PAEM) were tested. To detect tissue distribution by Maestro live animal imaging, three mice per sample group were injected. For time course studies of cellular distribution by immunofluorescence, one mouse was injected for each sample and sacrificed at each time point through 4 days. All the mice were housed under specific pathogen-free conditions and cared for in accordance with the University of Minnesota and NIH guidelines.

4.2.6. Maestro Live Animal Imaging

To assess tissue distribution of Cy3-labeled DNA in live animals after intradermal injection, mice were anesthetized using isofluorane at predetermined time points and imaged using a CRi Maestro live animal imaging system equipped with a Nikon AF Micro 60 mm camera. Three mice of the same experimental group were imaged together. The tails of the mice were marked to keep the order of mice (from left to right under the camera) the same for every time point. Cy3-labeled DNA fluorescence was detected using a 503-555-nm excitation filter and 580 nm long-pass emission filter. Emission signal was collected between 550 nm and 800 nm in 10-nm steps. Three images of each

group of mice were taken at each time point, rotating mice to be at different positions under the camera between images to account for any potential inconsistency due to different animal positions. All images were taken at the same stage height and light position with a constant exposure time of 5000 ms. The fluorescence signal at 560 nm was isolated and the threshold was set using Image J software. Image J was also used to quantify the total pixel area of signal for each sample at each time point.

4.2.7. Immunofluorescence

To determine cellular distribution of Cy3-labeled DNA in tissue sections, mice were euthanized using CO_2 at predetermined time points after injection. The skin of each injection site and the inguinal lymph node that drains the injection site were removed, embedded in OCT medium, and frozen in a bath of 2-methylbutane using liquid nitrogen. Frozen skin samples were cut into 10-µm sections using a cryotome and placed on SuperFrost (Fischer) glass slides. Slides were allowed to dry at room temperature for 1 h, fixed by incubating in cold acetone for 10 min, and stored at -20 °C.

For immunofluorescence staining, slides of tissues were removed from freezer and equilibrated to room temperature. A hydrophobic circle was drawn around tissue sections with a PAP pen (Research Products International Corps.) to help keep staining solutions from running off the slides. Slides were placed in a staining chamber and equilibrated in PBS for 30 min with slight agitation. Tissue was then blocked using Blocking Buffer (from Tyramide Signal Amplification (TSA) Biotin System, Perkin Elmer) for 30 min in a humidity chamber. Slides were also blocked with streptavidin and biotin solutions (Vector Laboratories) for 15 min each in the humidity chamber. Slides were then stained

with biotin-labeled anti-CD11c (for DCs) (BioLegend), biotin-labeled anti-F4/80 (for macrophages) (BioLegend), or rabbit anti-ER-TR7 (for reticular dermal fibroblasts) (Abcam) followed by biotin-labeled anti-rabbit IgG (Invitrogen). All antibody incubation times were 1 h, except for anti-CD11c which was 30 min. Signal was developed using Tyramide Signal Amplification (TSA) Biotin System (Perkin Elmer) and a streptavidin labeled with Alexa Fluor 350 (Invitrogen). Tissue sections were then mounted using Vectashield and visualized using an Olympus IX70 inverted microscope equipped with a standard FITC/TRITC/DAPI filter set, an Olympus DP72 camera, and CellSens software.

To analyze the images, the areas of fluorescence signal from Cy3-labeled DNA and antibody staining of cell type markers were quantified in Image J. The thresholding levels on the DNA signal were varied to adjust for differences in signal intensity. Cell-DNA interaction was quantified by calculating the area of overlap between the signals of DNA and cell markers using the "co-localize" plug-in for Image J. The results on co-localization were expressed as the fraction of total DNA signal that overlapped with cell marker signal. Two to five slides were stained with each cell marker for each time point and each sample.

4.2.8 Statistical Analysis

Statistical analysis was performed using the two-sample equal variance Student's *t*-test. A probability (p) value of <0.05 was deemed statistically significant.

4.3. Results

4.3.1. Selection of Cationic Polymers

Three cationic polymers with differing structures were selected to prepare polyplexes: branched 25-kDa PEI, linear PAEM, and linear PEG-*b*-PAEM, (Fig. 4.1). Branched PEI is well known for efficiently transfecting cells in vitro but is quite inefficient in vivo.[98] PEI from commercial sources has heterogeneous structure and broad molecular weight distribution. On the other hand, the PAEM polymer has a different, much more defined structure than PEI. We used ATRP to synthesize a PAEM polymer with average DP of 150 and narrow molecular weight distribution. To probe the impact of PEGylation, we also synthesized PEG-*b*-PAEM diblock copolymer using ATRP that contained the same PAEM block (DP = 150) and a PEG block of 5000. Next, we prepared polyplexes with the three cationic polymers and plasmid DNA at an N/P ratio of 8, which yielded the highest transfection efficiency in cultured cells (data not shown), for the following studies.

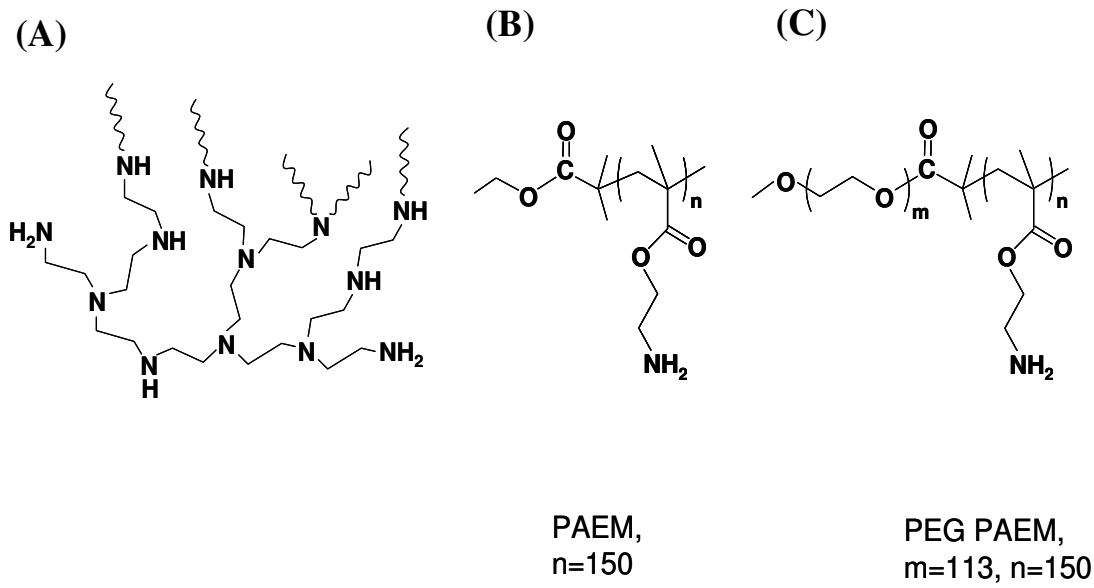

Figure 4.1. Chemical structures of branched PEI (A), PAEM (B), and PEG-*b*-PAEM (C).

4.3.2. Visual Assessment of Polyplex Stability in Simulated In Vivo Medium

Polyplexes containing Cy3-labeled plasmid DNA were dissolved in 5% glucose injection buffer or cell medium complete with serum and buffer salts to mimic the in vivo fluid environment, and visualized by fluorescence microscopy (Fig 4.2). Cy3-labeled naked DNA solutions remained clear with a slight reddish fluorescence background during the entire time of observation. Shortly after formation, aggregates of PEI and PAEM polyplexes were already visible in 5% glucose (used later for in vivo injection), especially after 1 hour (Fig. 4.2A), presumably because of the high polyplex concentration necessary to keep the injection volume low. More severe aggregation in these polyplexes was seen in serum-containing cell culture medium with aggregates ranging from several microns to nearly a hundred microns in size after 1 hour (Fig. 4.2B). Qualitatively, aggregates of the PAEM polyplexes appeared smaller than the PEI polyplexes. However, no visible aggregation was seen in the PEG-*b*-PAEM polyplexes after 1 h in either 5% glucose or complete cell culture medium (Fig. 4.2B). All the samples of polyplexes and naked DNA with or without incubation in complete cell medium were also analyzed by gel electrophoresis. There was no band corresponding to free plasmid DNA in any of the polyplex samples (Fig. 4.2C), confirming that DNA was still bound by the polymers during incubation in serum-containing medium.

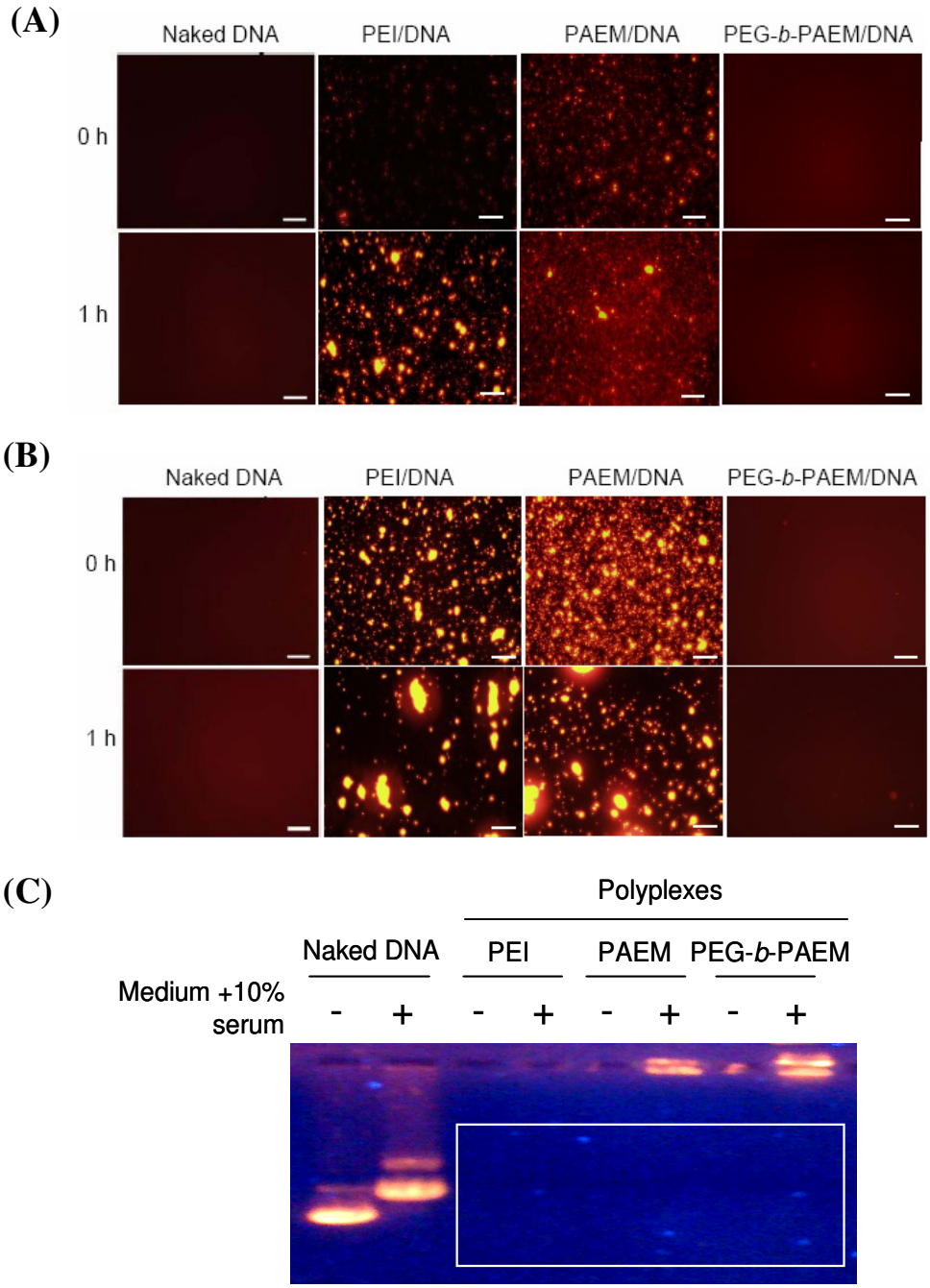

Figure 4.2. Visual assessment of polyplex stability in injection buffer (5% glucose) (A) and cell medium containing 10% serum (B) – conditions that mimic the in vivo fluid environment. Whereas PEI and PAEM polyplexes experienced much aggregation over time, PEGylated polyplexes remained stable without visible aggregation. Agarose gel electrophoresis of naked DNA and polyplexes before and after incubation in serum-containing medium (C) confirmed the absence of any free, unbound DNA. Scale bar: 100 µm.

4.3.3. Tissue Distribution of DNA in Live Animals

Cy3-labeled naked DNA and polyplexes were injected intradermally into the hind quadriceps of mice and were imaged using a Maestro live animal imaging instrument. We analyzed the area of the Cy3-DNA signal at various time points after injection to determine the difference, if any, between the distribution and persistence of the naked DNA and DNA delivered as various polyplexes. Naked DNA disseminated quickly in the skin in 4 hours, diminished after 24 hours, and completely disappeared by 3 days (Fig. 4.3). On the other hand, when DNA was delivered as polyplexes, tissue distribution was much reduced but persisted for at least 14 days (Fig. 4.4), and polyplexes were seen for as long as 27 days in some mice (data not shown). Furthermore, the PEGylated polyplexes appeared to have spread to significantly larger areas than the PEI and PAEM-based polyplexes through the first 3 days (Fig. 4.4).

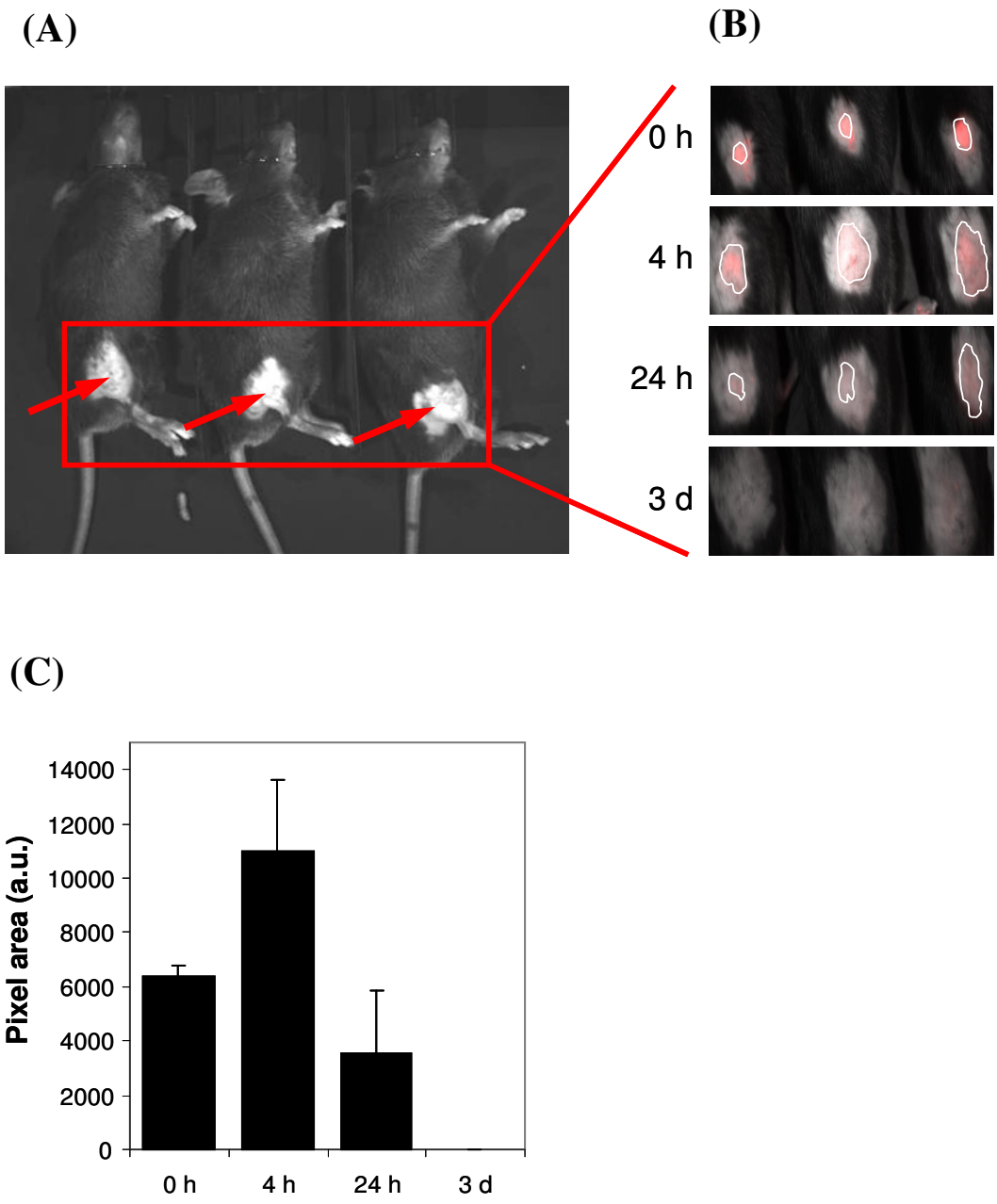

Figure 4.3. Tissue distribution of naked DNA in live animals after intradermal injection. Three mice were each injected with 10 µg of Cy3-labeled DNA in the right hind quadriceps and were imaged together (A). DNA distribution in three injected mice was shown at indicated time points as marked by a white outline (B) and the area of the signal was quantified (C).

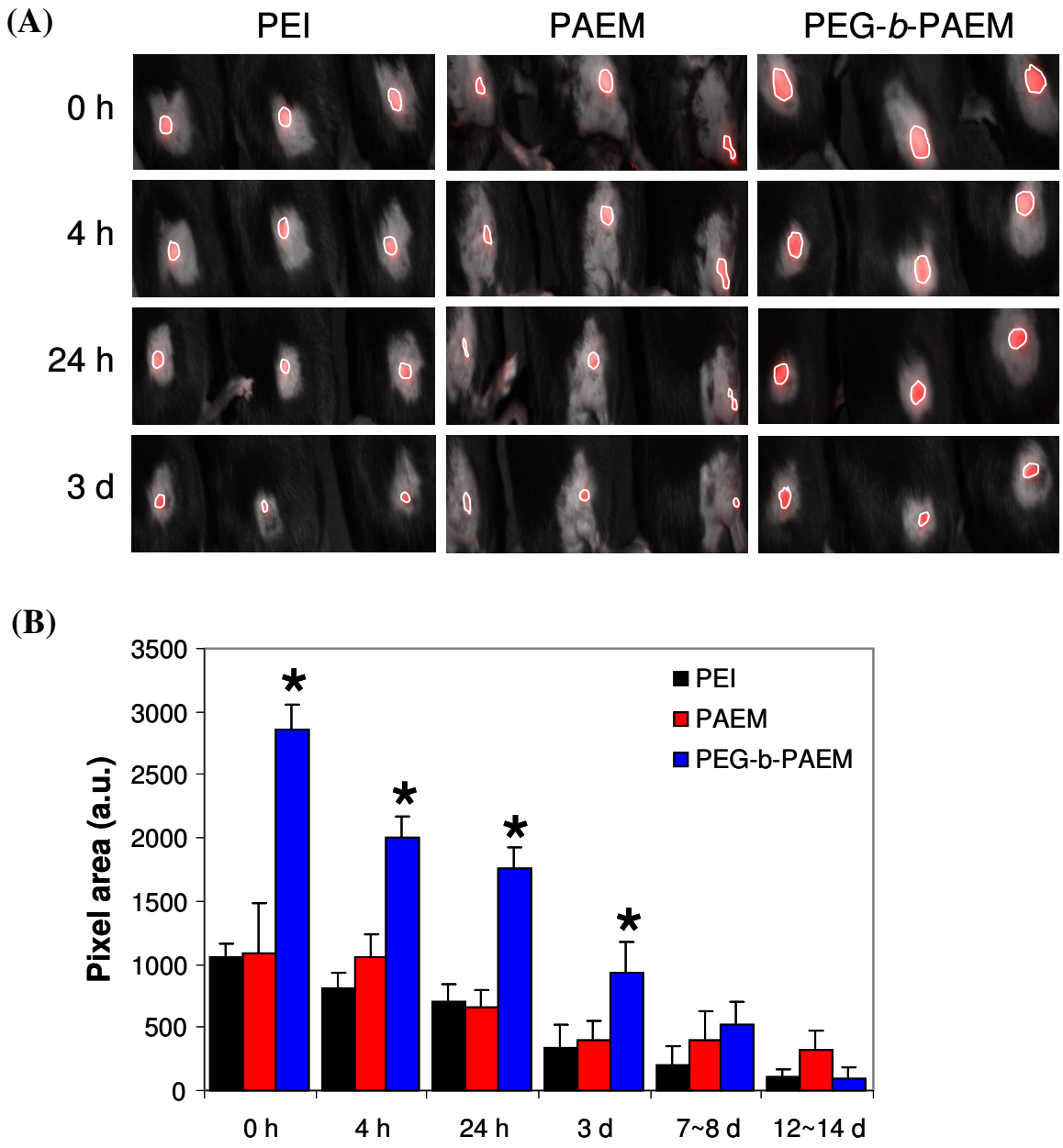

Figure 4.4. Tissue distribution of polyplexes in live animals after intradermal injection. Three mice were each injected with polyplexes containing 10 µg of Cy3-labeled DNA in the right hind quadriceps and were imaged together. DNA distribution in three injected mice was shown at indicated time points as marked by a white outline (A) and the area of spreading was quantified (B). *PEGylated polyplexes showed statistically larger area of spreading than PEI and PAEM-based polyplexes (*t* test, $p<0.001$).

4.3.4. Cellular Distribution of Naked DNA at the Injection Site

Mice were again injected in the hind quadriceps with naked or polyplexes of Cy3-labeled DNA and sacrificed at predetermined time points. Injection sites were harvested, sectioned, and stained for ER-TR7, CD11c, and F4/80 as markers for reticular dermal fibroblasts, DCs, and macrophages, respectively. The amount of interaction between DNA and stained cells 4 h after injection was estimated by determining co-localization (white) of fluorescence signals of the DNA label (Cy3, red) with the cell markers (blue) (Fig. 4.5). From the representative set of images we can see that the naked DNA spread very well throughout the injection site and had significant interaction (co-localization) with dermal fibroblasts that were abundant in the skin (Fig. 4.5). The numbers of DCs and macrophages present at the injection site 4 h post-injection were much lower, and the interaction with naked DNA was also less than with fibroblasts. Signal of the naked DNA was not visible in tissue sections after 4 h.

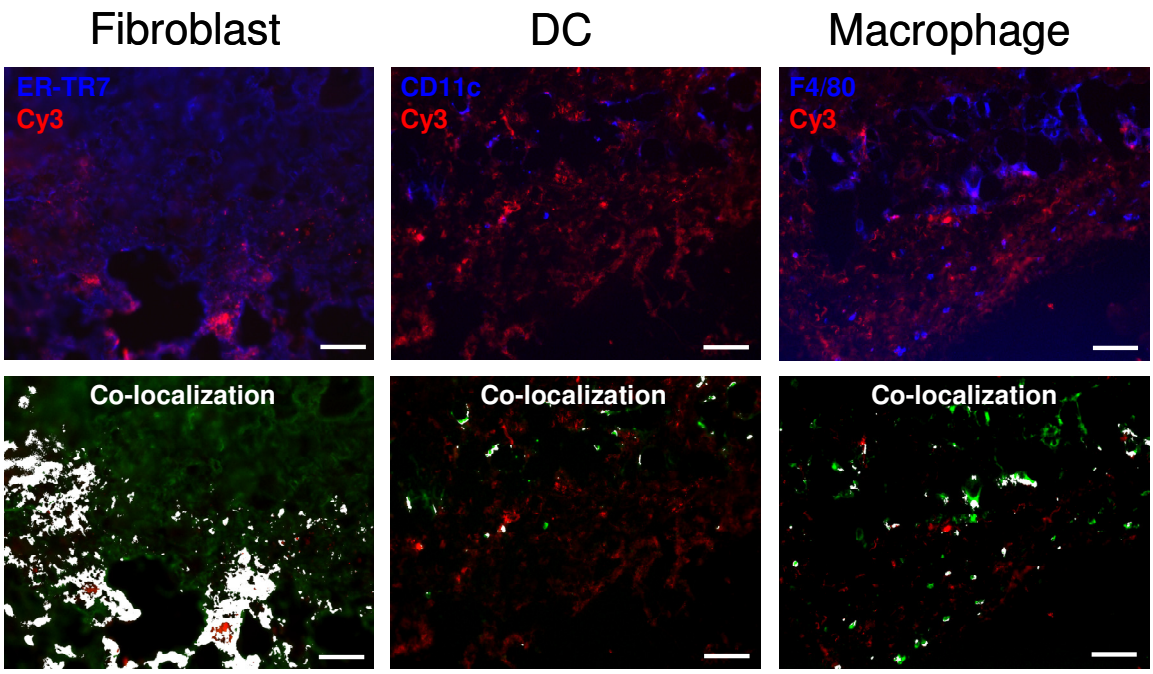

Figure 4.5. Cellular distribution of naked DNA at the injection site. Naked DNA was labeled with Cy3 (red). Reticular dermal fibroblasts, DCs, and macrophages were stained for ER-TR7, CD11c, and F4/80, respectively (blue or green). Areas of co-localization between DNA and cell marker were painted in white. Images shown are representative fields of view. Scale bar: 50 µm (for fibroblasts), 100 µm (for DCs and macrophages).

4.3.5. Cellular Distribution of Polyplexes at the Injection Site

4.3.5.1. Dermal Fibroblasts

Cellular distribution of Cy3-labeled polyplexes in tissue sections of the injection site was characterized. Consistent with live animal imaging studies (Fig. 4.3 and 4.4), polyplexes persisted much longer than naked DNA in the skin. While naked DNA appeared diffusive in the tissue (Fig. 4.5), all the polyplexes were more aggregated, forming depots of DNA (Fig. 4.6A). Both PEI and PAEM polyplexes remained aggregated throughout the 4-days of observation, whereas the PEGylated polyplexes dispersed into much smaller packets with faint signal intensity by day 4 (Fig. 4.6A, pointed by arrows). Much better dissemination of the PEGylated polyplexes among fibroblasts was also reflected in the quantification of the fraction of co-localization, which was defined as the ratio of pixel areas between co-localized DNA signal and the total DNA signal. Significantly more DNA-cell co-localization on day 1 and day 4 was shown for the PEGylated polyplexes, whereas co-localization of signals remained low throughout 4 days with both the PEI and PAEM polyplexes (Fig. 4.6B). PAEM polyplexes dispersed slightly better than PEI polyplexes, although the difference was not statistically significant.

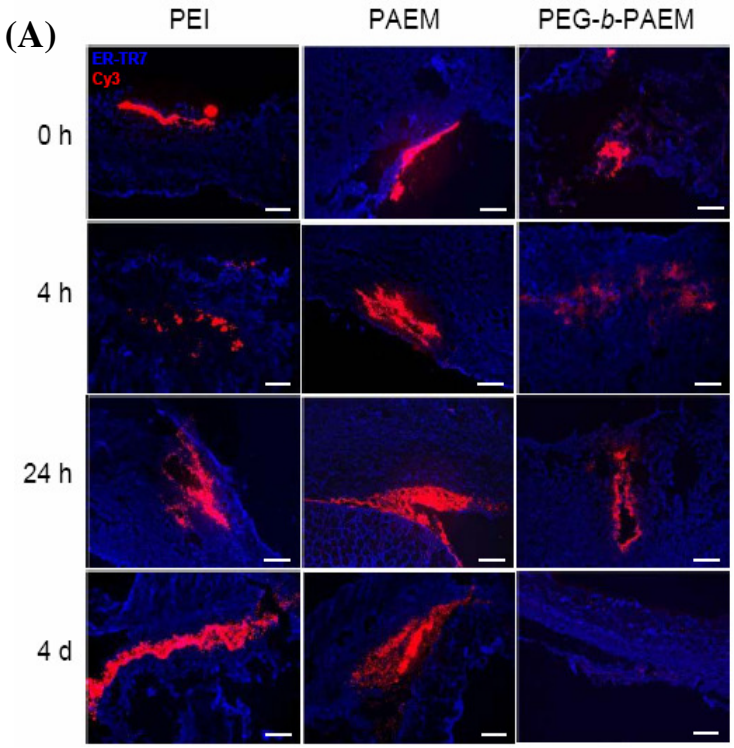

Figure 4.6: Cellular distribution of polyplexes and interaction with dermal fibroblasts at the injection site. (A) Representative fluorescence microscopy images showing DNA labeled with Cy3 (red), and fibroblasts stained for ER-TR7 (blue). Scale bar: 200 µm. (B) Quantification of the fraction of co-localization between DNA and fibroblasts defined as the ratio of pixel areas between co-localized DNA signal and the total DNA signal. *PEGylated polyplexes showed statistically more co-localization with fibroblasts than PEI and PAEM-based polyplexes (*t* test, $p<0.05$).

4.3.5.2. DCs

There was substantial infiltration of DCs into the injection site for all polyplexes 24 h after injection and the cells persisted through day 4 (Fig 4.7A). All polyplexes again showed considerable aggregation and much co-localization with DCs was observed after DCs infiltrated. By 24 h co-localization with DCs was significantly more pronounced with the PEGylated polyplexes compared to non-PEGylated PAEM polyplexes (Fig. 4.7B). From day 1 to 4 there was an increase in co-localization of both the PEI and PAEM polyplexes with DCs, and much of the co-localization or interaction between polyplexes and DCs was limited to the edges of the aggregates; apparently, DCs had little capacity of breaking apart the dense clumps of polyplex aggregates. Combining tissue sections through the edge of aggregates (where co-localization was high) with those through the middle of aggregates (where co-localization was rare) likely resulted in the large error range in the average value of fraction of co-localization for the PEI polyplexes at days 1 and 4 (Fig. 4.7B).

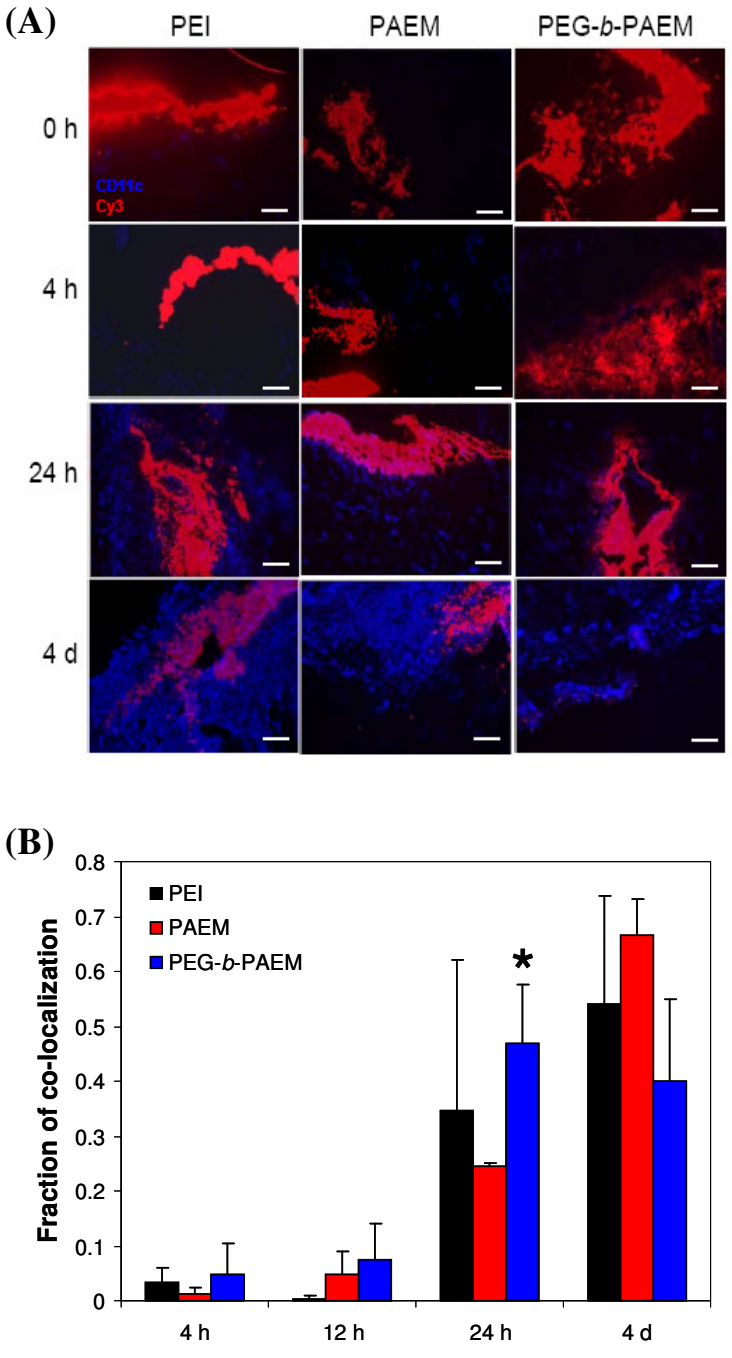

Figure 4.7: Cellular distribution of polyplexes and interaction with DCs at the injection site. (A) Representative fluorescence microscopy images showing DNA labeled with Cy3 (red), and DCs stained for CD11c (blue). Scale bar: 100 µm. (B) Quantification of the fraction of co-localization between DNA and DCs defined as the ratio of pixel areas between co-localized DNA signal and the total DNA signal. *PEGylated polyplexes showed statistically more co-localization with DCs than PAEM-based polyplexes at 24 h (*t* test, $p<0.05$).

4.3.5.3. Macrophages

Similar to the observations made on DCs, the infiltration to the injection site by macrophages occurred at least 1 day after injection (Fig. 4.8A). Co-localization of polyplexes with macrophages did not appear to be as substantial as with DCs, but did increase with time (Fig. 4.8B). More PEGylated polyplexes co-localized with macrophages than non-PEGylated polyplexes, but the differences were not statistically significant.

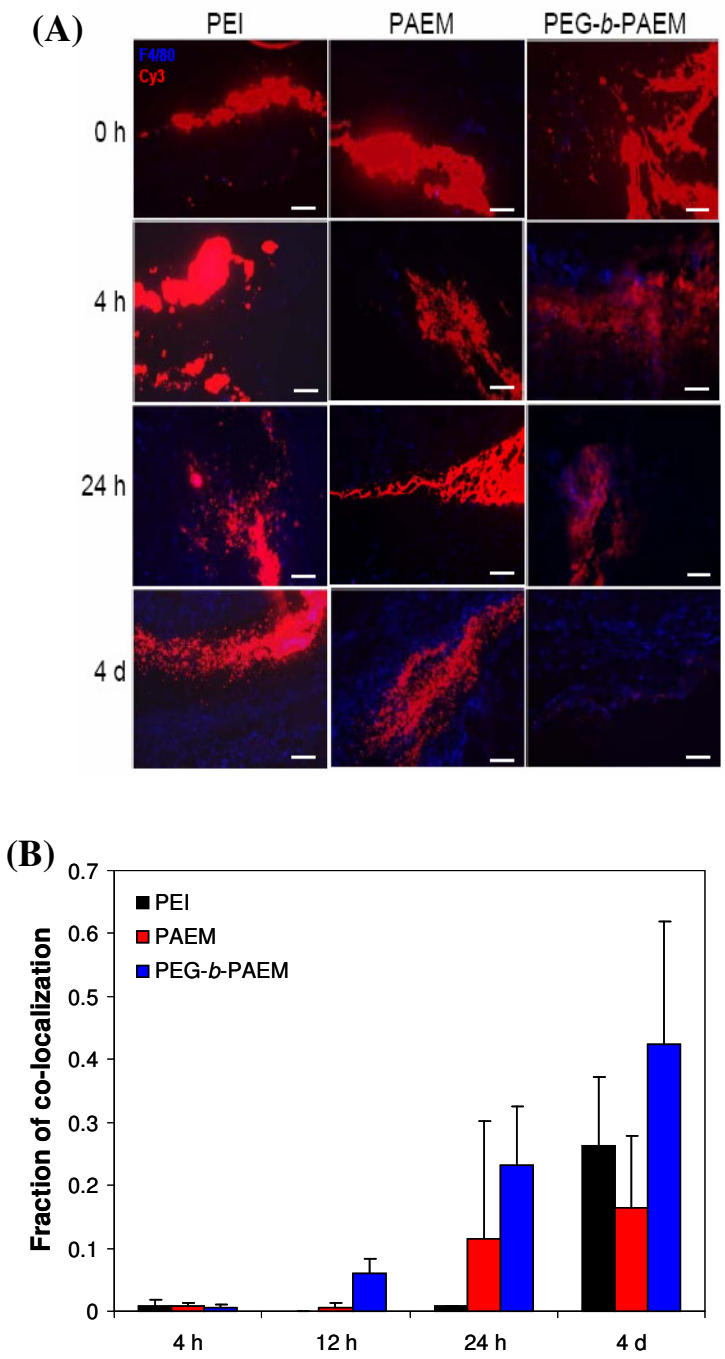

Figure 4.8: Cellular distribution of polyplexes and interaction with macrophages at the injection site. (A) Representative fluorescence microscopy images showing DNA labeled with Cy3 (red), and macrophages stained with F4/80 (blue). Scale bar: 100 µm. (B) Quantification of the fraction of co-localization between DNA and macrophages defined as the ratio of pixel areas between co-localized DNA signal and the total DNA signal.

4.3.6. Lymph Nodes

In addition to injection sites, the draining lymph nodes were also harvested, sectioned, and analyzed by fluorescence microscopy to determine possible draining of Cy3-labeled naked DNA and polyplexes. We found that naked DNA signal was not seen at any time point. A few punctate signals were visible beginning at 12 h after polyplex injection and increased slightly 4 days after injection (Fig. 4.9). Overall, the presence of polyplexes in the draining lymph nodes was rare. The punctuate signals of DNA was not necessarily co-localized with DCs stained by CD11c (data not shown), suggesting that perhaps some small fragments of polyplexes were able to migrate on their own through the lymphatic system from the injection site.

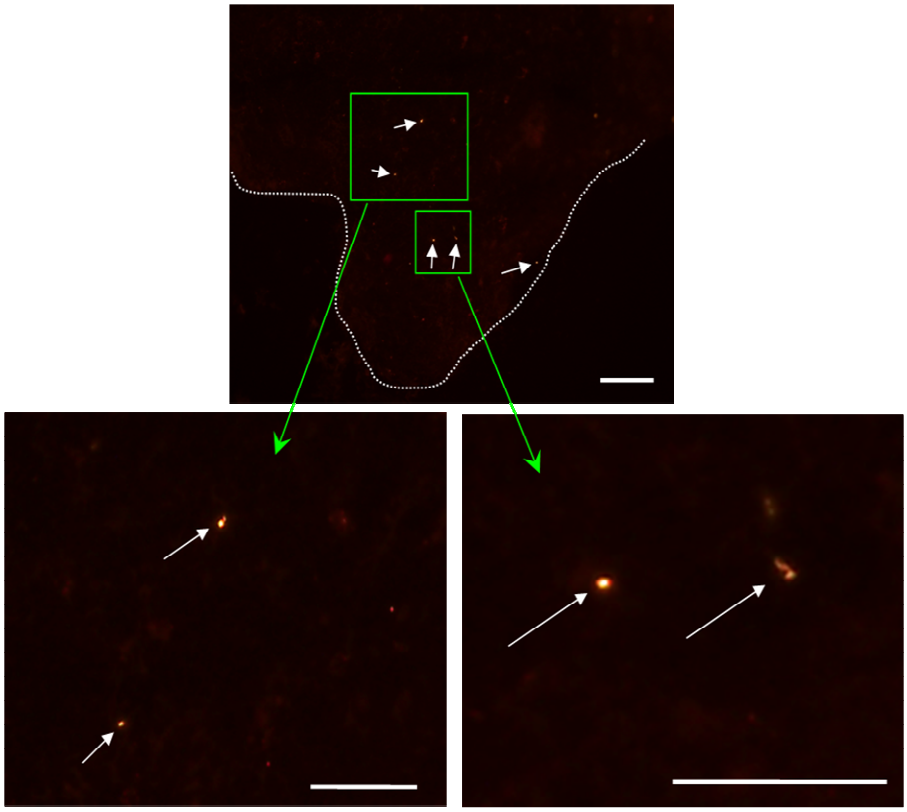

Figure 4.9: Polyplexes were rarely found in the draining lymph nodes of mice 4 days after intradermal injection. DNA was labeled with Cy3. Shown are representative images. White curve points to the outline of the lymph node tissue. Arrows point to punctate signals of polyplexes. No difference was found among different polymers. Drainage of naked DNA was not detected at any time point.

4.4. Discussion

This study focused on examining tissue and cellular distribution of naked DNA and polyplexes after intradermal injection into mice, aiming to uncover mechanisms and molecular design principles for more efficient polymer carriers for DNA vaccination in vivo. We paid special attention to the influence on in vivo distribution of DNA by using cationic polymer carriers with different molecular structures. With these studies we hope to shed light on the following three questions pertaining to polymer-mediated DNA vaccine delivery.

First, what are the benefits, if any, in using polyplexes rather than naked DNA for vaccination? Although it is well known that polymer carriers protect DNA from degradation and enhance cellular uptake, naked DNA vaccine alone has been quite successful in generating immune responses in vivo.[106] Here we have shown that from the standpoint of tissue and cellular distribution, it may be advantageous to use a cationic polymer carrier. Although naked DNA distributed to larger areas in the skin than polyplexes (Fig. 4.3), it persisted for only a short period of time (a few hours) and was depleted before the arrival of substantial number of APCs (DCs and macrophages) (Fig. 4.5). In contrast, polyplexes formed aggregates at the injection site, serving as reservoirs of DNA that persisted for much longer periods of time (days and weeks) (Fig. 4.4) and enabling subsequent interactions between DNA and APCs (Fig. 4.7 and 4.8). The presence of cationic polymers appeared to have attracted a large number of APCs by day 4, which is highly beneficial for the priming of immune responses.

Second, “to PEGylate or not to PEGylate”, that is still the question.[107] A popular drug delivery strategy, PEGylation has not yet been widely explored in DNA vaccine delivery

nor has its mechanism in vivo been clearly understood. PEGylation has long been used to enhance polyplex stability in high salt and serum environments.[31,98] Recently, Nomoto and colleagues observed directly the stabilization against aggregation by PEGylated polyplexes after intravenous injection in vivo.[108] We have carried out a similar experiment in simulated in vivo fluid environment by incubating fluorescently labeled DNA in complete cell culture medium containing serum. We visually observed substantial aggregation of non-PEGylated polyplexes and stabilization against aggregation by PEGylation (Fig. 4.2). Consistent with this in vitro finding, we found in live animals that the PEGylated polyplexes distributed to a broader area in the skin after intradermal injection than non-PEGylated polyplexes (Fig. 4.4). It was reported that PEGylated polyplexes and even naked DNA generated significantly more antigen expression and subsequent immune response than unprotected cationic polyplexes when delivered by tattooing.[8] The proposed explanation by the authors was the sequestration and deactivation of unprotected cationic polyplexes by negatively charged extracellular matrix.[109] While this is certainly possible, our in vitro and in vivo data here further suggest that limited diffusability of large, highly aggregated polyplexes inside tissue could be a major reason for the low efficiency of DNA vaccination reported earlier, and that PEGylated polyplexes would be advantageous due to their superior transport properties.

Third, what are the targeted cells in vivo for DNA vaccine? We showed that, due to its quick dispersion and transient presence at the injection site, naked DNA has mostly interacted with the dermal fibroblasts rather than with APCs, which arrived at the site late (Fig. 4.5). On the other hand, aggregates of polyplexes lasted much longer and were able

to interact with infiltrating APCs (Fig. 4.7 and 4.8), potentially leading to uptake and antigen expression. PEGylated polyplexes not only maintained a depot that attracted APC migration, but also appeared to spread more than non-PEGylated polyplexes, so as to encounter both incoming APCs and resident dermal fibroblasts (Fig. 4.6). Furthermore, in contrast to previous reports[99,110,111], we did not detect any direct draining of the naked DNA into the lymph node. This could be due to variations of the amount of DNA injected, injection volume, tissue section thickness, and fixation method. More importantly, lymphatic draining of the polyplexes was low and was observed only after 12 h regardless which polymer was used (Fig. 4.9), suggesting that direct targeting of resident APCs in the lymph node was not a significant pathway for the polyplexes studied, and perhaps for polyplexes in general as well.

Taken together, several lessons can be learned from our studies that may help improve the design of cationic polymers for DNA vaccine delivery. Much attention has been given to transfecting DCs directly with antigen-encoding DNA, since endogenous expression of antigen by DCs has been shown to result in strong cellular immune response.[68,71-73,112] To target DCs directly, one could use a polymer (such as PEI or PAEM) that protects and retains DNA at the peripheral site of administration for sufficiently long duration of time to allow DC infiltration and interaction. Comparing to the strategy of targeting DCs actively through DC-specific molecular ligands,[7,11] creating a depot of DNA at the periphery may be a more simple alternative approach to access DCs. Furthermore, instead of transfecting DCs directly, cross-presentation through bystander cells has been suggested to be an important pathway in the development of a cellular immune response by DNA vaccine.[79-82] In this case, bystander cells (such as

fibroblasts) can be transfected by polyplexes, express antigen, and be cross-presented by DCs through MHC-I molecules. To target the cross-presentation pathway, PEGylated polyplexes would be preferred because of their high stability, less aggregation, neutrally charged particle surface, and wider distribution among bystander cells. In fact, PEGylated carriers such as PEG-*b*-PAEM that combine good diffusivity in tissue with a moderate depot effect would be ideal for targeting DNA vaccine to both bystander cells and infiltrating APCs at the periphery, so as to exploit both pathways of cross-presentation and direct DC transfection. Thus, further studies will focus on illuminating the relationship between different polymer carrier designs and antigen presentation as well as immune responses in vivo.

4.5. Conclusions

The tissue and cellular distributions of plasmid DNA using different cationic polymers were analyzed after intradermal injection in mice. We found that naked DNA dispersed quickly in hours within the injected tissue and showed limited interaction with APCs. On the other hand, polyplexes formed depots at the injection site and persisted for up to 2 weeks to interact with infiltrating APCs. PEGylated polyplexes, in particular, possessed superior stability against aggregation than non-PEGylated polyplexes, and they distributed further inside tissue that promoted interaction with both the APCs and dermal fibroblasts. These findings provide in vivo evidence to support the use of PEGylated polymer carriers for DNA vaccine delivery and suggest possible approaches to further improve polymer design.

Chapter 5: Overall Conclusions and Future Prospects

Much attention has been given to developing polymeric delivery systems that will efficiently deliver DNA for vaccination. However, the efficiency of immune response generation by these vehicles has generally been very low. This thesis focuses on our attempts to optimize DNA vaccination using polymeric delivery systems. First, as described in Chapter 2, we evaluated the feasibility of using the CD40L as both a targeting moiety and adjuvant for delivery to dendritic cells. We did observe enhanced uptake of polystyrene particles coated with the CD40L to DCs in vitro. However, the stimulus of DC maturation was low, probably because a monomeric form of the binding domain, fused to a large maltose binding protein to improve expression in bacteria, was used. Targeting in vivo was also inefficient, likely because of complications present in the in vivo environment. Unfortunately, trimeric versions of the protein were attempted and were relatively unstable in solution at biologically useful concentrations.

In Chapter 3 we investigated the use of polyplex-mediated delivery to bystander cells to generate MHC class I antigen presentation and cellular immune response. We were able to confirm that delivery of antigen-encoding DNA to fibroblasts using PEI based polyplexes is able to generate MHC class I restricted expression on dendritic cells. The cross-presentation appears to dependent on toxicity in bystander cells, despite lower antigen expression in these conditions. Fibroblast toxicity also led to enhanced maturation of co-cultured DCs and improved antigen-specific T cell stimulation. These

finding suggest cross-presentation may be an ideal pathway for generating a cellular immune response and some cellular toxicity is not only acceptable but beneficial for vaccine efficiency.

These investigations, as well as those of many other groups, focused mainly on in vitro interactions. In order to better understand how cationic polyplexes interact with cells in vivo, we evaluated the macro- and microscopic distributions of polymer/DNA complexes after intradermal injection. Polyplexes were formed using Cy3-labeled DNA using various cationic polymers, including branched PEI, an unbranched cationic polymer developed in our lab, PAEM, and a PEGylated version of the same PAEM polymer. We quantified the distribution of DNA over time and characterized cell-specific interactions at the injection site. These observations yielded information about the timeline and cellular interactions of cationic polymers and how they are affected by tissue distribution. It was determined that complexes made with the PEGylated polymer had the best tissue distribution compared to unprotected polyplexes, and that this allowed for increased interaction with fibroblasts at early timepoints. DCs and macrophages were also able to penetrate the injection site of PEGylated polyplexes at earlier timepoints, though interaction with infiltrating DCs was similar by later timepoints. These interactions suggest optimal polyplex compositions, depending on the desired vaccination strategy.

Better characterization is still needed of polyplex interactions in vivo. It will be necessary in the future to evaluate not only polyplex interactions with specific cell types but also antigen expression and presentation on DCs, both at the injection site and in the lymph nodes. Transfection with plasmid DNA encoding fluorescent protein can be

difficult to visualize in vivo because of various sources of autofluorescence. However, using antibody staining to enhance the signal may provide clear information. In addition, it would be interesting to evaluate cellular interactions at later timepoints since we know the DNA signal is still present. It would then be possible to better evaluate at which time antigen expression, antigen presentation on DCs, and DC infiltration of the injection site peak with different polyplexes.

Our work with bystander cells suggests that some cellular toxicity is necessary for efficient cross-presentation. It would be interesting, therefore, to evaluate MHC class I restricted antigen expression on dendritic cells and correlate the results with toxicity and inflammation present at the injection site. Our results suggest that, particularly if bystander cells were transfected, some toxicity may be beneficial to both antigen presentation and maturation of DCs, leading to a more effective immune response. In moderation, allowing some polymer-mediated toxicity could be a viable option for increasing the cellular immune response, and could be particularly suited to vaccination targeted to tumor sites. It could also be useful to include plasmid DNA encoding proteins shown to enhance cross-presentation, such as heat shock proteins, into delivery vehicles. This could potentially further enhance antigen presentation on DCs. In fact, it has been shown that the delivery of hsp70 was effective in enhancing immune response generated by cell death against cancer cells.[90-93] Additionally, our observations in Chapter 3 indicated that the addition of LPS enhanced DC stimulation of T cells even past that achieved after co-culture with fibroblasts transfected at higher N/P ratios. This suggests that while some cyotoxicity is an effective adjuvant, alternative materials can be used to enhance the immune response further. This can be tested either by adding an adjuvant

days after initial DNA delivery or by delivering adjuvant-encoding DNA along with antigen-encoding plasmid. The timing, location, and method of adjuvant delivery will likely need to be further studied and optimized.

There are many factors that can affect DNA vaccines in vivo. The injection site or type chosen, maturation stimulus provided, even route of cellular uptake, all effect how DCs process and present antigen, as well as what type of immune response they will stimulate.[7,11] There are many different subsets of DCs, residing in separate tissues and each with their own functional strengths and weaknesses. The functions of these subsets are still not fully understood, but it is known, for example, that plasmacytoid DCs, which reside mainly in the lymphatic system, are particularly efficient at secreting type I IFNs, an important component of innate immune response stimulation.[9,11,113] Myeloid DCs, on the other hand, found mainly in interstitial tissues, can secrete high levels of IL-12, which generally leads to strong $CD8^+$ T cell stimulation and cellular immune response.[9,11] There are also many tissue specific DC subtypes, such as Langerhans cells in the skin, that appear to play an important role in generating immunity when vaccine is delivered there.[114] Therefore, the injection site can play an important role in the type of immune response generated and must be taken into account. For example, systemic immunization, such as with intramuscular injections, generally does not stimulate a strong mucosal immune response. However, when vaccine is delivered directly to mucosal regions, such as after vaccination through the airways, a stronger response in generated, at least to that specific mucosal site.[11] In addition, it seems that some DC subsets, particularly $CD8^+$ DCs, found primarily in the lymphatic system, are able to cross-present antigen more efficiently than others.[11,75,115] Therefore, careful characterization not only of general cell

types, but also of the specific subset of DCs interacting with injected polyplex would be informative. Since different subsets are present in different locations, characterizations should be performed and immune response should be evaluated after delivery to different injection sites.

There may also be better ways of delivering polyplex than injection with a needle. For example, some groups have evaluated the use of microneedles for delivery into skin. This technology consists of a patch containing many solid microneedles coated with the desired material to be delivered. It has been shown that these needles can penetrate murine skin and deliver PLGA-based delivery system.[116] This is an ideal delivery system as the skin is particularly suited for vaccination due to its relatively high concentration of DCs.[10] The use of a microneedle injection system could potentially expand the distribution of polymeric delivery and minimize aggregation, as it is equivalent to many small injections rather than one bolus injection. This could improve DNA delivery to both bystander cells and DCs. In addition, polyplex could be delivered to multiple levels of the skin, from the epidermal layer into the dermis. This would be a more efficient method to deliver material to the DC-rich environment of the epidermis, which contains relatively high concentrations of Langerhans cells,[10] since intradermal injection, especially in thin murine skin, is difficult to perform reliably.

This thesis focuses on investigations of various methods for improving vaccination using polymer-based DNA delivery. Our observations have demonstrated several methods for optimizing delivery vehicles. However, to generate immune responses applicable to the clinical settings, continued characterization and optimization will likely be necessary.

Chapter 6: References

[1] Figdor, C. G.; de Vries, I. J. M.; Lesterhuis, W. J.; Melief, C. J. M. Dendritic cell immunotherapy: mapping the way. *Nat. Med.* **2004**, 10, 475-480.

[2] Heiser, A.; Coleman, D.; Dannull, J.; Yancey, D.; Maurice, M. A.; Lallas, C. D.; Dahm, P.; Niedzwiecki, D.; Gilboa, E.; Vieweg, J. Autologous dendritic cells transfected with prostate-specific antigen RNA stimulate CTL responses against metastatic prostate tumors. *J Clin Invest.* **2002**, 109, 409-417.

[3] Nestle, F. O.; Farkas, A.; Conrad, C. Dendritic-cell-based therapeutic vaccination against cancer. *Curr. Opin. Immunol.* **2005**, 17, 163-169.

[4] Ribas, A. Genetically Modified Dendritic Cells for Cancer Immunotherapy. *Curr. Gene Ther.* **2005**, 5, 619-628.

[5] Ribas, A.; Butterfield, L. H.; Glaspy, J. A.; Economou, J. S. Cancer Immunotherapy Using Gene-Modified Dendritic Cells. *Curr. Gene Ther.* **2002**, 2, 57-78.

[6] Dullaers, M.; Thielemans, K. From pathogen to medicine: HIV-1-derived lentiviral vectors as vehicles for dendritic cell based cancer immunotherapy. *J. Gene Med.* **2006**, 8, 3-17.

[7] Nguyen, D. N.; Green, J. J.; Chan, J. M.; Langer, R.; Anderson, D. G. Polymeric Materials for Gene Delivery and DNA Vaccination. *Adv. Mater.* **2009**, 21, 847-867.

[8] van den Berg, J. H.; Nuijen, B.; Schumacher, T. N.; Haanen, J. B. A. G.; Storm, G.; Beijnen, J. H.; Hennink, W. E. Synthetic vehicles for DNA vaccination. *J. Drug Targ.* **2010**, 18, 1-14.

[9] Banchereau, J.; Briere, F.; Caux, C.; Davoust, J.; Lebecque, S.; Liu, Y.; Pulendran, B.; Palucka, K. Immunobiology of Dendritic Cells. *Annu. Rev. Immunol.* **2000**, 18, 767-811.

[10] Foged, C.; Sundblad, A.; Hovgaard, L. Targeting Vaccines to Dendritic Cells. *Pharm Res* **2002**, 3, 229-238.

[11] Hubbell, J. A.; Thomas, S. N.; Swartz, M. A. Materials engineering for immunomodulation. *Nature* **2009**, 462, 449-460.

[12] Adams, S.; O'Neill, D. W.; Bhardwah, N. Recent Advances in Dendritic Cell Biology. *J. Clin. Immunol.* **2005**, 25, 87-98.

[13] Banchereau, J.; Palucka, A. K. Dendritic Cells as Therapeutic Vaccines Against Cancer. *Nat. Rev. Immunol.* **2005**, 5, 296-306.

[14] Steinman, R. M.; Hawiger, D.; Liu, K.; Bonifaz, L.; Bonnyay, D.; Mahnke, K.; Iyoda, T.; Vetch, J. R.; Dhodapkar, M. V.; Inaba, K.; Nussenzweig, M. Dendritic Cell Function *in Vivo* during the Steady State: A Role in Peripheral Tolerance. *Ann. N. Y. Acad. Sci.* **2003**, 987, 15-25.

[15] Berntsen, A.; Geertsen, P. F.; Svane, I. M. Therapeutic Dendritic Cell Vaccination of Patients with Renal Cell Carcinoma. *Eur. Urol.* **2006**, 50, 34-43.

[16] Lepisto, A. J.; Moser, A. J.; Zeh, H.; Lee, K.; Bartlett, D.; McKolanis, J. R.; Geller, B. A.; Schmotzer, A.; Potter, D. P.; Whiteside, T.; Finn, O. J.; Ramanathan, R. K. A phase I/II study of a MUC1 peptide pulsed autologous dendritic cell vaccine as adjuvant therapy in patients with resected pancreatic and biliary tumors. *Cancer Ther.* **2008**, 6, 955-964.

[17] Lopez, M. N.; Pereda, C.; Segal, G.; Munoz, L.; Aguilera, R.; Gonzalez, F. E.; Escobar, A.; Ginesta, A.; Reyes, D.; Gonzalez, R.; Mendoza-Naranjo, A.; Larrondo, M.; Compan, A.; Ferrada, C.; Salazar-Onfray, F. Prolonged Survival of Dendritic Cell–Vaccinated Melanoma Patients Correlates With Tumor-Specific Delayed Type IV Hypersensitivity Response and Reduction of Tumor Growth Factor-Expressing T Cells. *J. Clin. Oncol.* **2009**, 27, 945-952.

[18] Nair, S.; McLaughlin, C.; Weizer, A.; Su, Z.; Boczkowski, D.; Dannull, J.; Vieweg, J.; Gilboa, E. Injection of Immature Dendritic Cells into Adjuvant-Treated Skin Obviates the Need for Ex Vivo Maturation. *J. Immunol.* **2003**, 171, 6275-6282.

[19] Tacken, P. J.; Torensma, R.; Figdor, C. G. Targeting antigens to dendritic cells in vivo. *Immunobiology* **2006**, 211, 599-608.

[20] O'Hagan, D. T.; Singh, M.; Ulmer, J. B. Microparticles for the delivery of DNA vaccines. *Immunol. Rev.* **2004**, 199, 191-200.

[21] Glover, D. J.; Lipps, H. J.; Jans, D. A. Towards Safe, Non-Viral Therapeutic Gene Expression in Humans. *Nat. Rev. Genetics* **2005**, 6, 299-311.

[22] Little, S. R.; Lynn, D. M.; Puram, S. V.; Langer, R. Formulation and characterization of poly (B amino ester)microparticles for genetic vaccine delivery. *J. Cont. Release* **2005**, 107, 449-462.

[23] O'Hagan, D. T.; Rappuoli, R. Novel Approaches to Vaccine Delivery. *Pharm. Res.* **2004**, 21, 1519-1530.

[24] Lutsiak, M. E. C.; Robinson, D. R.; Coester, C.; Kwon, G. S.; Samuel, J. Analysis of Poly(D,L-Lactic-Co-Glycolic Acid) Nanosphere Uptake by Human Dendritic Cells and Macrophages *In Vitro*. *Pharm. Res.* **2002**, 19, 1480-1487.

[25] Newman, K. D.; Elamanchili, P.; Kwon, G. S.; Samuel, J. Uptake of poly(D,L-lactic-*co*-glycolic acid) microspheres by antigen-presenting cells *in vivo*. *Journal of Biomedical Materials Research* **2002**, 60, 480-486.

[26] Singh, M.; Ugozzoli, M.; Briones, M.; Kazzaz, J.; Soenawan, E.; O'Hagan, D. T. The Effect of CTAB Concentration in Cationic PLG Microparticles on DNA Adsorption and *in Vivo* Performance. *Pharm. Res.* **2003**, 20, 247-251.

[27] Denis-Mize, K. S.; Dupuis, M.; MacKichan, M. L.; Singh, M.; Doe, B.; O'Hagan, D.; Ulmer, J. B.; Donnelly, J. J.; McDonald, D. M.; Ott, G. Plasmid DNA adsorbed onto cationic microparticles mediates target gene expression and antigen presentation by dendritic cells. *Gene Therapy* **2000**, 7, 2105-2112.

[28] Lungwitz, U.; Breunig, M.; Blunk, T.; Gopferich, A. Polyethylenimine-based non-viral gene delivery systems. *Eur. J. Pharm. Biopharm.* **2005**, 60, 247-266.

[29] Khalil, I. A.; Kogure, K.; Akita, H.; Harashima, H. Uptake Pathways and Subsequent Intracellular Trafficking in Nonviral Gene Delivery. *Pharm. Rev.* **2006**, 58, 32-45.

[30] Medina-Kauwe, L. K.; Xie, J.; Hamm-Alvarez, S. Intracellular trafficking of nonviral vectors. *Gene Ther.* **2005**, 12, 1734-1751.

[31] Lee, M.; Kim, S. W. Polyethylene Glycol-Conjugated Copolymers for Plasmid DNA Delivery. *Pharm. Res.* **2005**, 22, 1-10.

[32] Oster, C. G.; Kim, N.; Grodeb, L.; Barbu-Tudoran, L.; Schaper, A. K.; Kaufmann, S. H. E.; Kissel, T. Cationic microparticles consisting of poly(lactide-co-glycolide) and polyethylenimine as carriers systems for parental DNA vaccination. *J. Cont. Release* **2005**, 104, 359-377.

[33] Kasturi, S. P.; Sachaphibulkij, K.; Roy, K. Covalent conjugation of polyethyleneimine on biodegradable microparticles for delivery of plasmid DNA vaccines. *Biomaterials* **2005**, 26, 6375-6385.

[34] Kichler, A.; Chillon, M.; Leborgne, C.; Danos, O.; Frisch, B. Intranasal gene delivery with a polyethylenimine–PEG conjugate. *J. Cont. Release* **2002**, 81, 379-388.

[35] Blessing, T.; Kursa, M.; Holzhauser, R.; Kircheis, R.; Wagner, E. Different Strategies for Formation of PEGylated EGF-Conjugated PEI/DNA Complexes for Targeted Gene Delivery. *Bioconjugate Chem.* **2001**, 12, 529-537.

[36] Ogris, M.; Walker, G.; Blessing, T.; Kircheis, R.; Wolschek, M.; Wagner, E. Tumor-targeted gene therapy: strategies for the preparation of ligand-polyethylene glycol-polyethylenimine /DNA complexes. *J. Cont. Release* **2003**, 91, 173-181.

[37] Thiele, L.; Rothen-Rutishauser, B.; Jilek, S.; Wunderli-Allenspach, H.; Merkle, H. P.; Walter, E. Evaluation of particle uptake in human blood monocyte-derived cells in vitro. Does phagocytosis activity of dendritic cells measure up with macrophages? *J. Cont. Release* **2001**, 76, 59-71.

[38] Boussif, O.; Lezoualch, F.; Zanta, M. A.; Mergny, M. D.; Scherman, D.; Demeneix, B.; Behr, J. A versatile vector for gene and oligonucleotide transfer into cells in culture and *in vivo*: Polyethylenimine. *PNAS* **1995**, 92, 7297-7301.

[39] Walker, G. F.; Fella, C.; Pelisek, J.; Fahrmeir, J.; Boeckle, S.; Ogris, M.; Wagner, E. Toward Synthetic Viruses: Endosomal pH-Triggered Deshielding of Targeted Polyplexes Greatly Enhances Gene Transfer in Vitro and in Vivo. *Mol. Ther.* **2005**, 11, 418-425.

[40] Foged, C.; Brodin, B.; Frokjaer, S.; Sundblad, A. Particle size and surface charge affect particle uptake by human dendritic cells in an *in vitro* model. *Int. J. Pharm.* **2005**, 298, 315-322.

[41] Jilek, S.; Merkle, H. P.; Walter, E. DNA-loaded biodegradable microparticles as vaccine delivery systems and their interaction with dendritic cells. *Adv. Drug Deliv. Rev.* **2005**, 57, 377-390.

[42] Wang, C.; Ge, Q.; Ting, D.; Nguyen, D.; Shen, H.; Chen, J.; Eisen, H. N.; Heller, J.; Langer, R.; Putnam, D. Molecularly engineered poly(ortho ester) microspheres for enhanced delivery of DNA vaccines. *Nat. Mat.* **2004**, 3, 190-196.

[43] Reddy, S. T.; Rehor, A.; Schmoekel, H. G.; Hubbell, J. A.; Swartz, M. A. In vivo targeting of dendritic cells in lymph nodes with poly(propylene sulfide) nanoparticles. *J. Controlled Release* **2006**, 112, 26-34.

[44] Panyam, J.; Labhasetwar, V. Biodegradable nanoparticles for drug and gene delivery to cells and tissue. *Adv. Drug Deliv. Rev.* **2003**, 55, 329-347.

[45] O'Hagan, D. T.; Valiante, N. M. Recent advances in the discovery and delivery of vaccine adjuvants. *Nat. Rev. Drug. Discov.* **2003**, 2, 727-735.

[46] Jilek, S.; Ulrich, M.; Merkle, H. P.; Walter, E. Composition and surface charge of DNA-loaded microparticles determine maturation and cytokine secretion in human dendritic cells. *Pharm. Res.* **2004**, 21, 1240-1247.

[47] Reddy, S. T.; van der Vlies, A. J.; Simeoni, E.; Angeli, V.; Randolph, G. J.; O'Neil, C. P.; Lee, L. K.; Swartz, M. A.; Hubbell, J. Exploiting lymphatic transport and complement activation in nanoparticle vaccines. *Nat. Biotech.* **2007**, 25, 1159-1164.

[48] Wischke, C.; Borchert, H. H.; Zimmermann, J.; Siebenbrodt, I.; Lorenzen, D. R. Stable cationic microparticles for enhanced model antigen delivery to dendritic cells. *J Control Release* **2006**, 114, 359-368.

[49] Babensee, J. E. Interaction of dendritic cells with biomaterials. *Semin Immunol* **2008**, 20, 101-108.

[50] Wattendorf, U.; Coullerez, G.; Vörös, J.; Textor, M.; Merkle, H. P. Mannose-based molecular patterns on stealth microspheres for receptor-specific targeting of human antigen-presenting cells. *Langmuir* **2008**, 24, 11790-11802.

[51] Cruz, L. J.; Tacken, P. J.; Fokkink, R.; Joosten, B.; Stuart, M. C.; Albericio, F.; Torensma, R.; Figdor, C. G. Targeted PLGA nano- but not microparticles specifically deliver antigen to human dendritic cells via DC-SIGN *in vitro*. *J Control Release* **2010**, 144, 118-126.

[52] Kwon, Y. J.; James, E.; Shastri, N.; Frechet, J. M. J. In vivo targeting of dendritic cells for activation of cellular immunity using vaccine carriers based on pH-responsive microparticles. *PNAS* **2005**, 102, 18264-18268.

[53] van Kooten, C.; Banchereau, J. CD40-CD40 ligand. *J. Leukoc. Biol.* **2000**, 67, 2-17.

[54] Mackey, M. F.; Gunn, J. R.; Maliszewski, C.; Kikutani, H.; Noelle, R. J.; Barth Jr., R. J. Dendritic cells require maturation via CD40 to generate protective antitumor immunity. *J. Immunol.* **1998**, 161, 2094-2098.

[55] Kelleher, M.; Beverley, P. C. L. Lipopolysaccharide modulation of dendritic cells is insufficient to mature dendritic cells to generate CTLs from naïve polyclonal CD8+ T cells *in vitro*, whereas CD40 ligation is essential. *J. Immunol.* **2001**, 167, 6247-6255.

[56] Gurunathan, S.; Irvine, K. R.; Yu, C.; Cohen, J. I.; Thomas, E.; Prussin, C.; Seder, R. A. CD40 ligand/trimer DNA enhances both humoral and cellular immune responses and induced protective immunity to infectious and tumor challenge. *J. Immunol.* **1998**, 161, 4563-4571.

[57] Pereboev, V.; Nagle, J. M.; Shkhmatov, M. A.; Triozzi, P. L.; Matthews, Q. L.; Kawakami, Y.; Curiel, D. T.; Blackwell, J. L. Enhanced gene transfer to mouse dendritic cells using adnoviral vectors coated with a novel adapter molecule. *Mol Therapy* **2004**, 9, 712-720.

[58] Belousova, N.; Korokhov, N.; Krendelshchikova, V.; Simonenko, V.; Mikheeva, G.; Triozzi, P. L.; Aldrich, W. A.; Banerjee, P. T.; Gillies, S. D.; Curiel, D. T.; Krasnykh, V. Genetically targeted adenovirus vector directed to CD40-expressing cells. *J. Virol.* **2003**, 77, 11367-11377.

[59] Inaba, K.; Inaba, M.; Romani, N.; Aya, H.; Deguchi, M.; Ikehara, S.; Muramatsu, S.; Steinman, R. M. Generation of large numbers of dendritic cells from mouse bone marrow cultures supplemented with granulocyte/macrophage colony-stimulating factor. *J. Exp. Med.* **1992**, 176, 1693-1702.

[60] Armitage, R. J.; Fanslow, W. C.; Strockbine, L.; Sato, T. A.; Clifford, K. N.; Macduff, B. M. Molecular and biological characterization of a murine ligand for CD40. *Nature* **1992**, 357, 80-82.

[61] Stone, G. W.; Barzee, S.; Snarsky, V.; Kee, K.; Spina, C. A.; Yu, X. F.; Kornbluth, R. S. Multimeric soluble CD40 ligand and GITR ligand as adjuvants for human immunodeficiency virus DNA vaccines. *J Virol.* **2006**, 80, 1762-1772.

[62] Moris, A. E.; Remmele, R. L.; Klinke, R.; Macduff, B. M.; Fanslow, W. C.; Armitage, R. J. Incorporation of an isoleucine zipper motif enhances the biological activity of soluble CD40L (CD154). *J Biol Chem* **1999**, 274, 418-423.

[63] Tacken, P. J.; de Vries, I. J.; Torensma, R.; Figdor, C. G. Dendritic-cell immunotherapy: from ex vivo loading to *in vivo* targeting. *Nat Rev Immunol* **2007**, 7, 790-802.

[64] Ogawara, K.; Yoshida, M.; Takakura, Y.; Hashida , M.; Higaki, K.; Kimura, T. Interaction of polystyrene microspheres with liver cells: roles of membrane receptors and serum proteins. *Biochim Biophys Acta* **1999**, 1472, 165-172.

[65] Vonderheide, R. H.; Dutcher, J. P.; Anderson, J. E.; Eckhardt, S. G.; Stephans, K. F.; Razvillas, B.; Garl, S.; Butine, M. D.; Perry, V. P.; Armitage, R. J.; Ghalie, R.; Caron, D. A.; Gribben, J. G. Phase I study of recombinant human CD40 ligand in cancer patients. *J Clin Oncol* **2001**, 19, 3280-3287.

[66] Tong, A. W.; Stone, M. J. Prospects for CD40-directed experimental therapy of human cancer. *Cancer Gene Therapy* **2003**, 10, 1-13.

[67] Rock, K. L.; Shen, L. Cross-presentation: underlying mechanisms and role in immune surveillance. *Immunol. Rev.* **2005**, 207, 166-183.

[68] Hattori, Y.; Kawakami, S.; Suzuki, S.; Yamashita, F.; Hashida, M. Enhancement of immune responses by DNA vaccination through targeted gene delivery using mannosylated cationic liposome formulations following intravenous administration. *Biochemical and Biophysical Research Communications* **2004**, 317, 992-999.

[69] van Broekhoven, C. L.; Parish, C. R.; Demangel, C.; Britton, W. J.; Altin, J. G. Targeting Dendritic Cells with Antigen-Containing Liposomes: A Highly Effective

Procedure for Induction of Antitumor Immunity and for Tumor Immunotherapy. *Canc. Res.* **2004**, 64, 4357-4365.

[70] Nchinda, G.; Kuroiwa, J.; Oks, M.; Trumpfheller, C.; Park, C. G.; Huang, Y.; Hannaman, D.; Schlesinger, S. J.; Mizenina, O.; Nussenzweig, M. C.; Überla, K.; Steinman, R. M. The efficacy of DNA vaccination is enhanced in mice by targeting the encoded protein to dendritic cells. *J Clin Invest.* **2008**, 118, 1427-1436.

[71] Hattori, Y.; Kawakami, S.; Nakamura, K.; Yamashita, F.; Hashida, M. Efficient Gene Transfer into Macrophages and Dendritic Cells by in Vivo Gene Delivery with Mannosylated Lipoplex via the Intraperitoneal Route. *J Pharm Exp Ther* **2006**, 318, 828-834.

[72] Un, K.; Kawakami, S.; Suzuki, R.; Maruyama, K.; Yamashita, F.; Hashida, M. Enhanced Transfection Efficiency into Macrophages and Dendritic Cells by a Combination Method Using Mannosylated Lipoplexes and Bubble Liposomes with Ultrasound Exposure. *Human Gene Therapy* **2010**, 21, 65-74.

[73] Elnekave, M.; Furmanov, K.; Nudel, I.; Arizon, M.; Clausen, B. E.; Hovav, A. Directly Transfected Langerin+ Dermal Dendritic Cells Potentiate CD8+ T Cell Responses following Intradermal Plasmid DNA Immunization. *J. Immunol.* **2010**, 185, 3463-3471.

[74] Jilek, S.; Zurkaulen, H.; Pavlovic, J.; Merkle, H. P.; Walter, E. Transfection of a mouse dendritic cell line by plasmid DNA-loaded PLGA microparticles in vitro. *European Journal of Pharmaceutics and Biopharmaceutics* **2004**, 58, 491-499.

[75] Ackerman, A. L.; Cresswell, P. Cellular mechanisms governing cross-presentation of exogenous antigens. *Nat. Immunol.* **2004**, 5, 678-684.

[76] Burgdorf, S.; Scholz, C.; Kautz, A.; Tampe, R.; Kurts, C. Spatial and mechanistic separation of crosspresentation and endogenous antigen presentation. *Nat. Immunol.* **2008**, 9, 558-566.

[77] Winau, F.; Weber, S.; Sad, S.; de Diego, J.; Hoops, S. L.; Breiden, B.; Sandhoff, K.; Brinkmann, V.; Kaufmann, S. H. E.; Schaible, U. E. Apoptotic Vesicles Crossprime CD8 T Cells and Protect against Tuberculosis. *Immunity* **2006**, 24, 105-117.

[78] Coombes, B. K.; Mahony, J. B. Dendritic cell discoveries provide new insight into the cellular immunobiology of DNA vaccines. *Immunol. Lett.* **2001**, 78, 103-111.

[79] Cao, B.; Bruder, J.; Kovesdi, I.; Huard, J. Muscle stem cells can act as antigen-presenting cells: implication for gene therapy. *Gene Therapy* **2004**, 11, 1321-1330.

[80] Ulmer, J. B.; Deck, R. R.; Dewitt, C. M.; Donnelly, J. J.; Liu, M. A. Generation of MHC class I-restricted cytotoxic T lymphocytes by expression of a viral protein in muscle cells: antigen presentation by non-muscle cells. *Immunology* **1996**, 89, 59-67.

[81] Cho, J. H.; Youn, J. W.; Sung, Y. C. Cross-Priming as a Predominant Mechanism for Inducing CD8+ T Cell Responses in Gene Gun DNA Immunization. *J. Immunol.* **2001**, 167, 5549-5559.

[82] Hon, H.; Oran, A.; Brocker, T.; Jacob, J. B Lymphocytes Participate in Cross-Presentation of Antigen following Gene Gun Vaccination. *J. Immunol.* **2005**, 174, 5233-5242.

[83] Zhou, X.; Liu, B.; Yu, X.; Zha, X.; Zhang, X.; Wang, X.; Jin, Y.; Wu, Y.; Chen, Y.; Shan, Y.; Chen, Y.; Liu, J.; Kong, W.; Shen, J. Controlled release of PEI/DNA complexes from PLGA microspheres as a potent delivery system to enhance immune

response to HIV vaccine DNA prime/MVA boost regime. *European Journal of Pharmaceutics and Biopharmaceutics* **2008**, 68, 589-595.

[84] Ma, Y.; Yang, Y. Delivery of DNA-based cancer vaccine with polyethylenimine. *European Journal of Pharmaceutical Sciences* **2010**, 40, 75-83.

[85] Singh, M.; Briones, M.; Ott, G.; O'Hagan, D. Cationic microparticles: A potent delivery system for DNA vaccines. *PNAS* **2000**, 97, 811-816.

[86] Kurts, C.; Miller, J. F. A. P.; Subramaniam, R. M.; Carbone, F. R.; Heath, W. R. Major Histocompatibility Complex Class I–restricted Cross-presentation Is Biased towards High Dose Antigens and Those Released during Cellular Destruction. *The Journal of Experimental Medicine* **1998**, 188, 409-414.

[87] Binder, R. J.; Srivastava, P. K. Peptides chaperoned by heat-shock proteins are a necessary and sufficient source of antigen in the cross-priming of CD8+ T cells. *Nat. Immunol.* **2005**, 6, 593-599.

[88] Arnold-Schild, D.; Hanau, D.; Spehner, D.; Schmid, C.; Rammensee, H.; de la Salle, H.; Schild, H. Cutting Edge: Receptor-Mediated Endocytosis of Heat Shock Proteins by Professional Antigen-Presenting Cells. *The Journal of Immunology* **1999**, 162, 3757-3760.

[89] Doody, A. D. H.; Kovalchin, J. T.; Mihalyo, M. A.; Hagymasi, A. T.; Drake, C. G.; Adler, A. J. Glycoprotein 96 Can Chaperone Both MHC Class I- and Class II-Restricted Epitopes for In Vivo Presentation, but Selectively Primes CD8+ T Cell Effector Function. *The Journal of Immunology* **2004**, 172, 6087-6092.

[90] Daniels, G. A.; Sanchez-Perez, L.; Diaz, R. M.; Kottke, T.; Thompson, J.; Lai, M.; Gough, M.; Karim, M.; Bushell, A.; Chong, H.; Melcher, A.; Harrington, K.; Vile, R. G.

A simple method to cure established tumors by inflammatory killing of normal cells. *Nat. Biotech.* **2004**, 22, 1125-1132.

[91] Sanchez-Perez, L.; Kottke, T.; Daniels, G. A.; Diaz, R. M.; Thompson, J.; Pulido, J.; Melcher, A.; Vile, R. G. Killing of Normal Melanocytes, Combined with Heat Shock Protein 70 and CD40L Expression, Cures Large Established Melanomas. *J. Immunol.* **2006**, 177, 4168-4177.

[92] Kottke, T.; Sanchez-Perez, L.; Diaz, R. M.; Thompson, J.; Chong, H.; Harrington, K.; Calderwood, S. K.; Pulido, J.; Georgopoulos, N.; Selby, P.; Melcher, A.; Vile, R. Induction of hsp70-Mediated Th17 Autoimmunity Can Be Exploited as Immunotherapy for Metastatic Prostate Cancer. *Cancer Res.* **2007**, 67, 11970-11979.

[93] Kottke, T.; Pulido, J.; Thompson, J.; Sanchez-Perez, L.; Chong, H.; Calderwood, S. K.; Selby, P.; Harrington, K.; Strome, S. E.; Melcher, A.; Vile, R. G. Antitumor Immunity Can Be Uncoupled from Autoimmunity following Heat Shock Protein 70–Mediated Inflammatory Killing of Normal Pancreas. *Cancer Res.* **2009**, 69, 7767-7774.

[94] Peter, C.; Wesselborg, S.; Herrmann, M.; Lauber, K. Dangerous attraction: phagocyte recruitment and danger signals of apoptotic and necrotic cells. *Apoptosis* **2010**, 15, 1007-1028.

[95] Yang, Y.; Shen, S. Enhanced antigen delivery via cell death induced by the vaccine adjuvants. *Vaccine* **2007**, 25, 7763-7772.

[96] Shi, Y.; Rock, K. Cell death releases endogenous adjuvants that selectively enhance immune surveillance of particulate antigens. *Eur. J. Immunol.* **2002**, 32, 155-162.

[97] Shi, Y.; Zheng, W.; Rock, K. L. Cell injury releases endogenous adjuvants that stimulate cytotoxic T cell responses. *PNAS* **2000**, 97, 14590-14595.

[98] Mintzer, M. A.; Simanek, E. E. Nonviral Vectors for Gene Delivery. *Chem. Rev.* **2009**, 109, 259-302.

[99] Dupuis, M.; Denis-Mize, K.; Woo, C.; Goldbeck, C.; Selby, M. J.; Chen, M.; Otten, G. R.; Ulmer, J. B.; Donnelly, J. J.; Ott, G.; McDonald, D. M. Distribution of DNA Vaccines Determines Their Immunogenicity After Intramuscular Injection in Mice. *J. Immunol.* **2000**, 165, 2850-2858.

[100] Drabick, J. J.; Glasspool-Malone, J.; Somiari, S.; King, A. M.,Robert W. Cutaneous Transfection and Immune Responses to Intradermal Nucleic Acid Vaccination Are Significantly Enhanced by *in Vivo* Electropermeabilization. *Mol. Ther.* **2001**, 3, 249-255.

[101] Grønevik, E.; Tollefsen, S.; Sikkeland, L. I. B.; Haug, T.; Tjelle, T. E.; Mathiesen, I. DNA transfection of mononuclear cells in muscle tissue. *J. Gene Med.* **2003**, 5, 909-917.

[102] Peachman, K. K.; Rao, M.; Alving, C. R. Immunization with DNA through the skin. *Methods* **2003**, 31, 232-242.

[103] Kuroda, K.; DeGrado, W. F. Amphiphilic polymethacrylate derivatives as antimicrobialagents. *J. Am. Chem. Soc.* **2005**, 127, 4128-4129.

[104] Jankova, K.; Chen, X.; Kops, J.; Batsberg, W. Synthesis of amphiphilic PS-b-PEG-b-PS by atom transfer radical polymerization. *Macromolecules* **1998**, 31, 538-541.

[105] Tang, R.; Palumbo, R. N.; Wang, C. Well-defined block copolymers for gene delivery to dendritic cells: Probing the effect of polycation chain-length. *J. Control. Release* **2010**, 142, 229-237.

[106] Greenland, J. R.; Letvin, N. L. Chemical adjuvants for plasmid DNA vaccines. *Vaccine* **2007**, 25, 3731-3741.

[107] Park, K. To PEGylate or not to PEGylate, that is not the question. *J. Controlled Release* **2010**, 142, 147-148.

[108] Nomoto, T.; Matsumoto, Y.; Miyata, K.; Oba, M.; Fukushima, S.; Nishiyama, N.; Yamasoba, T.; Kataoka, K. In situ quantitative monitoring of polyplexes and polyplex micelles in the blood circulation using intravital real-time confocal laser scanning microscopy. *J. Controlled Release* , In Press, Corrected Proof.

[109] Burke, R. S.; Pun, S. H. Extracellular Barriers to in Vivo PEI and PEGylated PEI Polyplex-Mediated Gene Delivery to the Liver. *Bioconjugate Chem.* **2008**, 19, 693-704.

[110] Rush, C. M.; Mitchell, T. J.; Garside, P. A detailed characterisation of the distribution and presentation of DNA vaccine encoded antigen. *Vaccine* **2010**, 28, 1620-1634.

[111] Tuomela, M.; Malm, M.; Wallen, M.; Stanescu, I.; Krohn, K.; Peterson, P. Biodistribution and general safety of a naked DNA plasmid, GTU®-MultiHIV, in a rat, using a quantitative PCR method. *Vaccine* **2005**, 23, 890-896.

[112] Radcliffe, J. N.; Roddick, J. S.; Friedmann, P. S.; Stevenson, F. K.; Thirdborough, S. M. Prime-Boost with Alternating DNA Vaccines Designed to Engage Different Antigen Presentation Pathways Generates High Frequencies of Peptide-Specific CD8 + T Cells. *J. Immunol.* **2006**, 177, 6626-6633.

[113] Barchet, W.; Cella, M.; Colonna, M. Plasmacytoid dendritic cells—virus experts of innate immunity. *Seminars in Immunology* **2005**, 17, 253-261.

[114] Stoitzner, P.; Green, L. K.; Jung, J. Y.; Price, K. M.; Tripp, C. H.; Malissen, B.; Kissenpfennig, A.; Hermans, I. F.; Ronchese, F. Tumor Immunotherapy by Epicutaneous Immunization Requires Langerhans Cells. *J. Immunol.* **2008**, 180, 1991-1998.

[115] Lin, M.; Zhan, Y.; Villadangos, J. A.; Lew, A. M. The cell biology of cross-presentation and the role of dendritic cell subsets. *Immunology & Cell Biology* **2008**, 86, 353-362.

[116] DeMuth, P. C.; Su, X.; Samuel, R. E.; Hammond, P. T.; Irvine, D. J. Nano-Layered Microneedles for Transcutaneous Delivery of Polymer Nanoparticles and Plasmid DNA. *Adv. Mater.* **2010**, 2010, 4851-4856.